Chapter 2
Electromagnetic Processes and Interactions

The electron, the muon, and their neutrinos are important tools in testing the structure of the fundamental electromagnetic and weak interactions. On the other hand, if these interactions are known, they serve as ideal probes for the internal structure of complex hadronic targets such as nucleons and nuclei. Although electroweak interactions should in fact be discussed as a whole and on the same footing, purely electromagnetic interactions play a distinctive role, for obvious experimental reasons: At low and intermediate energies the effective electromagnetic coupling is larger by many orders of magnitude than the weak couplings, so that electromagnetic processes are measurable to much higher accuracy than purely weak processes.

The *fundamental* aspects of unified electroweak (and strong) interactions are discussed below, in Chap. 3. The present chapter deals primarily with *applications* of charged leptons to problems of nucleon and nuclear structure, and to selected precision tests of quantum electrodynamics (QED) at low momentum transfers. In most of these applications the electromagnetic interactions effectively appear in the form of external fields in the leptonic particle's Dirac equation. This is the domain where the physics of (electromagnetically) interacting leptons can still be described in the framework of an effective, though relativistic, single particle theory. In contrast to this, the topics discussed in Chap. 3 will make use of the full intrinsic many-body nature of Dirac theory.

2.1 Electron Scattering from a Composite Target: Qualitative Considerations

Electron scattering at high and very high energies is an important tool for the investigation of the structure of various strongly interacting particles (hadrons). Among these only proton, neutron and nuclei can be prepared as targets in scattering experiments. Hence most of what we know about internal hadronic structure

F. Scheck, *Electroweak and Strong Interactions*, Graduate Texts in Physics,
DOI 10.1007/978-3-642-20241-4_2, © Springer-Verlag Berlin Heidelberg 2012

concerns protons and neutrons. Nevertheless there is also some information on long-lived hadrons such as pions from electron–positron colliding beam experiments in which pairs of such hadrons are created.[1]

If electron scattering from a nucleon or a nucleus is to give more information on the target than just its electric charge, the electron's de Broglie wavelength $\lambda\!\!\!^{-} = 1/k$ must have a magnitude comparable to the *spatial size* of the nucleon or nucleus, respectively. The radius of the proton is about $r_{\mathrm{p}} \simeq 0.86\,\mathrm{fm}$; the charge radius of nuclei is approximately

$$r_{\mathrm{c}} \simeq 1.1\ \mathrm{fm}\ A^{1/3} \tag{2.1}$$

(A being the nuclear mass number). Thus $\lambda\!\!\!^{-}$ should be of the order of, or smaller than, about 1 fm. Hence its momentum must be of the order of or greater than

$$k = \hbar c/\lambda\!\!\!^{-} \simeq 200\ \mathrm{MeV}.$$

Obviously, at these energies the electron is highly relativistic, its energy is very large as compared to its rest mass

$$E = \sqrt{\boldsymbol{k}^2 + m^2} \gg m.$$

In fact, in most cases we will neglect the mass altogether. We then deal with a massless charged fermion which behaves in a way somewhat similar to neutrinos, with the exception that the electron spin can assume any direction. The following simple estimates may serve to illustrate qualitatively what one learns from the study of *elastic scattering* and of *inelastic scattering to discrete excited states* in a hadronic target (nucleon or nucleus). A more detailed and quantitative analysis of these processes follows in the next sections.

Consider first elastic scattering of an electron by an extended object with spherically symmetric charge density $\rho(r)$ and total charge Ze. $\rho(r)$ shall be normalized to unity,

$$\int \rho(r)\mathrm{d}^3r = 4\pi \int_0^\infty \rho(r) r^2 \mathrm{d}r = 1. \tag{2.2}$$

The corresponding electrostatic potential $\phi(r)$ is related to the charge density through Poisson's equation (in natural units),

$$\Delta\phi(r) = -Ze\rho(r).$$

We calculate the differential cross section for elastic scattering in Born approximation and, for the moment, neglect the spin of the electron. In fact, in

[1]The essential difference between these two types of experiments is that in electron scattering the invariant momentum transfer is *spacelike* while in electron–positron collisions it is *timelike*.

electromagnetic scattering of electrons at very high energies, the spin of the electron is not essential.[2] We shall show below that for $E \gg m$, a spherically symmetric, parity even, potential does not lead to polarization of an initially unpolarized electron beam. This is in contrast to low energies of the order of the mass, $E \simeq m$, where there is polarization through spin–orbit coupling (Mott scattering). With this approximation the electron is then described by a Klein–Gordon equation with external electrostatic potential

$$V(r) = -e\phi(r).$$

To order $(Z\alpha)$ the scattering amplitude is given by

$$f(\boldsymbol{p}', \boldsymbol{p}) \simeq -\frac{k}{2\pi} \int e^{-i\boldsymbol{p}'\boldsymbol{r}}(-e\phi(r))\mathrm{e}^{i\boldsymbol{p}\boldsymbol{r}}\mathrm{d}^3r \tag{2.3}$$

($\boldsymbol{p}$, $\boldsymbol{p}'$ being the initial and final momenta of the electron, respectively, $k = |\boldsymbol{p}| = |\boldsymbol{p}'|$).

Introducing the momentum transfer $\boldsymbol{q} = \boldsymbol{p} - \boldsymbol{p}'$, for which

$$q \equiv |\boldsymbol{q}| = 2k \ \sin(\theta/2) \tag{2.4}$$

(θ being the scattering angle), the amplitude $f(\boldsymbol{q})$ can be expressed in terms of the charge density $\rho(r)$ by integrating by parts twice and making use of Poisson's equation.[3] One obtains

$$f(\boldsymbol{q}) \simeq \frac{Ze^2k}{2\pi q^2} \int \mathrm{e}^{i\boldsymbol{q}\boldsymbol{r}}\rho(r)\mathrm{d}^3r = \frac{2Z\alpha k}{q^2} \int \mathrm{e}^{i\boldsymbol{q}\boldsymbol{r}}\rho(r)\mathrm{d}^3r, \tag{2.5}$$

where we have replaced $e^2/4\pi$ by α (natural units).

Thus, the differential cross section is

$$\left(\frac{d\sigma}{\mathrm{d}\Omega}\right)_{\text{no spin}} = |f(\boldsymbol{q})|^2 \simeq \left(\frac{Z\alpha}{2k}\right)^2 \frac{1}{\sin^4(\theta/2)}|F(\boldsymbol{q})|^2,$$

with the *charge form factor* $F(\boldsymbol{q})$ defined as follows:

$$F(\boldsymbol{q}) = \int \rho(r)\mathrm{e}^{i\boldsymbol{q}\boldsymbol{r}}\mathrm{d}^3r. \tag{2.6}$$

---

[2] This is true because electromagnetic interactions are invariant under parity.

[3] In order to do this in a mathematically correct manner the $1/r$ potential must be multiplied by a convergence factor, say $\mathrm{e}^{-\alpha r}$, and the limit $\alpha \to 0$ must be taken at the end.

When the electron spin in included, the scattering cross section for a spin zero target just gets another factor $\cos^2(\theta/2)$, so that we obtain

$$\frac{\mathrm{d}\sigma}{\mathrm{d}\Omega} = \left(\frac{\mathrm{d}\sigma}{\mathrm{d}\Omega}\right)_{\mathrm{Mott}} |F(\boldsymbol{q})|^2, \tag{2.7}$$

with

$$\left(\frac{\mathrm{d}\sigma}{\mathrm{d}\Omega}\right)_{\mathrm{Mott}} = \left(\frac{Z\alpha}{2k}\right)^2 \frac{\cos^2(\theta/2)}{\sin^4(\theta/2)}. \tag{2.8}$$

The Mott cross section (2.8) is derived below, including the necessary kinematics if recoil of the struck target becomes important. However, already at this point, we can read off a few qualitative physical features from these formulae.

(i) In the forward direction, $\boldsymbol{q} = 0$, the form factor $F(\boldsymbol{q})$ is equal to one, by virtue of the normalization condition (2.2): $F(0) = 1$. The same result obtains for *all* momenta $\boldsymbol{q}$ if the charge distribution is concentrated in a point,

$$\rho_{\mathrm{point}}(r) = \frac{1}{4\pi}\frac{1}{r^2}\,\delta(r) \to F(\boldsymbol{q}) \equiv 1 \quad \forall \boldsymbol{q}. \tag{2.9}$$

Thus, the Mott cross section (2.8) describes the scattering from a point charge Ze placed at the origin.

(ii) If the charge is not pointlike the cross section (2.7) is modulated by the form factor $F(\boldsymbol{q})$. It is this form factor which contains information about the target beyond its charge Ze. Hence, elastic electron scattering measures, in essence, the *spatial distribution* of the charge density $\rho(r)$. In particular, if the Born approximation is applicable, then (2.6, 2.7) show that the cross section is just the square of the Fourier transform of $\rho(r)$.

(iii) If the region over which $\rho(r)$ is appreciably different from zero is characterized by a radius R, the momentum transfer must be chosen such that

$$qR \gtrsim 1. \tag{2.10}$$

Indeed, if q is chosen too small, i.e. $qR \ll 1$ the form factor does not yet deviate much from unity and little information is obtained. If q is too large, i.e. $qR \gg 1$, the exponential in (2.6) oscillates rapidly and $F(\boldsymbol{q})$ becomes unmeasurably small. Thus q must be tuned to the size of the extended object that one wants to map. The quantitative details and the nature of the information obtained by means of elastic scattering are worked out in some of the following sections (Sects. 2.4, 5).

(iv) A similar situation is encountered when we consider inelastic scattering to discrete excited states. In that case the ground state charge density (which we assumed spherically symmetric, for simplicity) is replaced by a transition density $\rho_{\mathrm{fi}}(\boldsymbol{r})$ or more complicated functionals of charge and current densities of the target particle. Equivalently, the elastic charge form factor is replaced

by inelastic form factors. As in the case of elastic scattering, the cross section depends on a leptonic part which is known and some kinematics, whilst the hadronic structure is contained in the form factors.

In the simplest case (electric charge scattering from a nucleus to a discrete excited state) the form factor for the transition from state i to state f, and with multipolarity λ, will be proportional to

$$F_{\mathrm{fi}}(q) \propto \int_0^\infty \rho_{\mathrm{fi}}(r)\, j_\lambda(qr) r^2 \mathrm{d}r. \tag{2.11}$$

This follows from expanding the exponential $\mathrm{e}^{\mathrm{i}\boldsymbol{qr}}$ in terms of spherical harmonics and from the selection rules for angular momentum imposed by the spins and parities of initial and final target state. The expression (2.11) is reminiscent of the transition amplitude for the corresponding photoexcitation of state f. In that case q is replaced by the photon energy $k_\gamma = E_\mathrm{i} - E_\mathrm{f}$. For given energy this is a fixed number. Furthermore, in many cases $k_\gamma r$ is small compared to one over the domain where $\rho_{\mathrm{fi}}(r)$ is appreciably different from zero. In this case the Bessel function in (2.11) can be replaced by its limiting form for small argument,

$$j_\lambda(k_\gamma r) \simeq (k_\gamma r)^\lambda / (2\lambda + 1)!!. \tag{2.12}$$

Thus, the γ-transition depends essentially only on one specific *moment* of the transition charge density. The power behaviour $(k_\gamma r)^\lambda$ with $k_\gamma r \ll 1$ limits the γ-transition to the lowest possible multipolarity.

In *electron* scattering, in contrast, q is a variable momentum transfer which can be chosen as large as one wishes. This means that a complete mapping of $F_{\mathrm{fi}}(q)$ and, thereby, of $\rho_{\mathrm{fi}}(r)$ can be obtained, at least in principle. Also, all multipolarities compatible with the angular momentum and parity selection rules can contribute on equal footing if q is chosen appropriately. For instance, an E5 electro-excitation can have as large a cross section as an E2 transition.

(v) Finally, if both the momentum transfer and the energy transfer to the target are chosen sufficiently large one reaches a new domain where the electron starts to probe, in a rather general sense, the *constituent structure of the target*. In the case of scattering from nuclei this is called *quasi-free scattering*, expressing the fact that the energy transfer is much larger than the binding energy of the nucleons in the nucleus so that the nucleus behaves like a cloud of almost free nucleons.

In the case of *nucleons* the analogous domain is called the *deep inelastic* region. Although there are essential differences to the case of nuclei, the main idea is the same as in quasi-free scattering from nuclei: Deep inelastic scattering, where both momentum and energy transfers are large, must be sensitive to interactions within the target at very small distances.

2.2 Elastic Scattering from a Spin Zero Target, Born Approximation

The elastic scattering of an electron from a spin zero target is the simplest case. It can be dealt with by means of standard Green function techniques of potential scattering without having to invoke covariant perturbation theory and Feynman rules. The result is the correct covariant cross section in the Born approximation and contains many of the essential features of more complicated situations such as scattering on spin-1/2 targets or similar. Because of this simplicity we consider this case first.

The "spin-zero target" may be a pion or any nucleus whose spin is zero. We start with the kinematics of Fig. 2.1. Let

$$k = (E;\boldsymbol{k}), \quad k' = (E';\boldsymbol{k}') \tag{2.13}$$

be the four-momenta of the electron in the *laboratory system* before and after the scattering. Similarly,

$$p = (M;0), \quad p' = \left(\sqrt{M^2 + \boldsymbol{p}'^2};\boldsymbol{p}'\right) \tag{2.14}$$

denote the four-momenta of the target before and after the scattering process, respectively, with M the target mass. As the electron energy is chosen large compared to its rest mass, $E \simeq |k|$ and $E' \simeq |k'|$ and the square of the four-momentum transfer is

$$q^2 := -(k - k')^2 = -(E - E')^2 + (\boldsymbol{k} - \boldsymbol{k}')^2 \simeq 4EE' \sin^2(\theta/2) \tag{2.15}$$

[q^2 is the same as $-t$, see below, (2.36)].

Setting $m_e \simeq 0$, energy–momentum conservation gives the relationship

$$E' = E \frac{1}{1 + 2(E/M)\sin^2(\theta/2)}. \tag{2.16}$$

We note that the denominator of (2.16) is a typical recoil term. Whether or not this recoil term is important depends on the mass of the target. For a nucleus, for instance, $M \simeq A \cdot 940\,\text{MeV}$ will in general be large compared to E if the electron energy is chosen to be a few hundred MeV.

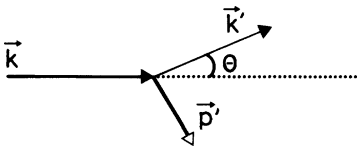

Fig. 2.1 Kinematics of electron scattering in the laboratory system

Suppose we can characterize the ground state of the target by a spherically symmetric charge distribution. In the case of a nucleus of charge number Z this is

$$Ze\rho(r) = \left\langle \psi_0 \left| e \sum_{i=1}^{Z} \delta(\boldsymbol{r} - \boldsymbol{r}_i) \right| \Psi_0 \right\rangle$$

with $\boldsymbol{\Psi}_0$ the (spherical) ground state wave function.[4] The corresponding electrostatic potential $V(r)$ is given by (1.186) and must be inserted into the Dirac equation (1.187) in which we neglect the mass term on the right-hand side.

We wish to construct solutions of (1.187) which describe the scattering of electrons whose incoming momentum is directed along the positive 3-axis. In order to avoid the complications due to the infinite range of the Coulomb potential we assume, as usual that $\lim_{r\to\infty} rV(r) = 0$. This means that we multiply the Coulomb potential by a screening factor and that we take the correct limit at the end of our calculation. As is well-known, using this mathematically incorrect procedure we miss the typical constant and logarithmic phases of the Coulomb scattering problem. However, very much like in the nonrelativistic case, these complications are irrelevant for our discussion; they may be inserted in the final results.

For $r \to \infty$ the two-component spinors $\phi(\boldsymbol{x})$ and $\chi(\boldsymbol{x})$ must be eigenstates of helicity. Thus, in the *centre-of-mass system* they have the asymptotic behaviour

$$\phi(\boldsymbol{x}) \sim u_+(0,0)\mathrm{e}^{\mathrm{i}k^* z} + f(\theta,\varphi)\frac{\mathrm{e}^{\mathrm{i}k^* r}}{r}u_+(\theta,\varphi), \tag{2.17a}$$

$$\chi(\boldsymbol{x}) \sim u_-(0,0)\mathrm{e}^{\mathrm{i}k^* z} + g(\theta,\varphi)\frac{\mathrm{e}^{\mathrm{i}k^* r}}{r}u_-(\theta,\varphi), \tag{2.17b}$$

where $k^* = |k_{\mathrm{c.m}}| = \left|k'_{\mathrm{c.m.}}\right| \simeq E^*$ and where

$$\begin{aligned} u_\pm(\theta,\varphi) &= D^{(1/2)*}(0,\theta,\varphi)u_\pm(0,0), \\ u_+(0,0) &= \begin{pmatrix} 1 \\ 0 \end{pmatrix}, \quad u_-(0,0) = \begin{pmatrix} 0 \\ 1 \end{pmatrix}, \end{aligned} \tag{2.18}$$

cf. (1.141). f and g denote the scattering amplitudes whose squares give the cross section in the c.m. system. $u_\pm(0,0)$ are positive and negative helicity eigenstates, respectively, of the incoming state whose momentum points in the positive 3-direction. Similarly

$$u_+(\theta,\varphi) = \begin{pmatrix} \mathrm{e}^{-\mathrm{i}\varphi/2}\cos(\theta/2) \\ \mathrm{e}^{\mathrm{i}\varphi/2}\sin(\theta/2) \end{pmatrix}, \quad u_-(\theta,\varphi) = \begin{pmatrix} -\mathrm{e}^{-\mathrm{i}\varphi/2}\sin(\theta/2) \\ \mathrm{e}^{\mathrm{i}\varphi/2}\cos(\theta/2) \end{pmatrix} \tag{2.19}$$

are the helicity eigenstates along the outgoing momentum.

[4] In the case of an elementary particle $\rho(r)$ is the Fourier transform of the form factor, see below. This leaves open the question of whether or not $\rho(r)$ may be computable from a constituent picture.

Two important properties follow from the equations (1.187) with m set equal to zero:

(i) Equations (1.187a) and (1.187b) are completely decoupled. The potential $V(r)$, which is spherically symmetric, cannot change the helicity.
(ii) From invariance under *parity* and under *rotations* one shows that $f(\theta, \varphi)$ and $g(\theta, \varphi)$ must be equal (see exercise 2.1). Thus, *a fast electron cannot be polarized by a spherically symmetric potential*. [Note that this is not so for energies comparable to the rest mass. At such energies the spin–orbit force can indeed flip the spin of the electron (Mott scattering).] Therefore, it is sufficient to solve one of the equations (1.187), for example the first one, which reads

$$(\mathrm{i}\boldsymbol{\sigma} \cdot \nabla + k^*)\phi(x) = V(r)\phi(x). \tag{2.20}$$

We solve this equation with the aid of the appropriate Green function which satisfies the equation

$$(\mathrm{i}\boldsymbol{\sigma} \cdot \nabla_x + k^*)G(\boldsymbol{x} - \boldsymbol{x}') = \delta(\boldsymbol{x} - \boldsymbol{x}'), \tag{2.21}$$

whereby

$$\phi(x) = u_+(0,0)\mathrm{e}^{\mathrm{i}k^* z} + \int G(\boldsymbol{x} - \boldsymbol{x}')V(r')\phi(\boldsymbol{x}')\mathrm{d}^3x'. \tag{2.22}$$

The Green function with the correct asymptotic behaviour is given by

$$G(\boldsymbol{x} - \boldsymbol{x}') = (\mathrm{i}\boldsymbol{\sigma} \cdot \nabla_x - k^*)\frac{\mathrm{e}^{\mathrm{i}k^*|\boldsymbol{x}-\boldsymbol{x}'|}}{4\pi|\boldsymbol{x} - \boldsymbol{x}'|}. \tag{2.23}$$

This follows from the equations

$$(\mathrm{i}\boldsymbol{\sigma} \cdot \nabla_x + k^*)(\mathrm{i}\boldsymbol{\sigma} \cdot \nabla_x - k^*) = -(\Delta + k^{*2}),$$
$$(\Delta + k^{*2})\frac{\mathrm{e}^{\mathrm{i}k^*|\boldsymbol{x}-\boldsymbol{x}'|}}{4\pi|\boldsymbol{x} - \boldsymbol{x}'|} = -\delta(\boldsymbol{x} - \boldsymbol{x}').$$

First Born approximation means replacing $\phi(\boldsymbol{x}')$ on the r.h.s. of (2.22) by the incoming plane wave. Thus

$$\phi(\boldsymbol{x}) \simeq u_+(0,0)\mathrm{e}^{\mathrm{i}k^* z} + \frac{1}{4\pi}\int \mathrm{d}^3x'(\mathrm{i}\boldsymbol{\sigma} \cdot \nabla_x - k^*)\frac{\mathrm{e}^{\mathrm{i}k^*|\boldsymbol{x}-\boldsymbol{x}'|}}{|\boldsymbol{x} - \boldsymbol{x}'|}V(r')u_+(0,0)\mathrm{e}^{\mathrm{i}k^* z},$$

from which we must now extract the scattering amplitude $f(\theta, \varphi)$. For finite r', but taking the limit $r \to \infty$, we have

$$(\mathrm{i}\boldsymbol{\sigma}\cdot\nabla_x - k^*)\frac{\mathrm{e}^{\mathrm{i}k^*|\boldsymbol{x}-\boldsymbol{x}'|}}{|\boldsymbol{x}-\boldsymbol{x}'|} = -(\mathrm{i}\boldsymbol{\sigma}\cdot\nabla_{x'} + k^*)\frac{\mathrm{e}^{\mathrm{i}k^*|\boldsymbol{x}-\boldsymbol{x}'|}}{|\boldsymbol{x}-\boldsymbol{x}'|}$$
$$\underset{r\to\infty}{\sim} -(\mathrm{i}\sigma\cdot\nabla_{x'} + k^*)\frac{\mathrm{e}^{\mathrm{i}k^* r}}{r}\mathrm{e}^{-\mathrm{i}k^*\hat{x}\cdot x'}.$$

If we set $\boldsymbol{k}' := k^*\cdot\hat{\boldsymbol{x}} = k^*\boldsymbol{x}/r$, this gives for $r\to\infty$

$$\phi(\boldsymbol{x}) \sim u_+(0,0)\mathrm{e}^{\mathrm{i}k^* z} - \frac{\mathrm{e}^{\mathrm{i}k^* r}}{r}\frac{1}{4\pi}\int \mathrm{d}^3x'\mathrm{e}^{\mathrm{i}\boldsymbol{q}\boldsymbol{x}}V(r')(\boldsymbol{\sigma}\cdot\boldsymbol{k}' + k^*)u_+(0,0) \tag{2.24}$$

with $\boldsymbol{q} := \boldsymbol{k} - \boldsymbol{k}'$. The r.h.s of (2.24) is to be identified with the general form (2.17a), giving

$$f(\theta,\varphi) = -\frac{1}{4\pi}\int \mathrm{d}^3x'\mathrm{e}^{\mathrm{i}\boldsymbol{q}\boldsymbol{x}}V(r')u_+^\dagger(\theta,\varphi)(\boldsymbol{\sigma}\cdot\boldsymbol{k}' + k^*)u_+(0,0).$$

The scalar product under the integral sign is easily worked out by making use of the equation satisfied by the spinor $u_+(\theta,\varphi)$:

$$u_+^\dagger(\theta,\varphi)\left(\boldsymbol{\sigma}\cdot\boldsymbol{k}' - k^*\right) = 0.$$

One finds

$$u_+^\dagger(\theta,\varphi)(\boldsymbol{\sigma}\cdot\boldsymbol{k}' + k^*)u_+(0,0) = 2k^*u_+^\dagger(\theta,\varphi)u_+(0,0) = 2k^*\mathrm{e}^{\mathrm{i}\varphi/2}\cos(\theta/2),$$

which then gives

$$f(\theta,\varphi) = -\frac{k^*}{2\pi}\mathrm{e}^{\mathrm{i}\varphi/2}\cos(\theta/2)\int \mathrm{d}^3r\mathrm{e}^{\mathrm{i}\boldsymbol{q}\cdot\boldsymbol{r}}V(r).$$

Alternatively, we may integrate by parts and make use of Poisson's equation $\Delta V(r) = Ze^2\rho(r)$ to obtain

$$f(\theta,\varphi) = -\frac{2Z\alpha k^*}{q^2}\mathrm{e}^{\mathrm{i}\varphi/2}\cos(\theta/2)\int \mathrm{d}^3r\mathrm{e}^{\mathrm{i}\boldsymbol{q}\cdot\boldsymbol{r}}\rho(r) \tag{2.25}$$

$\left(\alpha = \mathrm{e}^2/4\pi \simeq \frac{1}{137}\right)$. The differential cross section in the centre-of-mass system is then given by

$$\left(\frac{\mathrm{d}\sigma}{\mathrm{d}\Omega}\right)_{\text{c.m.}} = |f(\theta,\varphi)|^2 = \left.\frac{\mathrm{d}\sigma}{\mathrm{d}\Omega}\right|_{\text{Mott}} F^2(\boldsymbol{q}), \tag{2.26}$$

where

$$\left.\frac{\mathrm{d}\sigma}{\mathrm{d}\Omega}\right|_{\text{Mott}} = \frac{(Z\alpha)^2\cos^2(\theta/2)}{4k^{*2}\sin^4(\theta/2)} \tag{2.27}$$

is the Mott cross section (2.8), θ is the scattering angle in the c.m. system and $F(\boldsymbol{q})$ is the (real) charge form factor of the charge distribution $\rho(r)$ (Mott, 1929).

2.3 A Few Properties of Form Factor and Cross Section

Before we proceed to scattering from targets with nonvanishing spin we wish to discuss a few properties of the results obtained in the previous section.

The order of magnitude of the Mott cross section is easily estimated. Take, for instance, $k^* = 200\,\mathrm{MeV} \triangleq (200/\hbar c)\,\mathrm{fm}^{-1} = 1.01\,\mathrm{fm}^{-1}$, $\theta = 90°$ and $Z = 82$. This gives

$$\left.\frac{\mathrm{d}\sigma}{\mathrm{d}\Omega}\right|_{\mathrm{Mott}} = (82)^2 \times 2.6 \times 10^{-31}\,\mathrm{cm}^2 = 1.7 \times 10^{-27}\,\mathrm{cm}^2.$$

A few properties of the form factor have already been mentioned above, in Sect. 2.1. If the target is a nucleus the charge distribution can be calculated from the ground state wave function Ψ_0,

$$\rho(\boldsymbol{r}) = \frac{1}{Z}\int \mathrm{d}^3 r_1 \int \mathrm{d}^3 r_2 \ldots \int \mathrm{d}^3 r_A \sum_{\nu=1}^{z} \delta(\boldsymbol{r} - \boldsymbol{r}_\nu)|\boldsymbol{\Psi}_0(\boldsymbol{r}_1 \ldots \boldsymbol{r}_A)|^2,$$

so that

$$F(q^2) = \frac{1}{Z}\int \mathrm{d}^3 r_1 \int \mathrm{d}^3 r_2 \ldots \int \mathrm{d}^3 r_A \sum_{\nu=1}^{z} \mathrm{e}^{i\boldsymbol{q}\cdot\boldsymbol{r}_\nu}|\boldsymbol{\Psi}_0(\boldsymbol{r}_1 \ldots \boldsymbol{r}_A)|^2. \tag{2.28}$$

We verify the property $F(0) = 1$ which expresses the fact that forward scattering depends only on the total charge of the target. If $\rho(\boldsymbol{r})$ is spherically symmetric, the form factor (2.6) can be written as follows. We make use of the expansion

$$\mathrm{e}^{\mathrm{i}\boldsymbol{q}\cdot\boldsymbol{r}} = 4\pi \sum_{l=0}^{\infty} \mathrm{i}^l\, j_l(qr) \sum_{m=-l}^{+l} Y^*_{lm}(\hat{\boldsymbol{q}})\, Y_{lm}(\hat{\boldsymbol{r}}) \tag{2.29}$$

and of the orthogonality property of the spherical harmonics to obtain[5]

$$\begin{aligned} F(q^2) &= 4\pi \int_0^\infty \rho(r)\, j_0(qr) r^2 \mathrm{d}r \\ &= \frac{4\pi}{q}\int_0^\infty \rho(r)\sin(qr) r\,\mathrm{d}r. \end{aligned} \tag{2.30}$$

[5]If $\rho(\boldsymbol{r})$ is not spherically symmetric the formalism developed for inelastic scattering below may be consulted.

If (qr) is small over the domain where $\rho(r)$ is appreciably different from zero, one may expand the form factor in powers of q,

$$F(q^2) = 4\pi \int_0^\infty \rho(r) r^2 \mathrm{d}r - \frac{1}{6} q^2 4\pi \int_0^\infty \rho(r) r^4 \mathrm{d}r | \mathcal{O}(q^4)$$
$$= 1 - \frac{1}{6} q^2 \langle r^2 \rangle_{\text{r.m.s}} + \mathcal{O}(q^4 \langle r^4 \rangle). \tag{2.31}$$

Here $\langle r^2 \rangle_{\text{r.m.s.}}$ denotes the root-mean-square radius

$$\langle r^2 \rangle_{\text{r.m.s.}} = -6 \frac{\partial F(q^2)}{\partial q^2}\bigg|_{q^2=0} = 4\pi \int_0^\infty [\rho(r) r^2] r^2 \mathrm{d}r. \tag{2.32}$$

As the momentum transfer increases, more and more moments $\langle r^{2n} \rangle$ come into play. Eventually, if the form factor is known for all momenta q^2, all even moments are determined. This is equivalent to saying that the charge distribution $\rho(r)$ has been mapped completely and is obtained from the form factor by

$$\rho(r) = \frac{1}{(2\pi)^3} \int \mathrm{d}^3 q \mathrm{e}^{-\mathrm{i}\boldsymbol{q}\cdot\boldsymbol{r}} F(q^2), \tag{2.33}$$

In the case of *nuclei* $\rho(r)$ is given by the wave functions of the protons in the nuclear ground state. The r.m.s. radius is then the average r.m.s. radius of the protons (so-called *charge radius*),

$$\langle r^2 \rangle_{\text{r.m.s.}} = \frac{1}{Z} \sum_{i=1}^{Z} \langle r_i^2 \rangle. \tag{2.34}$$

In the case of the *nucleon* it is not clear a priori what causes its finite charge distribution. The finite extension of charge within the proton may be due to the virtual meson cloud surrounding the proton, and/or to a bound state substructure in which case the charge density reflects some properties of the ground state of the proton's constituents. In any event, the primary physical quantity is the form factor, not the charge density. It is the form factor which describes the particle's coupling to the photon (Coulomb field) and which enters in the expressions for scattering amplitudes and cross sections. Once the form factor is given, we may *define* the charge density through (2.33) and, in particular, the r.m.s. radius through the derivative of $F(q^2)$, cf. (2.32).

In Sect. 2.2 we have calculated the cross section in the c.m. system. It is not difficult to transform it to the laboratory system or any other system of reference. For that purpose it is useful to write first the cross section in a Lorentz invariant form. Let us introduce Lorentz-scalar variables (Mandelstam variables), s and t, and let us write these, in the c.m. frame, in terms of k^* and θ (neglecting the electron mass).

$$s = (k + p)^2 = M^2 + 2k^* \sqrt{M^2 + k^{*2}} + 2k^{*2},$$
$$t = (k - k')^2 = -2k^{*2}(1 - \cos\theta) \equiv -q^2.$$

Inverting these equations one obtains

$$k^* = (s - M^2)/2\sqrt{s},$$
$$\cos^2(\theta/2) = [(s - M^2)^2 + st]/(s - M^2)^2.$$

The invariant cross section $\mathrm{d}\sigma/\mathrm{d}t$ is calculated by means of

$$\frac{\mathrm{d}\sigma}{\mathrm{d}t} = \left(\frac{\mathrm{d}\sigma}{\mathrm{d}(\cos\theta)}\right)_{\text{c.m.}} \frac{\mathrm{d}\cos\theta}{\mathrm{d}t} = \int_0^{2\pi} \mathrm{d}\varphi \left(\frac{\mathrm{d}\sigma}{\mathrm{d}\Omega}\right)_{\text{c.m.}} \frac{\mathrm{d}\cos\theta}{\mathrm{d}t},$$

yielding

$$\frac{\mathrm{d}\sigma}{\mathrm{d}t} = \frac{4\pi(Z\alpha)^2}{t^2} F^2(t) \frac{(s - M^2)^2 + st}{(s - M^2)^2}. \tag{2.35}$$

It is now easy to calculate the cross section in the laboratory system, where

$$s = M^2 + 2ME,$$
$$t = -2EE'(1 - \cos\theta) = -2E^2 \frac{1 - \cos\theta}{1 + (E/M)(1 - \cos\theta)}. \tag{2.36}$$

Thus,

$$\frac{\mathrm{d}t}{\mathrm{d}(\cos\theta)} = \frac{2E^2}{[1 + (E/M)(1 - \cos\theta)]^2},$$
$$\frac{(s - M^2)^2 + st}{(s - M^2)^2} = \frac{\cos^2(\theta/2)}{1 + (E/M)(1 - \cos\theta)}.$$

Finally, knowing that

$$\int \frac{\mathrm{d}\sigma}{\mathrm{d}\Omega}\mathrm{d}\varphi = \frac{\mathrm{d}\sigma}{\mathrm{d}t}\frac{\mathrm{dt}}{\mathrm{d}\cos\theta}$$

we find

$$\left(\frac{\mathrm{d}\sigma}{\mathrm{d}\Omega}\right)_{\text{lab}} = \left(\frac{Z\alpha}{2E}\right)^2 \frac{\cos^2(\theta/2)}{\sin^4(\theta/2)} F^2(q^2) \frac{1}{1 + 2(E/M)\sin^2(\theta/2)}. \tag{2.35′}$$

Thus, the cross section in the laboratory system contains the recoil factor $\{1 + 2(E/M)\sin(\theta/2)\}^{-1}$ which we encountered earlier in (2.16).

Clearly, the method of transforming the cross section from one frame of reference to another that we have developed here, is quite general. It consists in writing first the cross section in Lorentz invariant form (2.35), and then in specializing to any desired frame of reference. In this context, we also refer to the general formulae collected in App. B.

2.4 Elastic Scattering from Nucleons

2.4.1 Current Matrix Elements and Form Factors

The scattering cross section (2.26, 2.35) that we have derived in the last two sections holds for any spin zero target, a nucleus, a pion or any other elementary or composite particle with spin zero. The result is fully covariant and thus may also be derived in the framework of covariant perturbation theory. In other words the same cross section must be obtained from the Feynman rules for quantum electrodynamics which are summarized in App. C (see exercise 2.2).

If a particle has no internal structure caused by interactions other than electromagnetic, we say it is *pointlike*. For example, to the best of our knowledge, electron and muon seem to be such particles. In this case the Feynman rules apply as they are given in App. C. In particular, at any photon–fermion vertex we have to write a factor γ_α, the Lorentz index having to be contracted with the photon polarization vector $\varepsilon^\alpha(k)$ for an external photon, or with one of the indices of the photon propagator $D^{\alpha\beta}(k)$ for an internal photon line. This is a reflection of the fact that the photon couples to the electromagnetic current j^{em}_α, and that for a pointlike fermion (on its mass shell) the matrix element of j^{em}_α leading from momentum state p to momentum state p' is given by

$$\left\langle p' \left| j^{\mathrm{em}}_\alpha(0) \right| p \right\rangle = \frac{1}{(2\pi)^3} Q \overline{u(p')} \gamma_\alpha u(p). \tag{2.37}$$

If, to the contrary, the particle does have internal structure due to other interactions not described by QED,[6] then the Feynman rules are incomplete. They cannot tell us the explicit form of the particle's coupling to an (external or internal) photon line. Nevertheless, these couplings can be reduced considerably and can be expressed in terms of a few real Lorentz scalar functions (form factors) which allow one to parametrize the internal structure of the particle in a very condensed form.[7] This is achieved by making use of some general properties of the electromagnetic current, such as its behaviour under Lorentz transformations, time reversal, current conservation, hermiticity, isospin content, etc.

We exemplify these matters for the case of proton and neutron, i.e. strongly interacting particles of spin 1/2. The spin zero case is similar though somewhat simpler. It is left as an exercise for the reader. The relevant matrix element of the electromagnetic current is

[6] For example, hadrons are composite objects and, to some extent, they are also "dressed" by pion clouds.

[7] Note that also a pointlike particle of QED builds up form factors i.e. internal structure by interaction with the Maxwell field. These effects are calculable from QED in higher order perturbation theory.

$$\left\langle p',\ s' \mid j_\alpha^{\mathrm{em}}(x) \mid\ p,\ s \right\rangle, \tag{2.38}$$

where initial and final states are on-mass-shell states of given momentum and spin, and $p^2 = p'^2 = M^2$. Let us work out the restrictions on this matrix element that follow from current conservation, from the space–time structure of the electromagnetic current and hermiticity.

(i) *Current conservation*. Let $x'_\mu = x_\mu + a_\mu$ be an arbitrary translation, that transforms a given field operator according to

$$F(x) \ \rightarrow\ F'(x') = U(a)F(x)U^{-1}(a) = F(x+a). \tag{2.39}$$

Using the generalized Heisenberg equations of motion

$$-\mathrm{i}\partial^\mu F(x) = [P^\mu, F(x)], \tag{2.40}$$

where P^μ are the four energy–momentum operators, one shows that (see exercise (2.3))

$$U(a) = \exp\{\mathrm{i}a_\mu P^\mu\}. \tag{2.41}$$

If we consider a matrix element of $F(x)$ between specific eigenstates of energy and momentum, we can make use of (2.39) to transform $F(x)$ to any other point $x' = x + a$ of Minkowski space, i.e.

$$\begin{aligned}\langle q_\mathrm{f}|F(x)|q_i\rangle &= \langle q_\mathrm{f}|U^{-1}(a)F(x+a)\ U(a)|q_\mathrm{i}\rangle \\ &= \langle U(a)q_\mathrm{f}|F(x+a)|\ U(a)q_\mathrm{i}\rangle \\ &= \mathrm{e}^{\mathrm{i}a\cdot(q_\mathrm{i}-q_\mathrm{f})}\ \langle q_\mathrm{f}|F(x+a)|q_\mathrm{i}\rangle. \end{aligned} \tag{2.42}$$

In particular, we may take $a_\mu = -x_\mu$ to obtain

$$\langle q_\mathrm{f}|F(x)|q_\mathrm{i}\rangle \ =\ \mathrm{e}^{-\mathrm{i}x\cdot(q_\mathrm{i}-q_\mathrm{f})}\ \langle q_\mathrm{f}|F(0)|q_\mathrm{i}\rangle. \tag{2.42$'$}$$

Thus, the x-dependence of any such matrix element between eigenstates of four-momentum is a simple exponential; the remaining factor $\langle q_\mathrm{f}|F(0)|q_\mathrm{i}\rangle$ no longer depends on x. Formulae such as (2.42) or (2.42′) in which space–time arguments are shifted may be called *translation formulae*.

Suppose $F(x)$ is a current operator $J_\alpha(x)$ and suppose that the divergence of J_α is known, $\partial_\alpha J^\alpha(x) = \phi(x)$. Then from (2.42′)

$$\begin{aligned}\langle q_\mathrm{f}|\partial^\alpha\ J_\alpha(x)|q_\mathrm{i}\rangle &= (\partial^\alpha \mathrm{e}^{-i(q_\mathrm{i}-q_\mathrm{f})\cdot x})\langle q_\mathrm{f}|J_\alpha(0)|q_\mathrm{i}\rangle \\ &= \langle q_\mathrm{f}|\phi(x)|q_\mathrm{i}\rangle = e^{-\mathrm{i}(q_\mathrm{i}-q_\mathrm{f})\cdot x}\ \langle q_\mathrm{f}|\phi(0)|q_\mathrm{i}\rangle. \end{aligned}$$

Thus, one finds the relation

$$(q_\mathrm{i} - q_\mathrm{f})^\alpha \, \langle q_\mathrm{f}| \, J_\alpha \, (0) \, |q_\mathrm{i}\rangle = \mathrm{i}\langle q_\mathrm{f}| \, \phi \, (0) \, |q_\mathrm{i}\rangle \, . \tag{2.43}$$

If the current is conserved–which is the case for the electromagnetic current – we obtain the condition

$$(q_\mathrm{i} - q_\mathrm{f})^\alpha \, \langle q_\mathrm{f}| \, j_\alpha \, (0) \, |q_\mathrm{i}\rangle = 0 \tag{2.44}$$

(we drop the superscript "em" for simplicity).
(ii) *Covariance*. As j_α is a Lorentz vector, its matrix elements between nucleon states must also transform as Lorentz vectors. For the construction of such vectors we have at our disposal the vectors p'_α and p_α as well as the γ-matrices and combinations thereof. The only vectors that can be formed are[8]

$$\overline{u(p')}\,\gamma_\alpha u(p), \qquad (p'-p)^\beta \, \overline{u(p')}\,\sigma_{\alpha\beta} u(p),$$
$$(p+p')_\alpha \, \overline{u(p')}\,u(p), \qquad (p-p')_\alpha \, \overline{u(p')}\,u(p),$$

where we have defined

$$\boldsymbol{\sigma}_{\alpha\beta} := \frac{1}{2}\,\mathrm{i}(\gamma_\alpha\gamma_\beta - \gamma_\beta\gamma_\alpha). \tag{2.45}$$

That the first two of these are indeed *vector* operators is not difficult to show. Indeed $\overline{\boldsymbol{\Psi}(x)}\gamma_\alpha\boldsymbol{\Psi}(x)$ is a vector operator as should be clear from Chap. 1 Similarly, $\overline{\boldsymbol{\Psi}(x)}\sigma_{\alpha\beta}\boldsymbol{\Psi}(x)$ is a tensor operator. Knowing that p_α and p'_α are vectors and making use of the expansion (1.122), the assertion is proved. Among these covariants only three are independent. The external particles are on their mass shell and obey the free Dirac equation. In this case one has the Gordon identity relating the first three covariants (exercise 2.14).

Thus, the most general covariant decomposition must have the form (dropping the spin indices $s,\ s'$, for the sake of clarity),

$$\langle p'| \, j_\alpha \, (0) \, |p\rangle$$
$$= \frac{1}{(2\pi)^3} \, \overline{u(p')} \left\{ \gamma_\alpha F_1 \, (q^2) + \frac{\mathrm{i}}{2M}\sigma_{\alpha\beta}q^\beta \, F_2 \, (q^2) + \frac{1}{2M}q_\alpha F_3(q^2) \right\} u(p), \tag{2.46}$$

where q is the momentum transfer

$$q := p' - p. \tag{2.47}$$

(We have set $Q = 1$, taking out a factor $|e|$ to be inserted at each photon vertex). The functions F_i must be Lorentz scalars and, thus, can only depend on Lorentz scalar quantities such as $p^2,\ p'^2$ and q^2. Since $p^2 = p'^2 = m^2$, these are in fact constants,

[8]The same forms apply for antiparticle states, with $u(p)$ replaced by $\upsilon(p)$.

so the only true variation must be in the variable q^2. The divergence condition (2.44) implies that $F_3(q^2)$ must vanish identically for $q^2 \neq 0$. The other two terms on the r.h.s. of (2.46) fulfill this condition separately, as one easily verifies by means of the Dirac equations (1.84,1.84').

(iii) *Hermiticity of electromagnetic current*. By definition we have

$$\left\langle p \,\middle|\, j_\alpha^\dagger(0) \,\middle|\, p' \right\rangle = \langle p' |\, j_\alpha(0) \,| p \rangle^* . \tag{2.48a}$$

As j_α is a hermitean operator this is also equal to

$$\langle p |\, j_\alpha(0) \,| p' \rangle . \tag{2.48b}$$

The expression (2.48a), more explicitly, gives

$$\begin{aligned}
&\left(u(p')^\dagger \, \gamma_0 \left[\gamma_\alpha F_1 + \frac{\mathrm{i}}{2M} \sigma_{\alpha\beta} \, (p'-p)^\beta \, F_2 \right] u(p) \right)^* \\
&= u^\dagger(p) \left[(\gamma_0 \gamma_\alpha)^\dagger \gamma_0 \, F_1^* - \frac{\mathrm{i}}{2M} \, (\gamma_0 \sigma_{\alpha\beta})^\dagger \, (p'-p)^\beta \, F_2^* \right] u(p') \\
&= \overline{u(p)} \left\{ \gamma_0 \gamma_\alpha^\dagger \gamma_0 \, F_1^* + \frac{\mathrm{i}}{2M} \gamma_0 \sigma_{\alpha\beta}^\dagger \gamma_0 \, (p-p')^\beta \, F_2^* \right\} u(p'),
\end{aligned}$$

where we have inserted $(\gamma_0)^2 = 1$ between $u^\dagger(p)$ and the square brackets and have interchanged p and p' in the second term. We know from (1.79b) that $\gamma_0 \gamma_\alpha^\dagger \gamma_0 = \gamma_\alpha$. Using the definition (2.45) one sees that also $\gamma_0 \sigma_{\alpha\beta}^\dagger \gamma_0 = \sigma_{\alpha\beta}$. As (2.48a) must equal (2.48b) we conclude that the form factors F_1 and F_2 are real:

$$F_1^*(q^2) = F_1(q^2), \quad F_2^*(q^2) = F_2(q^2). \tag{2.49}$$

We add a few comments on these results: The form factor F_2 has actually been defined such as to make it real by the choice of the factor i in front of the second term of (2.46). Without this factor F_2 would have come out pure imaginary. Similarly, the factor $1/2M$ is a matter of convention, chosen so as to give $F_2(q^2)$ the same dimension as $F_1(q^2)$. In applying the divergence condition (2.44) we have used the fact that the two spinors belong to the same mass. If the external fermions have different masses the relations following from current conservation look different. Similarly, if the electromagnetic current is taken between two *different* particles, hermiticity does not suffice to derive reality properties of form factors. However, if the interactions are invariant under time reversal, the combination of hermiticity and time reversal invariance implies again reality conditions for the form factors. Examples of this will be met below in the context of weak interactions.

2.4.2 Derivation of Cross Section

The physical interpretation of the form factors F_1 and F_2 is discussed below. For the moment, we note that $F_1(q^2 = 0) = 1$ is the charge of the particle in units of $|e|$, see below. We first turn to the computation of the differential cross section,

$$\mathrm{d}\sigma = \frac{(2\pi)^2\,\delta^{(4)}(p + k - p' - k')}{[2E_k/(2\pi)^3]\;[2E_p/(2\pi)^3]\;|\boldsymbol{v}_{12}|}\;\frac{1}{4}\sum_{\text{spins}}|T_{\text{fi}}|^2\;\frac{d^3k'\mathrm{d}^3p'}{2E_{k'}\,2E_{p'}}. \tag{2.50}$$

T_{fi} is the T-matrix element, to be obtained from Feynman rules for lowest order perturbation theory. $\boldsymbol{v}_{12}$ is the relative velocity of electron and nucleon in the initial state. It is useful to calculate $\mathrm{d}\sigma$ first in the centre-of-mass system and then, in a second step, to write it in a manifestly invariant form from which the cross section in any system of reference can be obtained. In the c.m. system,

$$k = \left(\sqrt{m^2 + q^{*2}}\,;\,\boldsymbol{q}\right),\quad p = \left(\sqrt{M^2 + q^{*2}}\,;-\boldsymbol{q}\right).$$

Introducing the invariant variables *s, t, u* one has

$$s = (p + k)^2 = (p' + k')^2 = m^2 + M^2 + 2(pk) = m^2 + M^2 + 2(p'k'), \tag{2.51a}$$

$$t = (k - k')^2 = (p' - p)^2 = 2\,m^2 - 2(kk') = 2M^2 - 2(pp'), \tag{2.51b}$$

$$\begin{aligned} u &= (k - p')^2 = (p - k')^2 = m^2 + M^2 - 2(p'k) \\ &= m^2 + M^2 - 2(pk') = 2m^2 + 2M^2 - t - s. \end{aligned} \tag{2.51c}$$

In particular, in the c.m. system

$$q^* := |\boldsymbol{q}| = \frac{1}{2\sqrt{s}}\;\sqrt{(s - M^2 - m^2)^2 - 4M^2m^2}, \tag{2.52}$$

$$t = -2q^{*2}(1 - \cos\theta). \tag{2.53}$$

The Møller factor in the denominator of (2.50) is an invariant and can be written as

$$\begin{aligned} E_k\,E_p|\boldsymbol{v}_{12}| &= \sqrt{(pk)^2 - p^2k^2} \\ &= \frac{1}{2}\;\sqrt{(s - M^2 - m^2)^2 - 4M^2m^2} = q^*\,\sqrt{s}. \end{aligned}$$

As we are interested in $\mathrm{d}\sigma/\mathrm{d}\Omega$ or, equivalently, $\mathrm{d}\sigma/\mathrm{d}t$, all other variables in the final state must be integrated over. The integration over $\boldsymbol{p}'$ may be done first, giving $\boldsymbol{p}' = -\boldsymbol{k}' \equiv \boldsymbol{q}'$:

$$\mathrm{d}\sigma = \frac{(2\pi)^{10}}{16q^*\,\sqrt{s}E'_k\,E'_p}\;\frac{1}{4}\sum|T_{\mathrm{fi}}|^2\,\delta^{(1)}\,(W-E_k-E_p)\;q^{*\prime 2}\,\mathrm{d}q^{*\prime}\,\mathrm{d}\Omega,$$

where

$$W := \sqrt{M^2+q^{*\prime 2}}+\sqrt{m^2+q^{*\prime 2}}.$$

$q^{*\prime}$ is the modulus of the three-momentum in the final state. By the remaining δ-function it becomes equal to q^*. This leaves us with the integration over $q^{*\prime}$ or, equivalently, over W, provided we make the replacement

$$\mathrm{d}q^{*\prime} = \frac{\mathrm{d}q^{*'}}{\mathrm{d}W}\mathrm{d}W = \frac{E_{p'}\,E_{k'}}{q^{*\prime}\,W}\,\mathrm{d}W.$$

This gives

$$\frac{\mathrm{d}\sigma}{\mathrm{d}\Omega} = \frac{1}{16s}(2\pi)^{10}\,\frac{1}{4}\sum|T_{\mathrm{fi}}|^2. \tag{2.54}$$

The invariant quantity $\mathrm{d}\sigma/\mathrm{d}t$ is obtained from this by integrating over the azimuth ϕ and by making the replacement

$$\frac{\mathrm{d}\sigma}{\mathrm{d}(\cos\theta)} = \frac{\mathrm{d}t}{\mathrm{d}(\cos\theta)}\frac{\mathrm{d}\sigma}{\mathrm{d}t} = 2q^{*2}\frac{\mathrm{d}\sigma}{\mathrm{d}t}.$$

with the expression (2.52) for q^{*2}, this gives

$$\frac{\mathrm{d}\sigma}{\mathrm{d}t} = \frac{(2\pi)^{11}}{8[(s-M^2-m^2)^2-4M^2m^2]}\,\frac{1}{4}\sum|T_{\mathrm{fi}}|^2. \tag{2.55}$$

The next step is the construction of the T-matrix element and the calculation of the spin summation. The Feynman rules give the R-matrix R_{fi}, which is related to T_{fi} by (B2) of App. B. So we have

$$R_{\mathrm{fi}} = \frac{-\mathrm{i}e^2}{(2\pi)^2}\int \mathrm{d}^4\,\kappa\,\overline{u(k')}\,\gamma_\alpha\,u(k)(\kappa^2+\mathrm{i}\varepsilon)^{-1}\,g^{\alpha\beta}\,\langle p'|j_\beta(0)|p\rangle$$
$$\times(2\pi)^3\,\delta^{(4)}\,(k-\kappa-k')\,\delta^{(4)}\,(p+\kappa-p').$$

The integration over κ, the momentum of the virtual photon, yields $\kappa = k - k' = p' - p$ and leaves us with one δ-function for overall energy-momentum conservation.

Thus

$$T_{\mathrm{fi}} = \frac{-e^2}{(2\pi)^3}\,\overline{u(k')}\,\gamma^\alpha u(k)\,\frac{1}{t}\,\langle p'|j_\alpha(0)|p\rangle.$$

For the actual calculation of the cross section it is useful to rewrite the nucleonic matrix element by means of the Gordon identity

$$\langle p'|j_\alpha(0)|p\rangle = \frac{1}{(2\pi)^3}\,\overline{u(p')}\,\{(F_1+F_2)\,\gamma_\alpha - \frac{1}{2M}(p+p')_\alpha F_2\}\,u(p). \quad (2.46')$$

The spin summations are best carried out by means of the trace techniques of App. C2. Here we have to calculate the expression

$$\begin{aligned}\mathscr{M} :&= \frac{1}{4}\sum_{\text{spins}}\left|\overline{(u(k')\,\gamma^\alpha\,u(k))}\left(\overline{u(p')}\left[\gamma_\alpha(F_1+F_2) - \frac{1}{2M}\,P_\alpha F_2\right]u(p)\right)\right|^2\\ &= \frac{1}{4}\,\mathrm{tr}\{\gamma^\alpha(\not{k}+m)\gamma^\beta\,(\not{k}'+m)\}\mathrm{tr}\left\{\left[(F_1+F_2)\gamma_\alpha - \frac{P_\alpha}{2M}F_2\right](\not{p}+M)\right.\\ &\quad\left.\times\left[(F_1+F_2)\gamma_\beta - \frac{P_\beta}{2M}\,F_2\right](\not{p}'+M)\right\},\end{aligned}$$

where we have set $p+p' = P$. There are basically four expressions to be calculated, namely

$$\begin{aligned}\text{(a)}\quad &\frac{1}{4}\,\mathrm{tr}\,\{\gamma^\alpha(\not{k}+m)\gamma^\beta(\not{k}'+m)\}\,\mathrm{tr}\{\gamma_\alpha(\not{p}+M)\,\gamma_\beta\,(\not{p}'+M)\}\\ &= 8\{2m^2M^2 - M^2(kk') - m^2(pp') + (pk)\,(p'k') + (pk')(p'k)\},\end{aligned}$$

which from (2.51) is equal to

$$\begin{aligned}&= 2\{2(s-M^2-m^2)^2 + 2st + t^2\}.\\ \text{(b)}\quad &\frac{1}{4}\,\mathrm{tr}\{\gamma^\alpha(\not{k}+m)\,\not{P}\,(\not{k}'+m)\}\,\mathrm{tr}\{\gamma_\alpha(\not{p}+M)\,(\not{p}'+M)\}\\ &= 4M\{m^2P^2 + 2(Pk)\,(Pk') - P^2(kk')\}\\ &= 8M\{(s-M^2-m^2)^2 + t(s-m^2)\}.\\ \text{(c)}\quad &\frac{1}{4}\mathrm{tr}\{\not{P}(\not{k}+m)\,\not{P}\,(\not{k}'+m)\}\\ &= m^2P^2 + 2(Pk)\,(Pk') - P^2(kk')\\ &= 2\{(s-M^2-m^2)^2 + t(s-m^2)\}.\\ \text{(d)}\quad &\frac{1}{4}\,\mathrm{tr}\{(\not{p}+M)\,(\not{p}'+M)\} = M^2 + (pp') = 2M^2 - \frac{1}{2}t.\end{aligned}$$

All traces in $\mathscr{M}$ are reducible to these prototypes. We find

$$\begin{aligned}\mathscr{M} &= 4[(s-M^2-m^2)^2+t(s-m^2)]\\ &\times\left[(F_1+F_2)^2-2F_1F_2-F_2^2-\frac{t}{4M^2}F_2^2\right]\\ &+2(t^2+2m^2t)\,(F_1+F_2)^2.\end{aligned}$$

Inserting this into (2.55) and replacing $e^2/4\pi=\alpha$, we finally obtain

$$\begin{aligned}\frac{\mathrm{d}\sigma}{\mathrm{d}t} &= \frac{4\pi\alpha^2}{t^2}\,\frac{(s-M^2-m^2)^2+t(s-m^2)}{(s-M^2-m^2)^2-4M^2m^2}\\ &\times\left\{F_1^2(t)-\frac{t}{4M^2}F_2^2(t)+\frac{t(t+2m^2)}{2[(s-M^2-m^2)^2+t(s-m^2)]}(F_1(t)+F_2(t))^2\right\}.\end{aligned}\tag{2.56}$$

This formula was first derived by Rosenbluth (1950). It applies to the scattering of any charged lepton of mass m from a complex target with spin 1/2. The target structure is contained entirely in the Lorentz scalar functions $F_1(t)$ and $F_2(t)$, the significance of which will become clear below.

As an exercise let us use (2.56) to derive the differential cross section in the laboratory system for electron scattering on the nucleon. The electron energy shall be chosen so large that the electron mass can be neglected. Setting $m=0$, the variables s and t in the laboratory system are

$$\begin{aligned}s &\simeq M^2+2ME,\\ t &\simeq -2EE'(1-\cos\theta)=-2E^2\,\frac{1-\cos\theta}{1+(E/M)(1-\cos\theta)}\end{aligned}$$

From this one obtains

$$\begin{aligned}\frac{t^2}{2[(s-M^2)^2+ts]} &\simeq \frac{-tE^2(1-\cos\theta)}{2M^2E^2(1+\cos\theta)}=-\frac{t}{2M^2}\mathrm{tg}^2(\theta/2),\\ \frac{\mathrm{d}t}{\mathrm{d}(\cos\theta)} &= \frac{2E^2}{(1+(E/M)(1-\cos\theta))^2},\end{aligned}$$

so that

$$\begin{aligned}\left(\frac{\mathrm{d}\sigma}{\mathrm{d}\Omega}\right)_{\mathrm{lab}} &= \left(\frac{\alpha}{2E}\right)^2\frac{\cos^2(\alpha/2)}{\sin^4(\theta/2)}\,\frac{1}{1+2(E/M)\,\sin^2(\theta/2)}\\ &\times\left\{F_1^2(t)-\frac{t}{4M^2}F_2^2(t)-\frac{t}{2M^2}[F_1(t)+F_2(t)]^2\,\mathrm{tg}^2(\theta/2)\right\}.\end{aligned}\tag{2.57}$$

This is the generalization of formula (2.35′) to a target with spin 1/2.

2.4.3 Properties of Form Factors

The form factors $F_1(t)$ and $F_2(t)$ are defined through the covariant decomposition (2.46) of the nucleonic one-particle matrix element of the electromagnetic current operator $j_\alpha(x)$. In this section we work out the physical interpretation of these form factors. For this purpose it is convenient to consider the matrix element (2.46) in the specific frame of reference where the sum of spatial three-momenta of initial and final nucleon states vanishes, i.e. $\boldsymbol{p} + \boldsymbol{p}' = 0$. In this frame the limit of vanishing four-momentum transfer, $q^2 \to 0$, leads us automatically into the rest frame of the particle. It is in the particle's rest frame that we are able to relate F_1 and F_2 to static properties of nucleons.

(i) *Electric form factor* . From (2.46, 2.46′) the charge density (fourth component of $j_\alpha(x)$) is given by

$$\langle \boldsymbol{p}|\, j_0(0)|\, -\boldsymbol{p}\rangle = \frac{1}{(2\pi)^3}\overline{u(\boldsymbol{p})}\left\{(F_1 + F_2)\gamma_0 - \frac{E_p}{M}F_2\right\} u(-\boldsymbol{p}).$$

Inserting the explicit form of the spinors (1.90) in the standard representation, one finds

$$\begin{aligned}\overline{u(\boldsymbol{p})}\,\gamma_0\, u(-\boldsymbol{p}) &= u^\dagger(\boldsymbol{p})\, u(-\boldsymbol{p}) = 2M,\\ \overline{u(\boldsymbol{p})}\, u(-\boldsymbol{p}) &= 2E_p,\end{aligned}$$

independently of the spin direction. Furthermore, $\boldsymbol{q} = 2\boldsymbol{p}$ and $t = (p' - p)^2 = -4\boldsymbol{p}^2 = -4E_p^2 + 4M^2$. Thus

$$(2\pi)^3\, \langle \boldsymbol{p}|\mathrm{j}_0(0)|\, -\boldsymbol{p}\rangle = 2M(F_1 + F_2) - \frac{2E_p^2}{M}\, F_2 = 2M\left[F_1 + \frac{t}{4M^2}\, F_2\right].$$

On the basis of this result it is natural to define

$$G_\mathrm{E}(t) := F_1(t) + \frac{t}{4M^2}\, F_2(t) \tag{2.58}$$

as the *electric form factor* of the nucleon. It is easy to verify that for the proton

$$F_1^{(\mathrm{p})}(0) = G_\mathrm{E}^{(\mathrm{p})}(0) = 1, \tag{2.59a}$$

which expresses the fact that the proton carries one unit of the positive elementary charge. Indeed, we know that

$$\left\langle p' \left| \int \mathrm{d}^3 x\, j_0(x) \right| p \right\rangle = 1\langle p'|p\rangle = 2E_p\delta(\boldsymbol{p} - \boldsymbol{p}').$$

On the other hand, from the decomposition (2.46), and using translation invariance as in (2.42′),

$$\begin{aligned}\int \mathrm{d}^3 x \langle p' \mid j_0(x) \mid p\rangle &= (2\pi)^3\, \delta(\boldsymbol{p}-\boldsymbol{p}')\ \langle p'|j_0(0)|p\rangle \\ &= \delta(\boldsymbol{p}-\boldsymbol{p}')\ F_1^{(p)}(0) u^\dagger(\boldsymbol{p})\, u(\boldsymbol{p}) = 2E_p F_1^{(p)} \delta(\boldsymbol{p}-\boldsymbol{p}').\end{aligned}$$

Thus $F_1^{(p)}(0) = 1$.

Similarly for the neutron

$$F_1^{(\mathrm{n})}(0) \;=\; G_\mathrm{E}^{(\mathrm{n})}(0) \;=\; 0. \tag{2.59b}$$

The r.m.s. radii of F_1 and G_E, which are defined by (2.32) are not the same, however. One finds the relationship

$$\langle r^2\rangle_{G_\mathrm{E}} = \langle r^2\rangle_{F_1} + \frac{1}{4M^2} F_2(0). \tag{2.60}$$

Here, $F_2(0)$ is found to be the anomalous magnetic moment below.

(ii) *Magnetic form factor*. We know from Sect. 1.9.2 that the magnetic properties are obtained from matrix elements of the spatial current density, i.e. from

$$\langle \boldsymbol{p}|j^i(0)|-\boldsymbol{p}\rangle = \frac{1}{(2\pi)^3}(F_1+F_2)\overline{u(\boldsymbol{p})}\gamma^i u(-\boldsymbol{p})$$

[where we have used (2.46′)]. With the explicit solutions (1.90) we have

$$\begin{aligned}\overline{u(\boldsymbol{p})}\,\gamma^i\, u(-\boldsymbol{p}) &= u^\dagger(\boldsymbol{p}) \begin{pmatrix} 0 & \sigma^{(i)} \\ \sigma^{(i)} & 0 \end{pmatrix} u(-\boldsymbol{p}) \\ &= \chi^\dagger[-\sigma^{(i)}(\boldsymbol{\sigma}\cdot\boldsymbol{p}) + (\boldsymbol{\sigma}\cdot\boldsymbol{p})\,\sigma^{(i)}]\chi \\ &= -2\varepsilon_{ikl}\, p_k \chi^\dagger \sigma^{(l)}\chi = -\varepsilon_{ikl} q_k \chi^\dagger \sigma^{(l)}\chi \\ \langle \boldsymbol{p}|j^i(0)|-\boldsymbol{p}\rangle &= -\frac{1}{(2\pi)^3}\,(F_1+F_2)\ \varepsilon_{ikl} q_k \chi^\dagger \sigma^{(l)}\chi.\end{aligned}$$

Comparing this to the formulae in Sect. 1.9.2 we see that the combination

$$G_\mathrm{M}(t) := F_1(t) + F_2(t) \tag{2.61}$$

may be interpreted as the *magnetic form factor*.[9] In particular, $G_\mathrm{M}(0)$ is equal to the total magnetic moment of the particle; $F_1(0)$ gives the "normal" magnetic moment; $F_2(0)$ the "anomalous" magnetic moment. In the case of proton and neutron,

[9] $G_\mathrm{E}(t)$ and $G_\mathrm{M}(t)$ are also called Sachs form factors.

$$F_1^{(\mathrm{p})}(0) = 1, \quad F_2^{(\mathrm{p})}(0) \equiv \mu_{\mathrm{an}}^{\mathrm{p}} = 1.792847351(28), \tag{2.62a}$$

$$F_1^{(\mathrm{n})}(0) = 0, \quad F_2^{(\mathrm{n})}(0) \equiv \mu_{\mathrm{an}}^{\mathrm{n}} = -1.9130427(5) \tag{2.62b}$$

When rewritten in terms of the Sachs form factors (2.58) and (2.61) the differential cross section (2.57) reads

$$\left(\frac{\mathrm{d}\sigma}{\mathrm{d}\Omega}\right)_{\mathrm{lab}} = \left(\frac{\alpha}{2E}\right)^2 \frac{\cos^2(\theta/2)}{\sin^4(\theta/2)} \frac{1}{1 + 2(E/M)\sin^2(\theta/2)} \times \left\{ \frac{1}{1 - t/4M^2} G_{\mathrm{E}}^2(t) - \frac{t}{4M^2} \left[\frac{1}{1 - t/4M^2} + 2\mathrm{tg}^2(\theta/2) \right] G_{\mathrm{M}}^2(t) \right\}. \tag{2.57′}$$

Therefore, if one plots the quantity in curly brackets at fixed t and multiplied by $\mathrm{ctg}^2(\theta/2)$, as a function of $\mathrm{ctg}^2(\theta/2)$, the data must fall onto a straight line with slope and intercept, respectively, as follows

$$\frac{G_{\mathrm{E}}^2 + \tau G_{\mathrm{M}}^2}{1 + \tau} \quad \text{and} \quad 2\tau G_{\mathrm{M}}^2$$

where $\tau = -t/4M^2$.

2.4.4 *Isospin Analysis of Nucleon Form Factors*

Isospin invariance is an approximate symmetry of strong interactions. It is a spectrum symmetry in the sense that strongly interacting particles can be classified in mass degenerate multiplets of the isospin group SU(2). While the strong interactions are invariant under isospin transformations, the electromagnetic interactions are not. That is, the strong interactions transform like scalars under isospin transformations, the electromagnetic interaction $j^\alpha A_\alpha$ does not. Nevertheless, it may be expanded in terms of multipole operators in isospin space, viz.

$$j_\alpha(x) = j_\alpha^{(0)}(x) + j_\alpha^{(1)}(x) + \cdots, \tag{2.63}$$

where $j_\alpha^{(0)}$ denotes an isoscalar operator, $j_\alpha^{(1)}$ denotes the third component of an isovector operator. There are good indications that the electromagnetic current operator contains only isoscalar and isovector operators, i.e. that the expansion (2.63) ends with the second term, but a priori this is not known. The two terms on the right-hand side carry the quantum numbers of the vector mesons ω, ϕ and ρ, respectively, as summarized in Table 2.1.

In the case of nucleons it is easy to isolate the isoscalar and isovector parts of the nucleon form factors. Proton and neutron form a doublet of isospin, the proton is assigned $I_3 = +1/2$, the neutron $I_3 = -1/2$. Let $O_{\mu=0}^{(\kappa)}$ be any tensor

Table 2.1 Properties of electromagnetic current.

	Isospin		Spin Parity J^π	Charge conjugation C	G-Parity G	Analogue vector meson states
	I	I_3				
$j_\alpha^{(0)}(x)$	0	0	$\left\{\begin{matrix}0^+\\1^-\end{matrix}\right\}$	$-$	$-$	$\omega(782)$
						$\phi(1020)$
$J_\alpha^{(1)}(x)$	1	0	$\left\{\begin{matrix}0^+\\1^-\end{matrix}\right\}$	$-$	$+$	$\rho(770)$

operator with isospin κ and three component $\mu = 0$ in isospin, having nonvanishing matrix elements between one nucleon states. Then from the Wigner–Eckart theorem, we have

$$\langle \frac{1}{2} I_3 | O_\mu^{(\kappa)} | \frac{1}{2} I_3 \rangle = (-)^{1/2-I_3} \begin{pmatrix} \frac{1}{2} & \kappa & \frac{1}{2} \\ -I_3 & 0 & I_3 \end{pmatrix} \left(\frac{1}{2} \parallel O^{(\kappa)} \parallel \frac{1}{2} \right), \tag{2.64}$$

where $\left(\frac{1}{2} \left\| O^{(\kappa)} \right\| \frac{1}{2}\right)$ denotes the reduced matrix element. The first two $3j$-symbols with $\mu = 0$ are given by [EDM57, DST63]

$$\begin{pmatrix} \frac{1}{2} & 0 & \frac{1}{2} \\ -I_3 & 0 & I_3 \end{pmatrix} = \frac{(-)^{1/2-I_3}}{\sqrt{2}} \begin{pmatrix} \frac{1}{2} & 1 & \frac{1}{2} \\ -I_3 & 0 & I_3 \end{pmatrix} = \sqrt{1/6}.$$

All other such symbols for $\kappa \geq 2$ vanish because the triangle rule is not fulfilled. Thus

$$\left\langle \frac{1}{2} I_3 \right| \sum_\kappa O_0^{(\kappa)} \left| \frac{1}{2} I_3 \right\rangle = \frac{1}{\sqrt{2}} \left(\frac{1}{2} || O^{(0)} || \frac{1}{2} \right) + (-)^{1/2-I_3} \sqrt{\frac{1}{6}} \left(\frac{1}{2} || O^{(1)} || \frac{1}{2} \right). \tag{2.65}$$

As a consequence, we see that the isoscalar may be isolated by taking the sum of matrix elements (2.65) over I_3, while the isovector is isolated by taking the difference. This leads to the following definitions of isoscalar and isovector nucleon form factors

$$F_i^{(s)} = \frac{1}{2}(F_i^{(\mathrm{p})} + F_i^{(\mathrm{n})}) \tag{2.66a}$$

$$(i = 1, 2).$$

$$F_i^{(\upsilon)} = \frac{1}{2}(F_i^{(\mathrm{p})} - F_i^{(\mathrm{n})}) \tag{2.66b}$$

Analogous definitions may be introduced for the electric and magnetic form factors (2.58) and (2.61).

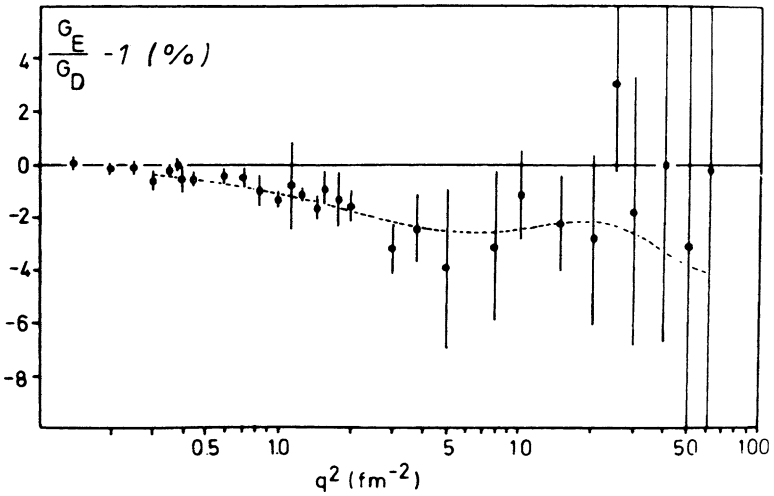

Fig. 2.2 The ratio $G_{\mathrm{E}}^{\mathrm{p}}/G_{\mathrm{D}}$ in percentage deviation from 1, versus q^2. Figure taken from Simon et al. (1980)

It is customary to show the measured electric form factor $G_{\mathrm{E}}^{\mathrm{p}}$ of the proton for low momentum transfers, divided by the so-called *dipole* fit:

$$G_{\mathrm{D}}(q^2) := \frac{1}{(1 + q^2/q_0^2)^2} \text{ with } \quad q_0^2 = 18.23\,\mathrm{fm}^{-2}. \tag{2.67}$$

This dipole dependence of the form factors $G_{\mathrm{E}}^{\mathrm{p}}(q^2)$ and $G_{\mathrm{M}}^{\mathrm{p}}(q^2)/\mu^{\mathrm{p}}$ on q^2 is only of historical interest insofar as early data seemed to be in good agreement with this simple ansatz. Better, empirical fits, useful for theoretical analyses, are found in the literature (Borkowski et al. 1976). Nevertheless, it is customary to plot the data in terms of this formula. From the data one deduces the following value for the r.m.s radius of the proton (Simon et al. 1980). As an example we quote:

$$\left\langle r_E^2 \right\rangle_P^{1/2} = (0.862 \pm 0.012)\,\mathrm{fm}.$$

Figures 2.2, 2.3 show the electric and magnetic form factors $G_{\mathrm{E}}^{\mathrm{p}}$ and $G_{\mathrm{E}}^{\mathrm{p}}/\mu^{\mathrm{p}}$ of the proton, in units of G_{D}, (2.67), and in the form of percent deviations from that ansatz. Figure 2.4, finally, shows data for the electron-proton elastic cross section, again in units of the dipole fit, i.e. in units of the cross section (2.57′) with

$$G_{\mathrm{E}}^{\mathrm{p}} = G_{\mathrm{M}}^{\mathrm{p}}/\mu^{\mathrm{p}} \equiv G_{\mathrm{D}}(q^2).$$

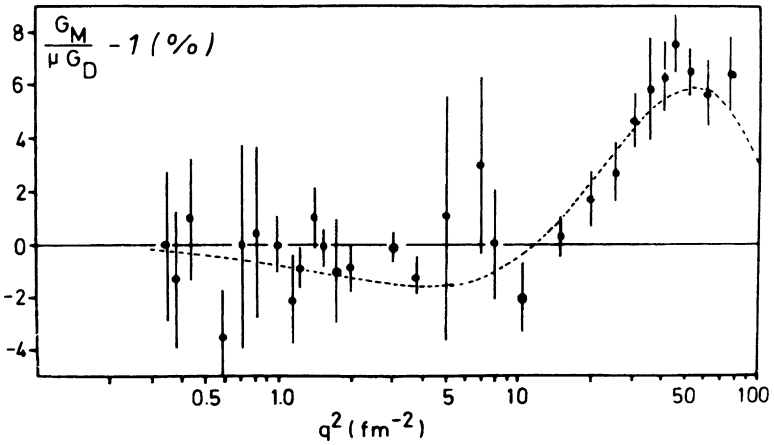

Fig. 2.3 The ratio $G_{\mathrm{M}}^{\mathrm{P}}/\mu^{\mathrm{P}}G_{\mathrm{D}}$ versus q^2. Figure taken from Simon et al. (1980)

2.5 *Elastic and Inelastic Electron Scattering from Nuclei

In Sects. 2.2, 2.4 we have derived the cross section for elastic scattering of electrons from spin zero and spin 1/2 targets. These formulae hold for any kind of target, composite or "elementary". The internal structure of the target is hidden in the Lorentz invariant form factors whose definition is based only on Lorentz covariance and current conservation.

We now extend these results to elastic scattering from nuclei of arbitrary spin, as well as to inelastic scattering to discrete nuclear excited states. As we have seen, *elastic* scattering from a target with spin zero depends on one single form factor, the electric form factor. In case of a target with spin 1/2 there are two form factors: the electric and the magnetic dipole form factor. For a target with spin $J = 1$ or higher there are, in addition, electric quadrupole form factors or more generally, form factors of multipolarity λ up to $\lambda_{\max} = 2J$. This is a consequence of conservation of angular momentum which requires that nuclear initial and final state spins form a triangle with λ, the multipolarity of the form factor, viz. $\boldsymbol{J}_{\mathrm{i}} + \boldsymbol{\lambda} + \boldsymbol{J}_{\mathrm{f}} = 0$. In addition, conservation of parity selects the kind of multipoles that can contribute to elastic scattering, e.g. electric monopole, magnetic dipole, electric quadrupole.

In studying inelastic scattering to discrete excited states of the nucleus we encounter a very similar situation. The initial state with spin and parity $J_{\mathrm{i}}^{\pi_{\mathrm{i}}}$ (this is generally the nuclear ground state), goes over into a final state with spin and parity $J_{\mathrm{f}}^{\pi_{\mathrm{f}}}$ through excitation by means of multipole fields with multi-polarity λ and π_λ such that

$$\boldsymbol{J}_{\mathrm{i}} + \boldsymbol{\lambda} + \boldsymbol{J}_{\mathrm{f}} = 0, \qquad \pi_{\mathrm{i}}\pi_\lambda = \pi_{\mathrm{f}}.$$

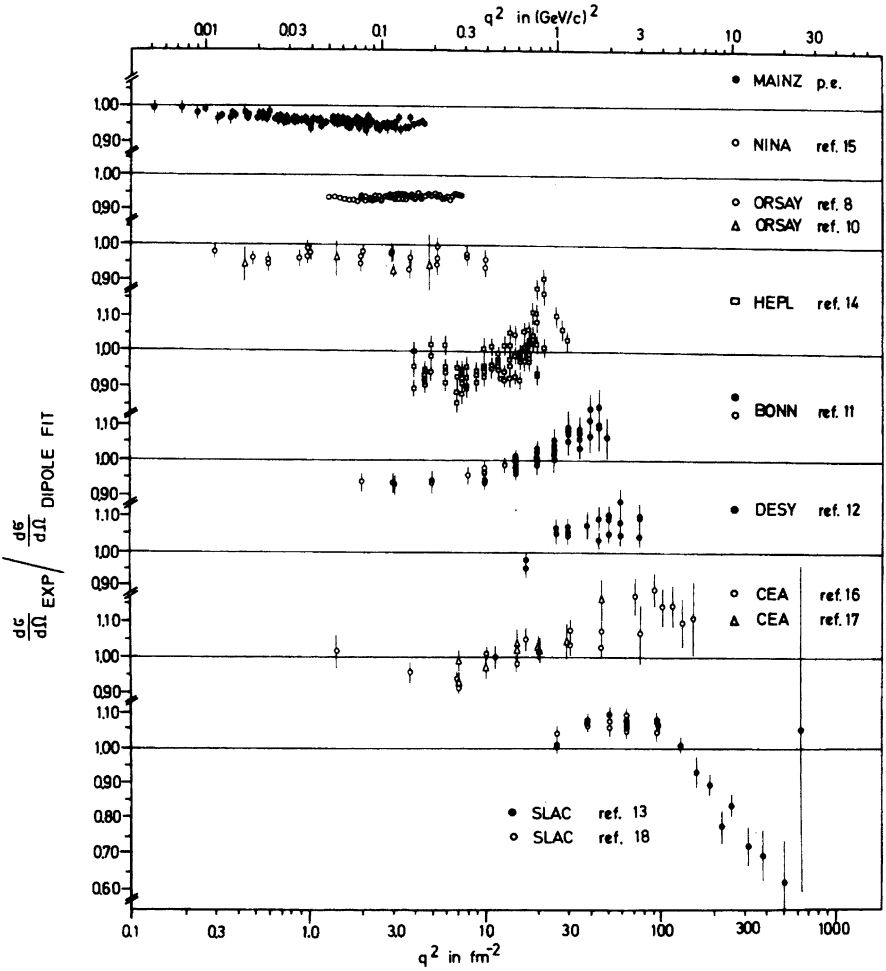

Fig. 2.4 Ratio of electron–proton scattering cross sections to the dipole formula, as measured in various laboratories, versus q^2. Compilation taken from Borkowski et al. (1975)

Because of the close similarity of these two situations we treat them within the same formalism. Everything that follows for inelastic scattering below can always be specialized to elastic scattering by taking $J_\mathrm{f} = J_\mathrm{i}$ and $\pi_\mathrm{f} = \pi_\mathrm{i}$.

In a first step we calculate the cross sections as before, using the Born approximation in describing initial and final states of the electron. This approximation is very good for the proton, $Z = 1$. Depending on the accuracy of experiments one wishes to analyze, the Born approximation may still be acceptable for light nuclei, up to about $Z \cong 10$. With increasing charge number of the nucleus it becomes less reliable; for heavy nuclei such as lead ($Z = 82$) it fails badly, as it neglects the strong distortion of initial and final electron waves due to the nuclear

Coulomb field. In this case a complete partial wave analysis on the basis of exact eigenstates in the nuclear electric field must be worked out. Nevertheless, it can be seen that the cross sections calculated in the Born approximation contain all relevant qualitative physical features of the scattering process. The exact cross sections, obtained from partial wave analysis, *differ quantitatively* from the Born cross sections but their structure carries the same (qualitative) physical information. Thus, Coulomb distortion is a problem of purely technical nature, and we leave its discussion to a later section.

2.5.1 Multipole Fields

The theory of electron scattering from nuclei leading to final states with definite spin and parity is based on an expansion of the virtual photon interaction in terms of multipole fields. In this subsection we collect a few results and formulae which are needed in the sequel [ROS55, JAC75]: We start from Helmholtz' differential equation for vector fields on $\mathbb{R}^3$,

$$(\nabla^2 + k^2)\boldsymbol{B}(\boldsymbol{r}) = 0. \tag{2.68}$$

This equation follows from the wave equation for any field $\boldsymbol{B}(\boldsymbol{r},\ t)$ with harmonic time dependence,

$$\boldsymbol{B}(\boldsymbol{r}, t) = \mathrm{e}^{\mathrm{i}\omega t}\boldsymbol{B}(r).$$

$\hbar\omega$ is the energy, $\hbar k$ the momentum, k the wave number of this field, and $\hbar\omega = \hbar ck$ or, in natural units, $\omega = k$. $\boldsymbol{B}(\boldsymbol{r})$ can be expanded in terms of a complete set of solutions of the Helmholtz equation with definite angular momentum and definite parity. These basic solutions are called *multipole fields*. They form a complete and orthogonal set of vector functions in the radial variable r and on the unit sphere.

Let us begin with the definition of *vector spherical harmonics*. Let ζ_m ($m = +1,\ 0,\ -1$) be spherical unit vectors, defined in terms of Cartesian unit vectors by

$$\begin{aligned}
\zeta_0 &= e_3, \\
\zeta_1 &= -\frac{1}{\sqrt{2}}(e_1 + \mathrm{i}e_2), \\
\zeta_{-1} &= \frac{1}{\sqrt{2}}(e_1 - \mathrm{i}e_2).
\end{aligned} \tag{2.69}$$

These vectors obey the symmetry relation

$$\zeta_m^* = (-)^m\zeta_{-m} \tag{2.70a}$$

and the orthogonality relation

$$\zeta_m^* \zeta_m = \delta_{mm}. \tag{2.70b}$$

As defined in (2.69) the ζ_m transform as a spherical tensor of rank one under rotations. The vector spherical harmonics are then defined as follows:

$$\boldsymbol{T}_{Jl M} := \sum_{m_l m_s} (l m_l, 1 m_s | JM) Y_{l m_l} \zeta_{m_s}, \tag{2.71}$$

where $(lm_l, 1m_s|JM)$ denotes the Clebsch–Gordan coefficients that couple the angular momenta l and 1 to $J = l + 1,\ l, l - 1$. By construction, T_{JlM} transform under rotations with the unitary rotation matrices $D^{(J)*}_{MM'}(\phi,\ \theta,\ \psi)$, i.e. they are spherical tensors of rank J. In addition they have vector character due to the fact that they contain the spherical unit vectors ζ. The m-th spherical component is given by

$$\begin{aligned}(\boldsymbol{T}_{Jl M})_m &\equiv (\boldsymbol{T}_{Jl M} \cdot \zeta_m) \\ &= (-)^m (l M + m, 1 - m | JM) Y_{l M+m}.\end{aligned}$$

The index l indicates the behaviour of the $\boldsymbol{T}_{JlM}$ under the parity operation. From their definition (2.71) one sees that under space reflection

$$\boldsymbol{T}_{Jl M}(\pi - \theta, \varphi + \pi) = (-)^l \boldsymbol{T}_{Jl M}(\theta, \varphi). \tag{2.72}$$

It is easy to verify the orthogonality property

$$\int \mathrm{d}\Omega (\boldsymbol{T}^*_{J'l'M'} \boldsymbol{T}_{Jl M}) = \delta_{JJ'} \delta_{ll'} \delta_{MM'}, \tag{2.73}$$

which follows from the orthogonality of the ordinary spherical harmonics and of the vectors ζ, as well as from some known properties of Clebsch-Gordan coefficients. Finally, we note that the vector harmonics also form a *complete* set of vector-like functions on the unit sphere. (The completeness follows from completeness of spherical harmonics). Some special cases are

$$\begin{aligned}\boldsymbol{T}_{10M} &= \frac{1}{\sqrt{4\pi}} \zeta_M, \\ \boldsymbol{T}_{10M} &= -\frac{1}{\sqrt{4\pi}} \frac{\boldsymbol{r}}{|\boldsymbol{r}|}.\end{aligned}$$

Returning to the Helmholtz equation (2.68), we now construct solutions with definite angular momentum and definite parity. These have the form

$$\boldsymbol{B}_{Jl M}(\boldsymbol{r}) = f_l(r) \boldsymbol{T}_{Jl M}(\theta, \varphi).$$

Inserting this ansatz into (2.68) we are led to a differential equation for the function $f_l(r)$ alone which reads

$$\left\{\frac{1}{r^2}\frac{\mathrm{d}}{\mathrm{d}r}\left(r^2\frac{\mathrm{d}}{\mathrm{d}r}\right)+k^2-\frac{l(l+1)}{r^2}\right\}f_l(r)=0,$$

or, with $z=kr$,

$$\left(\frac{\mathrm{d}^2}{\mathrm{d}z^2}+\frac{2}{z}\frac{\mathrm{d}}{\mathrm{d}z}+1-\frac{l(l+1)}{z^2}\right)f_l(z)=0. \tag{2.74}$$

This equation is well-known in the theory of Bessel functions. We choose the following fundamental system of solutions,

$$\begin{aligned} f_l^{\mathrm{I}}(r) &= j_l(kr) \qquad \text{spherical Bessel function,}\\ f_l^{\mathrm{II}}(r) &= h_l^{(1)}(kr) \qquad \text{spherical Hankel function of first kind}\\ &= j_l(kr)+\mathrm{i}n_l(kr) \end{aligned} \tag{2.75}$$

[$n_l(kr)$ is a spherical Neumann function]. This specific set is chosen in view of the physical boundary conditions that we require for the multipole fields: f_l^{I} is the solution regular at the origin $r=0$, whilst f_l^{II} describes asymptotically outgoing spherical waves,[10]

$$h_l^{(1)}(x)\underset{x\to\infty}{\sim}\frac{1}{x}\exp\left\{\mathrm{i}(x-(l+1))\frac{\pi}{2}\right\}. \tag{2.76}$$

Finally, the functions f_l satisfy the completeness relation

$$\int_0^\infty f_l^*(k'r)\,f_l(kr)r^2\mathrm{d}r=\frac{\pi}{2k^2}\delta(k-k'). \tag{2.77}$$

Equipped with this knowledge we can now define a set of *multipole fields*

(i) *magnetic multipole fields*

$$\boldsymbol{A}_{lm}(\mathrm{M}):=f_l(kr)\boldsymbol{T}_{j=l\,l\,m}; \tag{2.78}$$

(ii) *electric multipole fields*

[10]These and further properties of spherical Bessel and Hankel functions can be found in [ABS65] and in other monographs on special functions.

$$\boldsymbol{A}_{lm}(\mathrm{E}) = -\sqrt{\frac{l}{2l+1}}\, f_{l+1}(kr)\boldsymbol{T}_{ll+1m} + \sqrt{\frac{l+1}{2l+1}}\, f_{l-1}(kr)\boldsymbol{T}_{ll-1m}; \quad (2.79)$$

(iii) *longitudinal multipole fields*

$$\boldsymbol{A}_{lm}(\mathrm{L}) := \sqrt{\frac{l+1}{2l+1}}\, f_{l+1}(kr)\boldsymbol{T}_{ll+1m} + \sqrt{\frac{l}{2l+1}}\, f_{l-1}(kr)\boldsymbol{T}_{ll-1m}. \quad (2.80)$$

The properties of these fields, as well as the reason for the nomenclature, are discussed extensively in the literature on multipole fields [ROS55, JAC75]. In particular, differential properties of them can best be discussed by means of the techniques of angular momentum algebra for which we refer to standard monographs [FAR59, EDM57, ROS57]. Especially useful is the "gradient formula" which reads

$$\nabla f(r)Y_{lm} = -\sqrt{\frac{l+1}{2l+1}}\left(\frac{\mathrm{d}f}{\mathrm{d}r} - l\frac{f}{r}\right)\boldsymbol{T}_{ll+1m} + \sqrt{\frac{l}{2l+1}}\left(\frac{\mathrm{d}f}{\mathrm{d}r} + \frac{l+1}{r}f\right)\boldsymbol{T}_{ll-1m}. \quad (2.81)$$

By means of these techniques one shows that *magnetic* and *electric* multipole fields are divergence free

$$\nabla \cdot \boldsymbol{A}_{lm}(\tau) = 0, \ \tau = \mathrm{E}, M. \quad (2.82)$$

Both potentials vanish for $l = 0$. This is evident in the case of (2.79); in the case of (2.78) it follows from (2.71) since $(00,\ 1\,\mathrm{m}|00)$ vanishes. Thus, electric and magnetic multipole fields are transverse, i.e. fulfill (2.82), and may be used to describe photon states of definite angular momentum and parity. According to (2.72) their parities are $(-)^l$ and $(-)^{l+1}$, respectively. However, as the interaction with matter always involves the product of such vector fields with the current operator which is itself odd under parity, the rules for parity change in electromagnetic transitions are

$(-)^{l+1}$ in magnetic (Ml) transitions,
$(-)^l$ in electric (El) transitions.

The longitudinal fields (2.80) are not divergenceless (hence their name), and they exist also for $l = 0$. Thus, while there are no transverse monopole fields, a longitudinal field can carry total angular momentum zero.

On the basis of the orthogonality and completeness relations (2.73) and (2.77) one shows easily that the multipole fields fulfill the orthogonality relations

$$\int_0^\infty r^2 \mathrm{d}r \int \mathrm{d}\Omega \boldsymbol{A}^*_{l'm'}(\boldsymbol{r},\tau')\boldsymbol{A}_{lm}(\boldsymbol{r},\tau) = \frac{\pi}{2k^2}\delta(k-k')\delta_{\tau\tau'}\delta_{ll'}\delta_{mm'}. \quad (2.83)$$

The importance of these results lies in the fact that a given vector field $\boldsymbol{F}(\boldsymbol{r})$ which is sufficiently regular, can be expanded in terms of orthogonal multipole fields whose

parity and angular momentum properties are simple. Whenever matrix elements of $\boldsymbol{F}$ between states of definite angular momentum and parity are to be calculated, only one or a few terms of the multipole expansion give nonvanishing contributions.

Finally, using the techniques of angular momentum algebra, one can show that the multipole fields can also be written in terms of the orbital angular momentum operator applied to spherical harmonics, in terms of curl and gradient of such functions. This provides equivalent representations that are sometimes useful.

$$\boldsymbol{A}_{lm}(\mathrm{M}) = f_l(kr)\frac{1}{\sqrt{l(l+1)}}\boldsymbol{l}Y_{lm}, \tag{2.78′}$$

$$\begin{aligned}\boldsymbol{A}_{lm}(\mathrm{E}) &= -\frac{\mathrm{i}}{k}\nabla\times(f_l(kr)\boldsymbol{T}_{llm}) \\ &= -\frac{\mathrm{i}}{k\sqrt{l(l+1)}}\nabla\times\boldsymbol{l}(f_l(kr)Y_{lm}),\end{aligned} \tag{2.79′}$$

$$\boldsymbol{A}_{lm}(\mathrm{L}) = \frac{1}{k}\nabla(f_l(kr)Y_{lm}). \tag{2.80′}$$

The notation (2.78–2.80) is more useful in calculating matrix elements between states of good angular momentum and parity because one can then make use of the Wigner–Eckart theorem and all the tricks of angular momentum algebra. The representation (2.78′–2.80′) on the other hand, is very useful if one wants to use identities of vector calculus in order to transform interaction terms to a more convenient form.

2.5.2 *Theory of Electron Scattering*

There are several ways of deriving the Hamiltonian that describes the interaction of (arbitrarily relativistic) electrons with a static target.

(i) One may analyze the scattering process in a semi-classical treatment, starting from a retarded interaction between two given charge and current densities.

$$H_{\mathrm{ret}} = \int \mathrm{d}^3r_{\mathrm{n}} \int \mathrm{d}^3r_{\mathrm{e}} \frac{\mathrm{e}^{\mathrm{i}k|\boldsymbol{r}_{\mathrm{n}}-\boldsymbol{r}_{\mathrm{e}}|}}{|\boldsymbol{r}_{\mathrm{n}}-\boldsymbol{r}_{\mathrm{e}}|}\left\{\rho_{\mathrm{n}}(\boldsymbol{r}_{\mathrm{n}})\rho_{\mathrm{e}}(\boldsymbol{r}_{\mathrm{e}}) - \boldsymbol{j}_{\mathrm{n}}(\boldsymbol{r}_{\mathrm{n}})\boldsymbol{j}_{\mathrm{e}}(\boldsymbol{r}_{\mathrm{e}})\right\}. \tag{2.84}$$

One then expands the retarded Green function that appears in (2.84) in terms of transverse and longitudinal multipole fields. The procedure is conceptually simple but technically somewhat involved and we refer to the literature for details [ROS61] (Scheck 1966).

(ii) Alternatively, one can calculate the interaction in the framework of quantum electrodynamics, formulated in the Coulomb gauge. The interaction is then given by the *instantaneous* electrostatic Coulomb interaction plus the terms

arising from the exchange of virtual but still transverse photons between the electron and the target [HEI63, SAK84]. In this case, instead of using plane waves it is appropriate to expand and quantize the transverse photon field in terms of the magnetic and electric multipole fields (2.78, 2.79).

In either case the scattering matrix element is found to be

$$\begin{aligned}
&\langle \mathrm{f}; k' | H_{\mathrm{int}} | \mathrm{i}; k \rangle \\
&= \left\langle \mathrm{f}, k' \left| \sum_{l=1}^{\infty} \sum_{m=-l}^{+l} \frac{4\pi \mathrm{i}}{l(l+1)} \int \mathrm{d}^3 r_{\mathrm{n}} \int \mathrm{d}^3 r_{\mathrm{e}} \right.\right. \\
&\quad \times \left\{ \frac{1}{k} \left[\boldsymbol{j}_n \cdot \nabla \times \boldsymbol{l} \begin{pmatrix} j_l(kr_<) \\ h_l^{(1)}(kr_>) \end{pmatrix} Y_{lm}^*(\hat{\boldsymbol{r}}_{\mathrm{n}}) \right) \right] \left[\boldsymbol{j}_{\mathrm{e}} \cdot \nabla \times \boldsymbol{l} \begin{pmatrix} h_l^{(1)}(kr_>) \\ j_l(kr_<) \end{pmatrix} Y_{lm}(\hat{\boldsymbol{r}}_{\mathrm{e}}) \right) \right] \\
&\quad + k \left[\boldsymbol{j}_n \cdot \boldsymbol{l} \begin{pmatrix} j_l(kr_<) \\ h_l^{(1)}(kr_>) \end{pmatrix} Y_{lm}^*(\hat{\boldsymbol{r}}_n) \right) \right] \left[\boldsymbol{j}_e \cdot \boldsymbol{l} \begin{pmatrix} h_l^{(1)}(kr_>) \\ j_l(kr_<) \end{pmatrix} Y_{lm}(\hat{\boldsymbol{r}}_{\mathrm{e}}) \right) \right] \\
&\quad \left. + \int \mathrm{d}^3 r_n \int \mathrm{d}^3 r_e \frac{1}{r_>} \rho_n(\boldsymbol{r}_n) \rho_{\mathrm{e}}(\boldsymbol{r}_{\mathrm{e}}) \right| \mathrm{i}, k \Big\rangle . \qquad (2.85)
\end{aligned}$$

In this expression i and f denote initial and final state of the target, respectively; for example, i stands for initial total momentum p of the target and for all other target quantum numbers such as angular momentum, parity and any other internal quantum numbers as there may be. The notation $r_<$ and $r_>$ serves as a shorthand for the requirement that

$$\begin{aligned}
&\text{if } r_{\mathrm{e}} > r_{\mathrm{n}}, \quad \text{the combination } j_l(kr_{\mathrm{n}}) h_l^{(1)}(kr_{\mathrm{e}}), \quad \text{and} \\
&\text{if } r_{\mathrm{e}} > r_{\mathrm{n}}, \quad \text{the combination } h_l^{(1)}(kr_{\mathrm{n}}) j_l(kr_{\mathrm{e}})
\end{aligned}$$

must be taken in the first two terms on the r.h.s. of (2.85). This reflects the correct boundary conditions which are built into (2.85): It is always the smaller of the two radial variables that is to be inserted into j_l, the function regular at the origin, whilst the larger of the two is to be taken in $h_l^{(1)}$, the function that describes outgoing spherical waves.

Evidently, if we wish to explore the internal structure of the target, we have to choose the momentum transfer and, therefore, the electron energy high enough so that the electron penetrates sizeably into the target. In this case the integrations in (2.85) are entangled in a nontrivial way. The matrix element does not factor into a target structure function and a leptonic factor. This is unlike Coulomb excitation where penetration is unimportant (and, in fact, often unwanted) and where the lowest order cross section does factor into target and projectile properties.

The expression (2.85) is fairly general. It applies equally well to elastic and inelastic scattering. It holds independently of what basis we choose for the initial and final electron states. If we take plane waves we shall obtain the transition

matrix element in the Born approximation. In this case k is the magnitude of the three-momentum in the centre-of-mass system. If we wish to include the Coulomb distortion in the electronic states, we have to evaluate (2.85) with eigenstates of the electron in the static Coulomb field created by the target. In this case k is the asymptotic wave number determined by the electron energy.

The charge and current densities which appear in (2.85) are still very general. For the electron, we clearly have to set

$$\rho_{\mathrm{e}}(\boldsymbol{r}) = -e\gamma^0\delta(\boldsymbol{r}-\boldsymbol{r}_{\mathrm{e}}) \equiv -e\beta\delta(\boldsymbol{r}-\boldsymbol{r}_{\mathrm{e}}), \tag{2.86a}$$

$$\boldsymbol{j}_{\mathrm{e}}(\boldsymbol{r}) = -e\gamma^0\boldsymbol{\gamma}\delta(\boldsymbol{r}-\boldsymbol{r}_{\mathrm{e}}) \equiv -e\boldsymbol{\alpha}\delta(\boldsymbol{r}-\boldsymbol{r}_{\mathrm{e}}) \tag{2.86b}$$

Concerning the target, however, there are many options. For example, let the target be a nucleus treated in a nonrelativistic scheme. If we know the nuclear wave function in terms of states of individual nucleons then

$$\rho_{\mathrm{n}}(\boldsymbol{r}) = \sum_{i-1}^{A} e_i\delta(\boldsymbol{r}-\boldsymbol{r}_i), \tag{2.87a}$$

$$\boldsymbol{j}_{\mathrm{n}}(\boldsymbol{r}) = \sum_{i=1}^{A}\left[e_i\boldsymbol{v}_i\delta(\boldsymbol{r}-\boldsymbol{r}_i) + \frac{e}{2m}g_s^i(\nabla\times\boldsymbol{s}^i)\delta(\boldsymbol{r}-\boldsymbol{r}_i)\right]. \tag{2.87b}$$

These operators are taken between nonrelativistic nuclear states (e.g. shell model states). If the nucleus is to be described by some set of effective collective coordinates (such as vibrator coordinates in case of collective matter oscillations, or the set of Euler angles in case of rigid rotator motion, etc.) then the densities are semi-classical functions containing the collective coordinates in a way determined by the underlying model.

In the following two sections we present the essential steps of the derivation of cross sections in the Born approximation (Sect. 2.5.3) and including Coulomb distortion (Sect. 2.5.4).

2.5.3 Born Approximation

Before proceeding to the calculation of the matrix element (2.85) in the first Born approximation it is useful to transform the interaction to a more convenient form. The electric part of the interaction [first term on the right-hand side of (2.85)] is transformed by means of a well-known relation for spherical Bessel and Hankel functions [WAT58],

$$j_l(kr_<)h_l^{(1)}(kr_>) = \frac{2k}{\mathrm{i}\pi}\int_0^\infty \mathrm{d}q\,\frac{j_l(qr)\,j_l(qr')}{q^2-k^2} + \frac{1}{\mathrm{i}k}\frac{r_<^l r_>^{-l-1}}{2l+1}. \tag{2.88}$$

Likewise, the magnetic term (second term of eq. (2.85)) is transformed by means of the relation [WAT58]

$$j_l(kr_<)h_l^{(1)}(kr_>) = \frac{2}{\mathrm{i}\pi k}\int_0^\infty \frac{j_l(qr)j_l(qr')}{q^2-k^2}q^2\mathrm{d}q. \tag{2.89}$$

Finally, the electric term that comes from the second term on the right-hand side of (2.88), i.e.

$$\left\langle \mathrm{f};k'\right| \int \mathrm{d}^3r_\mathrm{n}\int \mathrm{d}^3r_\mathrm{e}\ \boldsymbol{j}_\mathrm{n}\cdot\nabla\times\boldsymbol{l}\left(\begin{matrix} r_<^l \\ r_>^{-l-1}\end{matrix} Y_{lm}^*\right)\boldsymbol{j}_\mathrm{e}\cdot\nabla\times\boldsymbol{l}\left(\begin{matrix} r_>^{-l-1} \\ r_<^l\end{matrix} Y_{lm}\right)\left|\mathrm{i};\ k\right\rangle$$

can be further transformed by means of the relation [ROS57]

$$\nabla\times\boldsymbol{l}(r^\alpha Y_{lm}) = \mathrm{i}(l+1)\nabla(r^\alpha Y_{lm}), \qquad \alpha = l, -l-1. \tag{2.90}$$

Partial integration allows to shift the nabla operators onto the current densities so that, eventually, the continuity equations[11]

$$\begin{aligned}\langle \mathrm{f}|\nabla\cdot\boldsymbol{j}_\mathrm{n}|\mathrm{i}\rangle &= -\mathrm{i}k\langle \mathrm{f}|\rho_\mathrm{n}|\mathrm{i}\rangle,\\ \langle k'|\nabla\cdot\boldsymbol{j}_\mathrm{e}|k\rangle &= +\mathrm{i}k\langle k'|\rho_\mathrm{e}|k\rangle\end{aligned}$$

may by used. In this manner we obtain the equivalent expression for the scattering matrix element (2.85):

$$\begin{aligned}&\langle \mathrm{f};k'|\boldsymbol{H}_\mathrm{int}|\mathrm{i};k\rangle\\ &= \Bigg\langle \mathrm{f};k'\Big|\sum_{l=1}^\infty\sum_{m=-l}^{+l}\frac{8}{l(l+1)}\int\mathrm{d}^3r_\mathrm{n}\int\mathrm{d}^3r_\mathrm{e}\int_0^\infty\frac{\mathrm{d}q'}{q'^2-k^2}\\ &\quad\times\{\boldsymbol{j}_\mathrm{n}\cdot\nabla\times\boldsymbol{l}(j_l(q'r_\mathrm{n})Y_{lm}^*(\boldsymbol{r}))\ \boldsymbol{j}_\mathrm{e}\cdot\nabla\times\boldsymbol{l}(j_l(q'r_\mathrm{e})Y_{lm}(\hat{\boldsymbol{r}}_\mathrm{e}))\\ &\quad+q'^2\boldsymbol{j}_\mathrm{n}\cdot\boldsymbol{l}(j_l(q'r_\mathrm{n})Y_{lm}^*(\hat{\boldsymbol{r}}_\mathrm{n}))\ \boldsymbol{j}_\mathrm{e}\cdot\boldsymbol{l}(j_l(q'r_\mathrm{e})Y_{lm}(\hat{\boldsymbol{r}}_\mathrm{e}))\}\\ &\quad+\sum_{l=0}^\infty\sum_{m=-l}^{+l}\frac{4\pi}{2l+1}\int\mathrm{d}^3r_\mathrm{n}\int\mathrm{d}^3r_\mathrm{e}\frac{r_<^l}{r_>^{l+1}}Y_{lm}^*(\hat{\boldsymbol{r}}_\mathrm{n})Y_{lm}(\hat{\boldsymbol{r}}_\mathrm{e})\rho_\mathrm{n}(\boldsymbol{r}_\mathrm{n})\rho_\mathrm{e}(\boldsymbol{r}_\mathrm{e})\Big|\mathrm{i};k\Bigg\rangle.\end{aligned} \tag{2.91}$$

In the last term of (2.91) the sum over l runs from zero to infinity; the terms from one to infinity stem from the transformed electric term (see above), whilst the term with $l = 0$ is the monopole term of (2.85). (Note that $Y_{00} = 1/\sqrt{4\pi}$). This last term, summed over *all* l, is nothing but the instantaneous Coulomb interaction

[11] The factor $k = \omega$, the energy variable, should not be confused with the initial electron's four-momentum, see also (2.68).

$$\int \mathrm{d}^3 r_\mathrm{n} \int \mathrm{d}^3 r_\mathrm{e} \frac{1}{|\boldsymbol{r}_\mathrm{n} - \boldsymbol{r}_\mathrm{e}|} \rho_\mathrm{n}(\boldsymbol{r}_\mathrm{n}) \rho_\mathrm{e}(\boldsymbol{r}_\mathrm{e}) \tag{2.92}$$

expanded in a multipole series. Therefore, the first two terms on the right-hand side of (2.91) must represent the contributions stemming from the exchange of transverse virtual photons with momentum q'.

To calculate (2.91) in the Born approximation means taking

$$|k\rangle = u(k)\mathrm{e}^{\mathrm{i}k\cdot r_\mathrm{e}} \text{ and } \quad |k'\rangle = u(k')\mathrm{e}^{\mathrm{i}k'\cdot r_\mathrm{e}}.$$

Inserting this into (2.91) one can then perform the integration over the electron coordinates $\boldsymbol{r}_\mathrm{e}$ and over the (virtual photon) momentum q. These calculations are somewhat lengthy and tedious. We therefore give only one example that shows the technique but do not work out all the details. Take for example the instantaneous interaction term (2.92) and use the relation (cf. exercise 2.4)

$$\frac{1}{|\boldsymbol{r}_\mathrm{n} - \boldsymbol{r}_\mathrm{e}|} = \frac{4\pi}{(2\pi)^3} \int \mathrm{d}^3 q' \frac{\mathrm{e}^{\mathrm{i}q'\cdot(\boldsymbol{r}_\mathrm{n} - \boldsymbol{r}_\mathrm{e})}}{\boldsymbol{q}'^2}. \tag{2.93}$$

Integration over $\boldsymbol{r}_\mathrm{e}$ gives, together with (2.86a),

$$\begin{aligned}
&\langle \mathrm{f}; k' | \int \mathrm{d}^3 r_\mathrm{n} \int \mathrm{d}^3 r_\mathrm{e} \frac{1}{|\boldsymbol{r}_\mathrm{n} - \boldsymbol{r}_\mathrm{e}|} \rho_\mathrm{n}(\boldsymbol{r}_\mathrm{n}) \rho_\mathrm{e}(\boldsymbol{r}_\mathrm{e}) | \mathrm{i}; k \rangle \\
&\quad = -4\pi e u^\dagger(k') u(k) \sum_{l,m} (-)^m \mathrm{i}^l \frac{4\pi}{q^2} Y_{lm}(\hat{\boldsymbol{q}}) \times \int \mathrm{d}^3 r_\mathrm{n} \langle \mathrm{f} | \rho_\mathrm{n}(\boldsymbol{r}_\mathrm{n}) | \mathrm{i} \rangle j_l(q r_\mathrm{n}) Y_{l-m}(\hat{\boldsymbol{r}}_\mathrm{n}),
\end{aligned}$$

where $\boldsymbol{q}$ is the three-momentum transfer, $\boldsymbol{q} = \boldsymbol{k} - \boldsymbol{k}'$ and $q = |\boldsymbol{q}|$. This last equation suggests that one define a multipole form factor of the target

$$M(\mathrm{C}l, m; q) := \frac{(2l+1)!!}{q^l} \int \mathrm{d}^3 r \rho_\mathrm{n}(\boldsymbol{r}) j_l(qr) Y_{lm}(\hat{\boldsymbol{r}}). \tag{2.94}$$

The factor in front of the integral has been chosen such that in the limit $q \to 0$, $M(Cl, m; q)$ goes over into the static l-pole moment of the target charge density.

The transverse electric and magnetic terms in (2.91) are worked out in a similar way. In analogy to (2.94) we are led to define

electric multipole form factors

$$M(\mathrm{E}l, m; q) := \frac{(2l+1)!!}{q^{l+1}(l+1)} \int \mathrm{d}^3 r \boldsymbol{j}_\mathrm{n}(\boldsymbol{r}) \cdot \nabla \times \boldsymbol{l}(j_l(qr) Y_{lm}(\hat{\boldsymbol{r}})), \tag{2.95}$$

and *magnetic multipole form factors*

$$M(\mathrm{M}l, m; q) := -\mathrm{i} \frac{(2l+1)!!}{q^l (l+1)} \int \mathrm{d}^3 r \boldsymbol{j}_\mathrm{n}(\boldsymbol{r}) \cdot \boldsymbol{l}(j_l(qr) Y_{lm}(\hat{\boldsymbol{r}})). \tag{2.96}$$

Here again, the factors have been chosen so that for $qr \ll 1$ the form factors go over into the corresponding transverse electric and magnetic multipole terms which describe the corresponding transition induced by photons [DST63] (in the approximation of long wavelengths).

We are concerned here only with the scattering cross section for unpolarized electrons and we do not discriminate the spin orientation of the electron in the final state. Therefore, we have to calculate the incoherent sum of squared matrix elements over all initial and final spin projections and have to divide by $2(2J+1)$, J being the nuclear spin, in order to account for the average over spin orientations in the initial state. The spin summation in the electronic part is done by means of the trace techniques (see Appendix). This is a straightforward but somewhat lengthy calculation that we do not wish to carry out here as the details can be found in the literature. The result is, in the unpolarized case [UEB71] (De Forest et al. 1966),

$$\frac{\mathrm{d}\sigma}{\mathrm{d}\Omega} = \sum_{l=0}^{\infty} \frac{\mathrm{d}\sigma_{\mathrm{E}l}}{\mathrm{d}\Omega} + \sum_{l=1}^{\infty} \frac{\mathrm{d}\sigma_{\mathrm{M}l}}{d\,\Omega}, \tag{2.97a}$$

where

$$\frac{\mathrm{d}\sigma_{\mathrm{E}l}}{\mathrm{d}\Omega} = \alpha^2 \frac{4\pi(l+1)}{l[(2l+1)!!]^2} \frac{q^{2l}}{E^2} \left\{ \frac{l}{l+1} B(\mathrm{C}l;q) V_{\mathrm{L}}(\theta) + B(\mathrm{E}l;q) V_{\mathrm{T}}(\theta) \right\} \tag{2.97b}$$

$$\frac{\mathrm{d}\sigma_{\mathrm{M}l}}{\mathrm{d}\Omega} = \alpha^2 \frac{4\pi(l+1)}{l[(2l+1)!!]^2} \frac{q^{2l}}{E^2} B(\mathrm{M}l;q) V_{\mathrm{T}}(\theta). \tag{2.97c}$$

Here the functions $V_{\mathrm{L}}(\theta)$ and $V_{\mathrm{T}}(\theta)$ stem from the summation over electron spins. In the high-energy limit ($E \gg m_{\mathrm{e}}$) they are

$$V_{\mathrm{L}}(\theta) \simeq \frac{\cos^2(\theta/2)}{4\sin^4(\theta/2)}, \quad V_{\mathrm{T}}(\theta) \simeq \frac{1+\sin^2(\theta/2)}{8\sin^4(\theta/2)}. \tag{2.98}$$

The functions $B(\tau l;q)$ are the spin-averaged, squared nuclear matrix elements of the operators (2.94)–(2.96), viz.

$$B(\tau l;q) = \sum_{M_{\mathrm{f}},m} |\langle J_{\mathrm{f}} M_{\mathrm{f}}|M(\tau l,m;q)|J_{\mathrm{i}} M_{\mathrm{i}}\rangle|^2, \tag{2.99}$$

with $\tau \equiv \mathrm{C}$ (longitudinal Coulomb multipoles), $\tau \equiv \mathrm{E}$ (electric multipoles), or $\tau \equiv \mathrm{M}$ (magnetic multipoles). As before, q is the magnitude of the three-momentum transfer, while E is the initial electron energy. Strictly speaking, the expressions (2.97) hold in the centre-of-mass frame. However, they may equally well be applied in the laboratory system provided the typical recoil terms of order of E/M, with M the target mass, can be neglected.

We note that there are no interference terms in the cross sections (2.97). The magnetic multipoles do not interfere with the electric and longitudinal multipoles

because they have different parity selection rules. The interference terms between electric and longitudinal multipoles disappear when the spin average is taken. Equations (2.97b,c), which hold for *elastic* as well as for *inelastic* scattering, demonstrate quite clearly the important new feature of electron scattering on an extended target: The scattering cross section depends on the momentum transfer q which can be chosen arbitrarily large. Thus, looking back at (2.94–2.96), the electron probes the *spatial structure* of charge and current densities within the target. In the case of elastic scattering, these are the charge, the electric and magnetic current densities of the ground state. In the case of inelastic scattering, we are probing off-diagonal matrix elements of these operators between the (initial) ground state and some (final) excited states of the target. Because of the close analogy to the elastic case one often calls these matrix elements *transition charge* and *transition current densities*.

The *selection rules* that apply to elastic and inelastic electron scattering derive from angular momentum conservation and from the behaviour of the transition operators and of the nuclear states under parity and time reversal.

Let

$$(J_\mathrm{i},\ \pi_\mathrm{i}) \quad \text{and} \quad (J_\mathrm{f},\ \pi_\mathrm{f})$$

be the spins and parities of initial and final nuclear states, respectively, and let us consider a given multipole operator $M(\tau l)$, (2.94–2.96), taken between these states. Angular momentum conservation implies that $(J_\mathrm{i},\ J_\mathrm{f},\ l)$ form a triangle $|J_\mathrm{i} - J_\mathrm{f}| \leq l \leq J_\mathrm{i} + J_\mathrm{f}$ with $l \geq 1$ for transverse electric and magnetic multipoles. Parity conservation implies that $\pi_\mathrm{i} \cdot \pi_\mathrm{f} = (-)^l$ for longitudinal and transverse electric multipoles, $\pi_\mathrm{i} \cdot \pi_\mathrm{f} = (-)^{l+1}$ for transverse magnetic multipoles. Finally, hermiticity of the electromagnetic current and invariance under time reversal give the additional relation for the nuclear reduced matrix element

$$(J_\mathrm{i}||M(\tau l)||J_\mathrm{f}) = (-)^{J_\mathrm{i}-J_\mathrm{f}+l+\eta}(J_\mathrm{f}||M(\tau l)||J_\mathrm{i}), \tag{2.100}$$

with $\eta = 0$ for $\tau = \mathrm{C}$; $\eta = 1$ for $\tau = \mathrm{E}$ or M (Donnelly et al. 1975). If the nuclear states are also eigenstates of isospin with eigenvalues $I_\mathrm{i},\ I_\mathrm{f}$, respectively, there is an additional phase factor $(-)^{I_\mathrm{i}-I_\mathrm{f}}$ in (2.100). In this case the reduced matrix element implies reduction with respect to both angular momentum and isospin (Donnelly et al. 1975).

For elastic scattering, in particular, J_i and J_f are identical. From (2.100) we then must have $(-)^{l+\eta} = +1$, $l + \eta$ must be even. Thus, only *even longitudinal* and only *odd transverse magnetic multipoles* contribute to elastic scattering.

As an illustration let us consider some examples:

(i) Elastic scattering on ^{3}He $\left(J^\pi = \frac{1}{2}^+\right)$ and ^{209}Bi $\left(\mathrm{J}^\pi = \frac{9}{2}^-\right)$. Only the following multipoles give nonvanishing contributions

^{3}He : C0,M1,
^{209}Bi : C0,C2,C4,C6,C8;M1,M3,M5,M7,M9.

(ii) Inelastic scattering from the ground state to the electric dipole giant resonance in $^{16}\mathrm{O}\left(J_{\mathrm{i}}^{\pi_{\mathrm{i}}} = 0^{+} \rightarrow J_{\mathrm{f}}^{\pi_{\mathrm{f}}} = 1^{-}\right)$. In this case only the multipoles E1 and C1 can contribute.

These selection rules for El and Ml transitions are the same as for the corresponding photonic electric and magnetic multipole transitions. (There are no Cl transitions in the case of real photons.) There is, however, one essential difference betweeen photo- and electroexcitation: In the case of photonic processes, the momentum transfer q is replaced by

$$k = E_{\mathrm{f}} - E_{\mathrm{i}} \stackrel{\Delta}{=} (E_{\mathrm{f}} - E_{\mathrm{i}})/\hbar c,$$

the photon momentum (or energy). In most practical cases $k \cdot r$ is smaller than 1 for r of the order of, or smaller than, the typical size of the nucleus. Thus, as a consequence of the behaviour of the spherical Bessel function for small argument [see (2.12)], a transition of high multipolarity l_{H} is suppressed relative to a transition of low multipolarity l_{L} by a typical factor

$$\frac{(kr)^{l_{\mathrm{H}}}}{(2l_{\mathrm{H}}+1)!!} \Big/ \frac{(kr)^{l_{\mathrm{L}}}}{(2l_{\mathrm{L}}+1)!!}. \tag{2.101}$$

For example, an E3 γ-transition amplitude is suppressed relative to an E1 transition by a factor of the order of $\frac{1}{35}(kr)^2$. Thus, the lowest multipolarity which is compatible with the selection rules will also be the dominant one.

No such ordering of successive multipoles occurs in electron scattering. Indeed, the modulus of the momentum transfer q can become arbitrarily large and the quantity $q \cdot r$ can assume any value, greater or smaller than one. So, in general, high multipoles can be equally important as low multipoles. In the limit of small momentum transfer only, $q \rightarrow 0$, we recover the ordering of photonic multipole transitions. Actually, apart from the electonic kinematic factors, El and Ml transition probabilities in electron scattering must go over, in the limit $q \rightarrow 0$, into the corresponding γ-transition probabilities. This is called the "photon point."

Examples for the use of the Born approximation in the description of electron scattering as well as an analysis of the information carried by elastic and inelastic form factors are postponed until Sects. 2.5.5,6, where we have completed the discussion of Coulomb distortion, so that we can compare the two methods of analysis, at the same time. For the moment, it may suffice to stress that, whilst a γ-transition gives us just one *moment* of the transition charge density or current density, the matrix elements of the multipole operators (2.94–2.96) which are relevant for the cross sections for electron scattering (2.97) yield continuous information on these quantities. As the momentum transfer is varied, these matrix elements probe the spatial structure of nuclear charge and current density. If it were possible to measure the cross sections up to very large momentum transfers we would eventually obtain a complete mapping of $\rho_{\mathrm{n}}(\boldsymbol{r})$ and $\boldsymbol{j}_{\mathrm{n}}(\boldsymbol{r})$.

In practice, this is not possible, however. The scattering cross section to any specific excited state falls off faster than q^{-4} with increasing momentum transfer and, at some point, becomes unmeasurably small. Furthermore, as the energy transfer and the momentum transfer increase (into what is called the "deep inelastic" region), the number of possible final states increases so much that one may not be able to follow up one particular excitation. One then measures instead fully *inclusive scattering* (i.e. summing over all final states), or *semi-inclusive scattering* (where some property of the final state is recorded). The cross section for inclusive scattering quickly starts to dominate over all exclusive reaction channels.

In summary, only limited information on the spatial structure of the target densities is obtained in practice. At low momentum transfer, one starts probing the nuclear periphery, i.e. the charge density in the neighbourhood of the nuclear radius (distance at which the density has dropped to about half its central value). As the momentum transfer increases, more and more information on the nuclear interior appears in the elastic scattering cross sections. The densities at the origin always remain the least well known. Examples of practical analysis are given below.

2.5.4 The Problem of Coulomb Distortion

The Born approximation in the calculation of electron scattering has the great advantage of being simple and transparent. The form factors are the Fourier transforms of the nuclear matrix elements of charge and current densities and thus provide us with a direct mapping of these important quantities. On the other hand, the Born approximation also has serious deficiencies: It does not take into account the distortion of the electron waves in the static Coulomb field of the nucleus. Depending on the accuracy of the available data, the neglect of Coulomb distortion may be tolerable for light nuclei, $Z = 1$ to ~ 10. However, for larger values of the nuclear charge these effects quickly become large and must be taken into account. What are the most prominent effects of Coulomb distortion?

(i) It is not difficult to see that a form factor can have zeroes at physical values of the momentum transfer q. These diffraction zeroes which reflect specific properties of the charge and current densities in coordinate space will also appear in the cross section[12]. The cross section will then exhibit a typical diffraction pattern. The diffraction zeroes, strictly speaking, are not realistic and do not appear in the exact expression for the cross section. This is easy to understand in a qualitative manner. Suppose we describe the scattering amplitude in terms of partial waves. Partial waves carry definite angular

[12]This is true if the cross section depends only on one form factor and, in the case of inelastic scattering, if retardation effects are neglected. If it contains several form factors which have their zeroes at different q^2 then cross sections do not go to zero. Obviously, this does not invalidate our discussion.

momenta. Classically, the angular momentum, with respect to the center of the nucleus, is proportional to the impact parameter b times the momentum transfer q. Thus low partial waves penetrate into the nucleus, high partial waves pass by far outside, whilst some intermediate partial waves graze the nuclear edge. In the Born approximation the diffraction zeroes come about as a result of destructive interference of partial wave amplitudes. On the other hand, if the effect of the static Coulomb field is taken into account, low partial waves are more distorted than intermediate partial waves, while very high partial waves will be affected only very little. As a consequence, the interference of the partial waves of the Born approximation is perturbed. The diffraction zeroes disappear and are replaced with *diffraction minima* of the scattering amplitude of nonvanishing value. Furthermore, the position of these minima will be displaced from the positions of the Born zeroes.

(ii) A second important effect of Coulomb distortion may also be understood qualitatively. The static field is attractive. Therefore, the exact partial waves are attracted towards the nuclear interior. In terms of the Born approximation, this means, effectively, that at least the low and intermediate partial waves are scattered at a higher effective energy k. As the previous zero occurs at a fixed value of the product

$$q \cdot R \simeq 2kR \sin(\theta/2) = \text{const.}$$

(R being the nuclear size parameter), the diffraction minimum is expected at a somewhat lower value of the scattering angle. As a simple example, consider elastic scattering from a spinless nucleus whose charge density is taken to be

$$\rho(r) = \frac{3}{4\pi R_0^3}\Theta(R_0 - r) \quad \text{(homogeneous density)}. \tag{2.102}$$

It is not difficult to calculate the charge form factor from (2.6,2.30), for this density (see exercise 2.5). One finds

$$F(q^2) = \frac{3}{z} j_1(z) = \frac{3}{z^3}(\sin z - z\cos z), \tag{2.103}$$

where $z = q \cdot R_0$. The cross section in the Born approximation is given by (2.7), and depends only on the variable

$$qR_0 \simeq 2kR_0 \sin(\theta/2).$$

Thus if we choose the energy such that $k_1 R_0^1 = k_2 R_0^2$ for two different nuclei with charges Z_1, Z_2 and radii R_0^1, R_0^2, the quantity $(k/Z)^2\, \mathrm{d}\sigma/\mathrm{d}\Omega$ will be the same

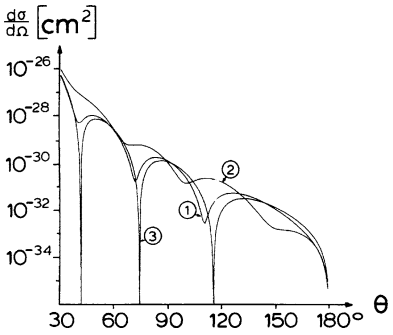

Fig. 2.5 Differential cross section for elastic electron scattering on calcium ($Z = 20$, $A = 40$) and lead ($Z = 82$, $A = 208$). Curve 1: exact result for Ca; curve 2: exact result for Pb; curve 3: cross section in the first Born approximation for Ca and Pb. The two cross sections for Ca are multiplied by the factor $(82\ R_0(\mathrm{Pb})/20 R_0(\mathrm{Ca}))^2$, so that the cross sections in the Born approximation of Ca and Pb coincide. In all three cases the nuclear charge density is assumed to be homogeneous, cf. e.g. (2.102). The radius for lead is $R_0(\mathrm{Pb}) = 4.26\,\mathrm{fm}$, the energy is $E = 300\,\mathrm{MeV}$, so that $kR_0 = 6.48$

for the two cases. This is illustrated by Fig. 2.5 which shows the scaled Born cross sections for $Z = 20$ (calcium) and $Z = 82$ (lead), with $k\ R_0 = 6.48$ (curve marked 3). The spherical Bessel function of order 1 has zeroes at $z_1 = 4.493$, $z_2 = 7.725$, $z_3 = 10.904$, etc.,[13] that is, the form factor and the Born cross section vanish at $\theta_1 = 40.6°$, $\theta_2 = 73.2°$, $\theta_3 = 114.7°$, ... For comparison, the figure also-shows the cross sections calculated by means of a full partial wave analysis. (The cross section for calcium is multiplied by the same scale factor as in the Born approximation.) We note that, even with the cross section on calcium being rescaled, the exact cross sections do not coincide.

The zeroes are replaced with minima whose position is shifted towards lower scattering angles. The shift is larger for $Z = 82$ than for $Z = 20$.

One may ask whether these strong distortion effects render useless the method of Born approximation in electron scattering. Fortunately, this is not so. As will be seen below, the physical information contained in specific features of the cross section is the same, independently of whether the Born approximation or the more exact partial wave analysis is used. Coulomb distortion is a technical complication which does not obscure the connection between properties of the nuclear densities and the cross sections. The technical and conceptual simplicity of the Born approximation can be made use of in many systematic investigations. Only when comparison with the data is made must the distortion be taken into account.

[13] See Table 10.6 of [ABS65].

2.5.5 *Partial Wave Analysis for Elastic Scattering*

On our way to constructing the partial wave decomposition of electron scattering amplitudes we need central field solutions of the Dirac equation carrying definite angular momentum. According to the formulate of App. E these have the form

$$\psi_{\kappa m}(r,\theta,\varphi) = \begin{pmatrix} g_\kappa(r)\varphi_{\kappa m} \\ \mathrm{i} f_\kappa(r)\varphi_{-\kappa m} \end{pmatrix}, \tag{2.104}$$

where κ is Dirac's quantum number. The radial wave functions g_κ and f_κ obey the system of differential equations

$$\begin{aligned} \frac{\mathrm{d}f_\kappa}{\mathrm{d}r} &= \frac{\kappa-1}{r} f_\kappa - (E - V(r) - m) g_\kappa, \\ \frac{\mathrm{d}g_\kappa}{\mathrm{d}r} &= -\frac{\kappa+1}{r} g_\kappa + (E - V(r) + m) f_\kappa. \end{aligned} \tag{2.105}$$

In the case of electron scattering at high energies we can neglect the mass term in (2.105). In this case we have the following symmetry relations

$$g_{-\kappa}(r) \simeq f_\kappa(r), \qquad f_{-\kappa}(r) \simeq -g_\kappa(r), \tag{2.106}$$

which can be read off from (2.105). Furthermore, it is appropriate to use the high-energy representation (1.187) of the Dirac equation. Using the transformation matrix S, p. 25, the central field solutions (2.104) now appear in the form

$$\psi_{\kappa m} = \begin{pmatrix} \phi_{\kappa m} \\ \chi_{\kappa m} \end{pmatrix} = \frac{1}{\sqrt{2}} \begin{pmatrix} g_\kappa \varphi_{\kappa m} + \mathrm{i} f_\kappa \varphi_{-\kappa m} \\ g_\kappa \varphi_{\kappa m} - \mathrm{i} f_\kappa \varphi_{-\kappa m} \end{pmatrix}. \tag{2.107}$$

For vanishing mass the symmetry relations (2.106) apply and thus

$$\psi_{-\kappa m} = -\frac{\mathrm{i}}{\sqrt{2}} \begin{pmatrix} g_\kappa \varphi_{\kappa m} + \mathrm{i} f_\kappa \varphi_{-\kappa m} \\ -g_\kappa \varphi_{\kappa m} + \mathrm{i} f_\kappa \varphi_{-\kappa m} \end{pmatrix}.$$

Furthermore, we know from (2.17,2.20) in Sect. 2.2, that the two asymptotic helicity states have the same scattering amplitudes. Thus, it is sufficient to study two-component spinors $\phi_{\kappa m}$ [e.g. upper two components of (2.107)] for *positive* κ. Replacing $\kappa > 0$ by $j = \kappa - 1/2$ and introducing $F_j(r) = r f_\kappa(r)$, $G_j(r) = r g_\kappa(r)$, equations (2.105) (in the limit $m = 0$) transform into

$$\begin{aligned} \frac{\mathrm{d}F_j}{\mathrm{d}r} &= \frac{j+1/2}{r} F_j - (E - V(r)) G_j, \\ \frac{\mathrm{d}G_j}{\mathrm{d}r} &= -\frac{j+1/2}{r} G_j + (E - V(r)) F_j. \end{aligned} \tag{2.105$'$}$$

As an example consider the case $V(r) \equiv 0$. From (2.105′) one derives

$$\frac{\mathrm{d}^2 G_j}{\mathrm{d}r^2} + \left(E^2 - \frac{\kappa(\kappa+1)}{r^2}\right) G_j = 0 \qquad (\kappa = j + 1/2),$$

whose solutions can be expressed in terms of the spherical Bessel functions,

$$G_j = Nrj_\kappa(kr) = Nrj_{j+1/2}(kr)$$

F_j is obtained from the second equation (2.105′) and the well-known relation

$$j_l'(z) = \frac{l}{z} j_l - j_{l+1} = -\frac{l+1}{z} j_l + j_{l-1}.$$

One finds

$$F_j(r) = Nrj_{\kappa-1}(kr) = Nrj_{j-1/2}(kr),$$

so that, with $\kappa = j + 1/2$

$$\phi_{\kappa m}^{(V\equiv 0)} = \frac{N}{\sqrt{2}} \{ j_{j+1/2}(kr)\varphi_{\kappa m} + \mathrm{i} j_{j-1/2}(kr)\varphi_{-\kappa m} \}. \tag{2.108}$$

In deriving the partial wave decomposition of the scattering amplitude we assume, at first, that the potential $V(r)$ decreases at infinity faster than $1/r$, i.e. $\lim_{r\to\infty} rV(r) = 0$. (See discussion in Sect. 2.2) The modifications due to the long range of the Coulomb potential are considered at the end of this section.

Following (2.17) we require the solutions to have the following asymptotic form:

$$\phi_{m=1/2} \sim \begin{pmatrix} 1 \\ 0 \end{pmatrix} \mathrm{e}^{\mathrm{i}kz} + \frac{f(\theta,\varphi)}{r} \begin{pmatrix} \mathrm{e}^{-i\varphi/2} \cos(\theta/2) \\ \mathrm{e}^{i\varphi/2} \sin(\theta/2) \end{pmatrix} \mathrm{e}^{\mathrm{i}kr}. \tag{2.109}$$

For the solution at all values of $\boldsymbol{x}$ we write the series expansion

$$\phi_{m=1/2} = \sum_{j=1/2}^{\infty} a_{j1/2} \phi_{j1/2}$$

in terms of the angular momentum eigenstates (2.107).

The incoming part of ϕ, i.e. the first term of (2.109), is readily expanded in terms of partial waves

$$\phi_{\text{in}} \equiv \begin{pmatrix} 1 \\ 0 \end{pmatrix} \mathrm{e}^{\mathrm{i}kz} = \begin{pmatrix} 1 \\ 0 \end{pmatrix} \sum_{l=0}^{\infty} \mathrm{i}^l \, j_l(kr) \, \sqrt{(2l+1)4\pi} Y_{l0}$$

$$= \sqrt{4\pi} \sum_{j=1/2}^{\infty} \sum_{l=j-1/2}^{j+1/2} \mathrm{i}^l \, \sqrt{2l+1} \, j_l(kr) \left(l0, \tfrac{1}{2}\tfrac{1}{2} | j \tfrac{1}{2}\right) \varphi_{jl1/2}. \quad (2.110)$$

Here we have expressed the product of the spin up state $\left(\begin{smallmatrix} 1 \\ 0 \end{smallmatrix}\right)$ and of the eigenstate Y_{l0} of orbital angular momentum in terms of states in which l and spin 1/2 are coupled to total angular momentum $j = l \pm 1/2$. Remembering the definition of the Dirac quantum number κ, we have for positive κ

$$\begin{aligned} \varphi_{\kappa m} &\equiv \varphi_{j=l-1/2, l=\kappa, m} \\ & \qquad\qquad (\kappa > 0) \\ \varphi_{-\kappa m} &\equiv \varphi_{j=\bar{l}+1/2, \bar{l}=\kappa-1, m} \end{aligned}$$

This allows us to rewrite (2.110) by inserting the explicit values of the Clebsch–Gordan coefficients, as given in Table 2.2.

One finds

$$\phi_{\text{in}} = \sum_{j=1/2}^{\infty} \mathrm{i}^{j-3/2} \, \sqrt{4\pi \left(j + \tfrac{1}{2}\right)} \{ j_{j+1/2}(kr) \, \varphi_{\kappa \, 1/2} + \mathrm{i} j_{j-1/2}(kr) \, \varphi_{-\kappa \, 1/2} \}. \quad (2.110')$$

[The reader may check that this is the same as the free solution (2.108).] For the purpose of reference we note here the well-known asymptotic behaviour of spherical Bessel functions

$$j_l(z) \underset{z \to \infty}{\sim} \frac{1}{z} \sin(z - l\pi/2). \quad (2.111)$$

Indeed, if we make the following ansatz for the full solution:

Table 2.2 Explicit expressions for Clebsch–Gordan coefficients $\left(lm_l = m - m_s; \tfrac{1}{2} m_s | jm\right)$

j	$m_s = +\frac{1}{2}$	$-\frac{1}{2}$
$l + \frac{1}{2}$	$\left(\dfrac{l + \frac{1}{2} + m}{2l+1}\right)^{1/2}$	$\left(\dfrac{l + \frac{1}{2} - m}{2l+l}\right)^{1/2}$
$l - \frac{1}{2}$	$-\left(\dfrac{l + \frac{1}{2} - m}{2l+1}\right)^{1/2}$	$\left(\dfrac{l + \frac{1}{2} + m}{2l+1}\right)^{1/2}$

$$\phi_{m=1/2} = \frac{1}{kr} \sum_{j=1/2}^{\infty} \sqrt{4\pi(j+1/2)}\, \mathrm{i}^{j-3/2}\, \mathrm{e}^{\mathrm{i}\eta_j} \{ G_j\, \varphi_{\kappa\, 1/2} + \mathrm{i} F_j\, \varphi_{-\kappa 1/2} \}. \tag{2.112}$$

the asymptotic behaviour of the radial functions can be taken to be

$$G_j \sim \sin\left(kr - \frac{j+1/2}{2}\pi + \eta_j\right), \tag{2.113a}$$

$$F_j \sim \cos\left(kr - \frac{j+1/2}{2}\pi + \eta_j\right). \tag{2.113b}$$

The asymptotic ansatz (2.113) makes sure that the *in*coming wave of ϕ, (2.112), i.e. the piece proportional to $\mathrm{e}^{-\mathrm{i}kr}/r$, is indeed equal to the incoming part of ϕ_{in}, (2.110′). η_j is the phase shift caused by the potential $V(r)$ as compared to the force-free situation where $V \equiv 0$. In order to identify the scattering amplitude $f(\theta, \varphi)$ we must isolate the *out*going spherical wave $\mathrm{e}^{\mathrm{i}kr}/r$ in the asymptotic expansion of ϕ, (2.112). We find

$$\phi|_{\mathrm{out}} \sim -\frac{\mathrm{e}^{\mathrm{i}kr}}{2\mathrm{i}kr} \sqrt{4\pi} \sum_j \sqrt{j+1/2}\, \mathrm{e}^{2\mathrm{i}\eta_j} \{\varphi_{\kappa 1/2} - \varphi_{-\kappa 1/2}\}.$$

The asymptotic piece of ϕ_{in}, (2.110′), which contains the *out*going spherical wave is determined in exactly the same way. Obviously, it is of the same form, but with $\eta_j = 0$. Upon comparison of the difference $(\phi - \phi_{\mathrm{in}})_{\mathrm{outg.spher.wave}}$ to the asymptotic form (2.109) we have

$$f(\theta, \varphi) \begin{pmatrix} \mathrm{e}^{-\mathrm{i}\varphi/2} \cos(\theta/2) \\ \mathrm{e}^{\mathrm{i}\varphi/2} \sin(\theta/2) \end{pmatrix} = -\frac{1}{2\mathrm{i}k} \sum \sqrt{4\pi(j+1/2)}\, (\mathrm{e}^{2\mathrm{i}\eta_j} - 1)\, \{\varphi_{\kappa 1/2} - \varphi_{-\kappa 1/2}\}. \tag{2.114}$$

By means of the Clebsch–Gordan coefficients of Table 2.2 we have, with $l = \kappa = j + \frac{1}{2}$,

$$\{\varphi_{\kappa 1/2} - \varphi_{-\kappa 1/2}\} = -\left(\sqrt{\frac{l}{2l+1}}\, Y_{l0} + \sqrt{\frac{l}{2l-1}}\, Y_{l-1,0} \right) \begin{pmatrix} 1 \\ 0 \end{pmatrix} + \left(\sqrt{\frac{l+1}{2l+1}}\, Y_{l1} - \sqrt{\frac{l-1}{2l-1}}\, Y_{l-1,1} \right) \begin{pmatrix} 0 \\ 1 \end{pmatrix}.$$

Using the definition

$$Y_{lm} = (-)^m \sqrt{\frac{(2l+1)(l-1)!}{4\pi(l+1)!}}\, p_l^m\, \mathrm{e}^{\mathrm{i}\varphi} \tag{2.115}$$

and two recurrence relations for the associated Legendre functions

$$P_l^m - xP_{l-1}^m - (l+m-1)\ \sqrt{1-x^2}\ P_{l-1}^{m-1} = 0,$$
$$xP_l^m - (l-m+1)\ \sqrt{1-x^2}\ P_l^{m-1} - P_{l-1}^m = 0,$$
$$(x = \cos\theta)$$

from which we derive

$$P_l^1 - P_{l-1}^1 = l\frac{\sqrt{1-x^2}}{1+x}\ (P_l + P_{l-1}) = l\,\mathrm{tg}(\theta/2)\,(P_l + P_{l-1}),$$

one finds

$$\{\varphi_{\kappa 1/2} - \varphi_{-\kappa 1/2}\} = -\sqrt{\frac{l}{4\pi}}\,(P_l + P_{l-1})\ \left\{\begin{pmatrix}1\\0\end{pmatrix} + \mathrm{e}^{\mathrm{i}\varphi}\,\mathrm{tg}(\theta/2)\begin{pmatrix}0\\1\end{pmatrix}\right\}$$
$$= -\sqrt{\frac{1}{4\pi}}\ \frac{\mathrm{e}^{\mathrm{i}\varphi/2}}{\cos\theta/2}\ (P_l + P_{l-1})\begin{pmatrix}\mathrm{e}^{-\mathrm{i}\varphi/2}\cos(\theta/2) \\ \mathrm{e}^{\mathrm{i}\varphi/2}\ \sin(\theta/2)\end{pmatrix}.$$

Comparing this to (2.114) and setting $l = j + 1/2$ we obtain at once the final result

$$f(\theta,\ \varphi) = \frac{1}{2\mathrm{i}k}\ \frac{\mathrm{e}^{\mathrm{i}\varphi/2}}{\cos(\theta/2)}\ \sum_{j=1/2}^{\infty}(j+1/2)\ (\mathrm{e}^{2\mathrm{i}\eta_j} - 1)\ (P_{j+1/2} + P_{j-1/2}). \tag{2.116}$$

The phase factor $\mathrm{e}^{\mathrm{i}\varphi/2}$ is the same as the one obtained in the Born approximation, (2.25). As the potential $V(r)$ and hence the scattering process are axially symmetric about the 3-axis we may set $\varphi = 0$ without loss of generality.

Extension to the Coulomb potential. For potentials which do not decrease faster than $1/r$, the asymptotic form (2.109) is not correct. Very much like in the analogous nonrelativistic situation the phase factor $\mathrm{e}^{\mathrm{i}kr}$ is modified by an additional phase factor which depends on $\ln(2kr)$, so that in (2.109) we should make the replacement

$$\mathrm{e}^{\mathrm{i}kr} \ \to\ \mathrm{e}^{\mathrm{i}(kr + Z\alpha\ln(2kr))}.$$

In the expression (2.116) the phases η_j, so far, were the scattering phases due to the potential relative to the *force-free case*. In the case of a potential decreasing like $1/r$ a different procedure is indicated: The electrostatic potential created by a nucleus with spherically symmetric charge density $\rho(r)$ is, cf. (1.186),

$$V(r) = -4\pi Ze^2\left\{\frac{1}{r}\int_0^r \rho(r')r'^2\mathrm{d}r' + \int_r^\infty \rho(r')r'\mathrm{d}r'\right\}. \tag{2.117}$$

As $\rho(r)$ vanishes (or becomes negligibly small) beyond some distance R of the order of the nuclear radius, $V(r)$ approaches the pure $1/r$ potential

$$V_C(r) = -Ze^2/r \tag{2.118}$$

for $r > R$. Like in the nonrelativistic case, the radial Dirac equations (2.105) can be solved analytically for the case of the potential (2.118) of point-like charges. In particular, the scattering phases η_j^{C} of this potential can be given explicitly and the scattering amplitude f_{C} be computed from (2.116). Therefore, the scattering problem for the true potential (2.117) is solved most economically by computing the *additional* phase shift due to $V(r)$

$$\delta_j := \eta_j - \eta_j^{\mathrm{C}}, \tag{2.119}$$

where η_j is the full phase shift of the potential $V(r)$. The construction of the continuum solutions g_κ^{C} and $\mathrm{f}_k^{\mathrm{C}}$ for the potential V_{C} is straightforward but tedious and we do not work them out here[14]. The solutions which are regular at the origin have the asymptotic behaviour (in the mass zero limit),

$$\begin{aligned} rg_\kappa^{\mathrm{C}} &\sim \sin\left(kr + y\ \ln(2kr) + \delta_\kappa^0\right), \\ rf_\kappa^{\mathrm{C}} &\sim \cos\left(kr + y\ \ln(2kr) + \delta_\kappa^0\right), \end{aligned} \tag{2.120}$$

where

$$\delta_\kappa^0 \equiv \bar{\eta}_\kappa - \sigma_\kappa - (\gamma_\kappa - 1)\pi/2, \quad y = Z\alpha, \tag{2.121}$$

with

$$\begin{aligned} &\gamma_\kappa = \sqrt{\kappa^2 - (Z\alpha)^2}, \\ &\bar{\eta}_\kappa\ (m=0) = -\frac{1}{2}\ \mathrm{arctg}\ \frac{y}{\gamma_\kappa} - \frac{\pi}{2}\ \frac{1+\mathrm{sign}\kappa}{2}, \\ &\sigma_\kappa = \arg\Gamma(\gamma_\kappa + \mathrm{i}y); \end{aligned}$$

comparing this to the general form (2.113) we see that the Coulomb phase is given by

$$\eta_k^{\mathrm{C}} = \bar{\eta}_\kappa - \sigma_\kappa + (l - \gamma_\kappa + 1)\,\pi/2. \tag{2.122}$$

(up to the logarithmic term $Z\alpha$ In $2kr$), or

$$\eta_j^{\mathrm{C}} = \bar{\eta}_j - \sigma_j + \left(j + \frac{3}{2} - \gamma_j\right)\pi/2. \tag{2.122'}$$

In (2.122′) we have written the index j, not κ since we need to consider only positive κ, here; equation (2.122) holds for all κ, positive and negative. For the sake of simplicity, we have neglected the mass of the electron. If one wishes to retain the

[14] See e.g. [ROS 61].

mass terms then $y = Z\alpha\ E/\kappa$ and $\bar{\eta}_\kappa$ of (2.121) is replaced with[15]

$$\bar{\eta}_\kappa(m) = -\frac{1}{2}\mathrm{arctg}\ \frac{y\left(1+\frac{\gamma_\kappa}{\kappa}\ \frac{m}{E}\right)}{\gamma_\kappa - \frac{1}{\kappa}y^2\ \frac{m}{E}} - \frac{\pi}{2}\ \frac{1+\mathrm{sign}\,\kappa}{2}. \tag{2.123}$$

All other formulae (2.120–2.122) remain unchanged provided k is now understood to be the wave number $k = \sqrt{E^2 - m^2} \cdot \eta_j^{\mathrm{C}}$ can therefore be obtained analytically form (2.122). The additional phase shifts δ_j, (2.119), which are caused by the *difference* of the true potential (2.117) and the pointlike potential (2.118) may be obtained as follows: One calculates solutions of the Dirac equations (2.105′), for a given energy and for $V(r)$ as obtained from (2.117), which are regular at the origin. As $V(r)$ goes over into $V_{\mathrm{C}}(r)$ at some finite radius R outside the nuclear charge radius, we need the full solution (f, g) only in the inner region $0 \le r \le R$. In the outer region $r \ge R$ the exact solution is a superposition of regular (R) and irregular (I) solutions of (2.105′) with $V_{\mathrm{C}}(r)$, viz.

$$\begin{aligned} f_\kappa &= a f_\kappa^{\mathrm{C,R}} + b f_\kappa^{\mathrm{C,I}}, \\ g_\kappa &= a g_\kappa^{\mathrm{C,R}} + b g_\kappa^{\mathrm{C,I}}. \end{aligned} \tag{2.124}$$

The phase differences δ_j may be obtained by direct comparison of the exact solution to the regular solutions $\left(f^{\mathrm{C,R}}, g^{\mathrm{C,R}}\right)$ at some $r > R$ at which an asymptotic expansion of these functions is meaningful. In this case, however, $rf^{\mathrm{C.R}}$ and $rg^{\mathrm{C.R}}$ must be expanded beyond the form (2.120), up to, say, terms of order $1/r^2$. Alternatively, the phases may be obtained from the asymptotic form of (2.124), expressing them as functions of b/a and η_j^{C} (Ravenhall et al. 1954).

As an example, Table 2.3 shows the Coulomb phases η_j^{C} for V_{C} with $Z = 82$, as well as the phase shifts δ_j for the Fermi charge density (2.125) for lead, $Z = 82$, $c = 6.6475$, $t = 2.30$. The electron energy is $k = 300\,\mathrm{MeV}$. At this energy the nine lowest partial waves are modified appreciably by the deviation of the actual charge density from the point-like charge.

2.5.6 *Practical Analysis of Scattering Data and Information Content of Partial Waves*

In the early stages of this kind of nuclear physics it was customary to analyze elastic scattering data in terms of specific functional forms for the nuclear charge density. An ansatz that was particularly popular is the so-called *Fermi distribution*,

$$\rho(r) = N\frac{1}{1+\exp\left[(r-c)/z\right]}, \tag{2.125}$$

[15] Arctg is defined such that it goes to zero as the argument goes to zero.

Table 2.3 Coulomb phases and phase shifts, equation (2.119) for electron scattering on $^{208}_{82}$Pb. The charge density is described by (2.125) with $c = 6.6475\,\text{fm}$, $t = 2.30\,\text{fm}$

j	η_j^C	δ_j
$\frac{1}{2}$	0.4441	−1.4779
$\frac{3}{2}$	−0.2401	−0.8046
$\frac{5}{2}$	−0.5491	−0.5137
$\frac{7}{2}$	−0.7512	−0.3367
$\frac{9}{2}$	−0.9017	−0.2181
$\frac{11}{2}$	−1.0218	−0.1361
$\frac{13}{2}$	−1.1217	−0.0801
$\frac{15}{2}$	−1.2072	−0.0434
$\frac{17}{2}$	−1.2820	−0.0214
$\frac{19}{2}$	−1.3485	−0.0095
$\frac{21}{2}$	−1.4083	−0.0039

where the normalization factor

$$N = \frac{3}{4\pi c^3}\left[1 + \left(\frac{\pi z}{c}\right)^2 - 6\left(\frac{z}{c}\right)^3 \mathrm{e}^{-c/z} \sum_{n=1}^{\infty} \frac{(-)^n}{n^3} \mathrm{e}^{-nc/z}\right]^{-1}$$
$$\simeq \frac{3}{4\pi c^3} \frac{1}{1 + (\pi z/c)^2} \tag{2.126}$$

is chosen such as to normalize $\rho(r)$ to one, cf. (2.2). The parameter c is called the *radius of half-density* because $\rho(r = c) = 0.5\ \rho(r = 0)$. The parameter a is a measure for the rate at which the density falls off in the nuclear surface. A good measure for this fall-off is the so-called *surface thickness* t which is defined as follows: Let $\rho(r)$ be a function which decreases monotonically for increasing r. Let $r_{(90)}$ and $r_{(10)}$ be the radii at which the density is 90% and 10% of its value at $r = 0$, respectively. Then

$$t := r_{(10)} - r_{(90)}.$$

In the case of the Fermi distribution (2.125) one has the relation $t = 4z \ln 3 \simeq 4.394z$. The shape of the Fermi density is illustrated by Fig. 6.7, curve marked ρ_0.

As a matter of fact, the Fermi density (2.125) gives a surprisingly good description of charge and matter densities in practically all spherical nuclei except

the very lightest ones. It depends on two parameters, c and t, which have the typical values

$$c \simeq 1.1 \times Z^{1/3}\,\text{fm}, t \simeq 2.2\text{–}2.5\,\text{fm}. \tag{2.127}$$

There are, of course, deviations from this simple pattern, especially at, and close to, magic shells but these deviations are never very large. (We shall come back to this, in connection with muonic atoms, below.) Even though a functional form such as the Fermi function (2.125) may be quite useful as a rough parametrization, it is not adequate for the analysis of precise measurements of the elastic cross section extending over many orders of magnitude, for several reasons: Assuming a specific functional form implies a prejudice about possible shapes of the charge density and, therefore, cannot be the basis of a model-free analysis of the data. Furthermore, such an ansatz contains a finite number of parameters [two in the case of the Fermi distribution (2.125)] which are then determined by a best fit to the data. What if the data are so numerous and so precise that they contain more information on the charge distribution than what can be described by these parameters? Finally, a specific function such as (2.125) does not reflect the fact that different parts of $\rho(r)$ have different weights in the angular dependence of cross sections. In summary, one would prefer a model independent way of analysis whose final result would be an empirical density function $\rho(r)$, along with an error band that depends on r and reflects the type of experimental input as well as its error bars.

Such methods of analysis which do not rely on specific model densities have been proposed and have been applied successfully to high-precision experiments (Lenz 1969, Friedrich et al. 1972, Sick 1974, Friar et al. 1973, 1975). Figures 2.6 and 2.7 show typical examples of nuclear charge densities as determined from experiment. Instead of describing these specific methods here we prefer to discuss, in a qualitative manner, the physical information carried by the various low, intermediate and high partial waves.

Sensitivity of scattering phase to details of charge density. Obviously, the nature of charge density moments and the number of them that can be obtained from elastic scattering, depend on:

(i) the primary energy of the electron,
(ii) the range of momentum transfers, and
(iii) the experimental error bars of the differential cross section.

The essential features of such an analysis can be made transparent by studying integral representations for the scattering phases. To this end, let us consider two different charge densities $\rho^{(1)}(r)$, $\rho^{(2)}(r)$ which are both normalized to one, as before, but which differ from each other over the domain of the nucleus. Both are assumed to go quickly to zero for $r \gtrsim R$. The corresponding potentials $V^{(1)}(r)$ and $V^{(2)}(r)$, calculated from (2.117), then differ only for $r \lesssim R$ and both go over into $V_C(r)$ outside the nucleus.

Let $F_j^{(1)}$, $G_j^{(1)}$ and $F_j^{(2)}$, $G_j^{(2)}$ be the solutions of (2.105′) for $V^{(1)}$ and $V^{(2)}$, respectively, and let $\delta_j^{(1)}$ and $\delta_j^{(2)}$ be the corresponding phase shifts as defined in (2.119). From (2.105′) and from the properties of the generalized Wronskian (see

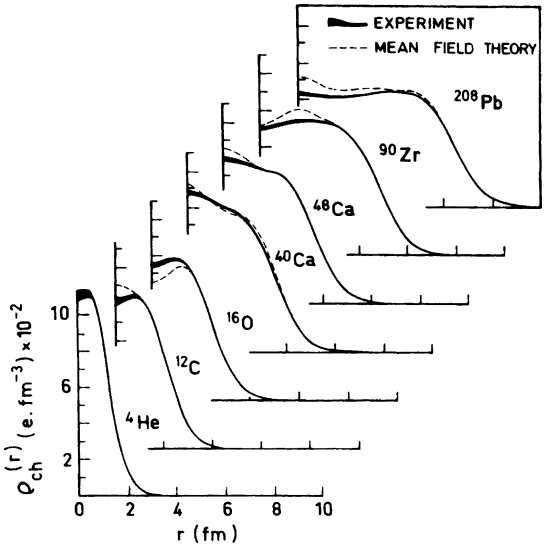

Fig. 2.6 Charge density distributions of doubly closed-shell nuclei. Thickness of solid lines corresponds to experimental uncertainties. Dashed lines are calculated densities. Taken from Frois and Papanicolas (1987)

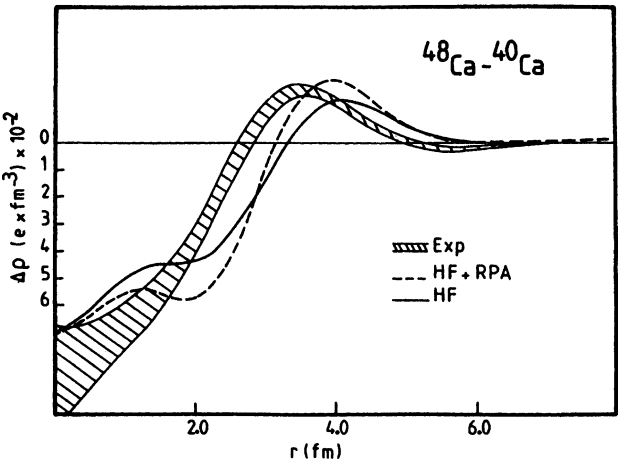

Fig. 2.7 Difference of charges densities of ^{48}Ca and ^{40}Ca. The shaded band is the result of a quasi model-independent determination from elastic electron scattering; its width reflects experimental errors of the cross sections as well as the lack of knowledge of their behaviour at large momentum transfers. Figure taken from Lect. Notes in Phys. 108 (1979), p. 58 (Proceedings of Conf. on Nuclear Physics with Electromagnetic Interactions, Mainz 1979)

exercise 2.6),

$$W(r) = F_j^{(1)}(r)G_j^{(2)}(r) - G_j^{(1)}(r)F_j^{(2)}(r), \tag{2.128}$$

one derives the relation

$$\sin\left(\delta_j^{(1)} - \delta_j^{(2)}\right) = -\int_0^\infty \mathrm{d}r (V^{(1)} - V^{(2)}) \left(F_j^{(1)} F_j^{(2)} + G_j^{(1)} G_j^{(2)}\right). \tag{2.129}$$

The potentials are related to the charge densities through Poisson's equation. Inserting this into (2.129) and integrating by parts twice yields the final result

$$\sin\left(\delta_j^{(1)} - \delta_j^{(2)}\right) = 4\pi \int_0^\infty r^2 \mathrm{d}r (\rho^{(1)}(r) - \rho^{(2)}(r)) \chi_j(r), \tag{2.130}$$

where χ_j stands for

$$\chi_j(r) = \int_0^r \frac{\mathrm{d}r'}{r'^2} \int_0^{r'} \mathrm{d}r'' \left(F_j^{(1)} F_j^{(2)} + G_j^{(1)} G_j^{(2)}\right). \tag{2.131}$$

What does (2.130) tell us about the sensitivity of the phase shifts to the charge density? To answer this question it is useful to consider high, intermediate, and low partial waves separately:

(a) *High partial waves*. Classically speaking, these partial waves correspond to electron trajectories which pass by, far outside, and do not penetrate the nucleus. The phases $\eta_j^{(i)}$ coincide practically with the phases η_j^{C} of a point-like source. As $\rho^{(1)} \simeq \rho^{(2)}$ these phases do not contain information on the nuclear charge density other than its total charge. (In the example of Table 2.3: $j \gtrsim 19/2$).

(b) *Intermediate partial waves*. These partial waves start penetrating the nucleus somewhat. However, the centrifugal potential terms in (2.105′) are still predominant so that the radial functions can be approximated, over the entire nuclear domain, by their power behaviour at the origin

$$F_j^{(i)} \sim r^{j+1/2}, \quad G_j^{(i)} \sim r^{j+3/2}, \tag{2.132}$$

Inserting this into (2.131) we find that $\chi_j(r)$ may be approximated by a simple power behaviour too, $\chi_j \sim r^{2j+1}$. Equation (2.130) then becomes

$$\sin\left(\delta_j^{(1)} - \delta_j^{(2)}\right) \sim 4\pi \int_0^\infty r^2 \mathrm{d}r (\rho^{(1)} - \rho^{(2)}) r^{2j+1}. \tag{2.130′}$$

Thus, intermediate partial waves are determined by even moments of the charge density. Obviously, these depend primarily on the density at the nuclear surface.

(c) *Low partial waves*. The low partial waves, finally, for which the approximation (2.132) becomes invalid, contain information about the nuclear interior. If these partial waves occur at all, i.e. if they are really distinct from the class b (in fact,

this is only the case if the energy is high enough), then they cannot be expressed in terms of simple moments

$$\int_0^\infty r^2 \mathrm{d}r\ \rho(r) r^{2j+1}$$

and a full partial wave analysis must be carried out.

Summarizing, we may say that the type and quality of information that is obtained from a partial wave analysis of electron scattering is very similar to the information content of the form factor in the Born approximation. Therefore, Coulomb distortion, even though important on a quantitative level, is not much more than a technical complication that does not alter the physics of the process.

2.5.7 Miscellaneous Comments

We close this somewhat lengthy discussion of electron scattering with a few comments and supplementary remarks, as well as some suggestions for further reading. The first three supplements concern elastic scattering, the last one concerns inelastic scattering.

Dispersion corrections to elastic scattering. In our treatment of elastic scattering we have assumed the nucleus to be an inert system of stationary charge and current densities. In other terms, we have calculated the fields created by the nuclear ground state at the site of the electron and we have calculated the cross sections from a one-particle wave equation for the electron, in the *external field approximation*. In reality, the nucleus is a dynamical system and has its own internal degrees of freedom which manifest themselves in its rich excitation spectra. These internal degrees of freedom may play a role in elastic scattering if second-order processes of the type sketched symbolically in Fig. 2.8 become important: In a first step the electron excites the nuclear ground state A to some excited intermediate state A* which deexcites again to the ground state in a second scattering process.

These dispersion corrections are notoriously difficult to calculate in a reliable manner. Fortunately, they are not large and can be neglected in most practical situations.

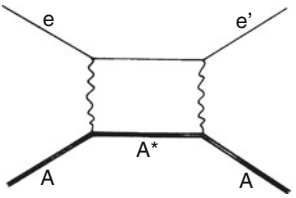

Fig. 2.8 So-called disperision corrections to electron scattering: a two-step process in which the nucleus is excited to a intermediate state

Elastic scattering on strongly deformed nuclei. So far we have considered only spherically symmetric nuclear charge densities $\rho(r)$. This situation allowed us to separate angular and radial motion of the electron. Obviously, this situation applies only for nuclei with spin zero, $J = 0$. For nuclei with $J = 1/2$ we have formally the same situation as for the nucleon: Here there is charge scattering from a spherically symmetric charge density as before, plus scattering on a magnetic moment density (M1 scattering). For nuclei with $J \geq 1$ the nuclear charge density also has nonvanishing higher (even) moments, viz.

$$\rho(\boldsymbol{r}) = \left\langle JM = J \left| \sum_{i=1}^{Z} \delta(\boldsymbol{r} - \boldsymbol{r}_i) \right| J\ M = J \right\rangle$$
$$= \rho_0(r) + \sum_{\kappa=1}^{[J]} \sqrt{\frac{4\kappa+1}{16\pi}} \rho_{2\kappa}(r) Y_{2\kappa,0}(\theta). \tag{2.133}$$

In the case of strongly deformed nuclei the quadrupole term will, in general, be predominant, i.e.

$$\rho(\boldsymbol{r}) \simeq \rho_0(r) + \sqrt{\frac{5}{16\pi}} \rho_2(r) Y_{20}(\theta), \tag{2.134}$$

where $\rho_2(r)$ denotes the radial quadrupole density. The factors in (2.133) have been chosen such that the nuclear spectroscopic quadrupole moment, by its traditional definition, is given by the second moment of $\rho_2(r)$

$$Q_s = \int_0^\infty [\rho_0(r) r^2] r^2 \mathrm{d}r. \tag{2.135}$$

While the calculation of the scattering cross section in the Born approximation is straightforward (see above), the corresponding partial wave analysis is technically more complicated, but still feasible. There may be a difficulty on the experimental side; Such strongly deformed nuclei have rotational excitations of rather low energy, 50–200 keV. It then depends on the energy resolution of a given experimental set up whether or not the truly elastic scattering from the nuclear ground state can be distinguished from the excitation cross sections for these low-lying rotator states. Thus, elastic scattering of electrons may not be the ideal tool for investigating the charge density of deformed nuclei. We will see below that in this case muonic atoms offer a more direct approach to this quantity.

Summation of partial wave amplitudes. There is a technical difficulty in summing the partial wave series (2.116): As it stands this series converges very slowly. The origin of this problem is not difficult to understand. For this purpose let us consider first the scattering on a point charge in the nonrelativistic case. The potential $V_C(r)$ of a point charge introduces a $1/r$ singularity into the Schrödinger equation. The corresponding scattering amplitude, which can be derived in closed form, is proportional to $1/\sin^2(\theta/2)$ and hence becomes singular at $\theta = 0$. This singularity

can be "smoothed" and the convergence of the partial wave series accelerated by means of the following procedure. Suppose we wish to sum an expression of the form (Ravenhall et al. 1954).

$$F(\theta) = \sum_{l=0}^{\infty} a_l P_l(\cos\theta).$$

If this series converges only very slowly in practice, one may replace it by a so-called reduced series which is defined by

$$(1-\cos\theta)^m F(\theta) = \sum_{l=0}^{\infty} c_l^{(m)} P_l(\cos\theta),$$

and where m is some positive integer. Using standard recurrence formulae for Legendre polynomials one derives the recurrence relations for the coefficients $c_l^{(m)}$

$$c_l^{(m+1)} = c_l^{(m)} - \frac{l}{2l-1} c_{l-1}^{(m)} - \frac{l+1}{2l+3} c_{l+1}^{(m)},$$

$$c_l^{(0)} = a_l.$$

The modified series which is obtained after a few iterations converges more rapidly than the original series.

Inelastic scattering and partial wave analysis. The problem of Coulomb distortion in inelastic electron scattering is essentially the same as in elastic scattering. For light nuclei the conceptually simple method of Born approximation may still be adequate (depending, again, on the accuracy of the data). For medium and heavy nuclei it is not. The inelastic form factors of the Born approximation, in general, have zeroes in the physical domain of momentum transfers. Therefore, the cross section, if it is dominated by one form factor, again exhibits the typical diffraction pattern of the Born approximation. The diffraction zeroes are replaced with minima and are shifted from their initial position if Coulomb distortion is taken into account. Also the absolute values of the cross section can be widely different from what they are in the Born approximation, depending on the value of the scattering angle.

The partial wave analysis of inelastic scattering is conceptually similar to the case of elastic scattering but technically much more involved. The first such analyses were carried out in the mid-nineteen-sixties[16]. (Griffy et al. 1963, Scheck 1966). A good starting point is the interaction term in the form of (2.85). It is appropriate to expand the electron wave functions in terms of the central field solutions (2.104). The initial state $|k\rangle$ is determined by the requirement that in the asymptotic domain it contain the plane wave and incoming spherical waves. Similarly, the

[16]The much simpler case of monopole excitations was treated in Alder et al. (1963).

final state is the analogous superposition of plane wave and outgoing spherical wave. Inserting these (properly normalized) functions into the matrix element (2.85) yields a multiple sum of matrix elements of the interaction between states of good angular momentum and parity. This fact allows one to make use of the selection rules due to angular momentum and parity conservation and to perform all angular and spin integrals by means of standard angular momentum algebra. This leaves one with a sum over radial integrals involving the radial functions $f_k(r)$, $g_k(r)$ and some nuclear radial quantity. We know from the analysis of elastic scattering that for $E \simeq 300\,\mathrm{MeV}$ about the nine lowest partial waves penetrate into the nucleus. Obviously, these are the ones which are sensitive to details of the transition charge and current densities. Here, the radial integrals entering the expansion of the scattering amplitude are obtained by numerical integration. For the higher partial waves the eigenfunctions of the point charge may be used and, if one is lucky, the radial integrals can be done analytically (Reynolds et al. 1964). The complexity of such calculations lies in the high number of partial waves which contribute and in the complicated pattern of terms allowed by the selection rules of angular momentum.

2.6 Muonic Atoms – Introduction

Like any other long-lived negatively charged particle the muon can be captured in the static Coulomb field of a nucleus and thus can form a hydrogen-like exotic atom. This system has peculiar and unique properties, regarding both its *spatial dimensions* and its dynamical *time structure*, which make it an important tool both in exploring electroweak interactions and in probing properties of the nucleus.

This section summarizes first the properties of the muon which are relevant for the subsequent sections of this chapter. We then give a first qualitative picture of the properties of the muonic atoms and their applications. The section closes with a derivation of bound central field solutions in static Coulomb potentials.

Specific and quantitative applications of muonic atoms to quantum electrodynamics and to the investigation of nuclear properties are treated in Sects. 2.7 and 2.8, respectively.

2.6.1 Properties of Free Muons

The muon has all properties of a "heavy electron". It appears in two charge states μ^- and μ^+, which are antiparticles of each other. Its charge is equal to the charge

of the electron[17]; its spin is 1/2; it carries *lepton number* (see Chap. 3). Its *mass* is about 207 times larger than the electron mass. More precisely

$$m_\mu/m_e = 206.768259(62). \tag{2.136}$$

This number is obtained by combining the measured values of

(i) the ratio of magnetic moments μ_μ/μ_p of muon and proton;
(ii) the hyperfine splitting $\Delta E = E(F = 1) - E(F = 0)$ of muonium;
(iii) the anomaly of the g-factor of the muon, $a_\mu = \frac{1}{2}(|g_\mu| - 2)$.[18]

[The same combination of data gives very precise information on the equality of the charges of the muon and the electron].

The mass value is known to better than 1 ppm [RPP94]:

$$m_\mu = 105.658367(4)\text{MeV}/c^2. \tag{2.137}$$

The fact that μ^- carries the charge $Q = -|e|$ means that it has exactly the same coupling to the electromagnetic field as the electron. In Chap. 3 we shall see that also the weak interactions of muons are exactly the same as those of electrons. Actually, the same statements seem to apply also to the τ-lepton with mass

$$m_\tau = 1776.82(16)\text{MeV}/c^2. \tag{2.138}$$

In this sense the interactions of leptons are *universal*: The structure of the coupling terms to the Maxwell field and to the bosons of weak interactions are identically the same for the three kinds of "electrons" e^-, μ^-, τ^-. Their coupling strengths (i.e. their electric and weak "charges", respectively) to photons and to weak bosons respectively are the same.

All *quantitative* differences in physical properties of electrons, muons and τ-leptons (such as anomaly of magnetic dipole moments, scattering cross sections, decay amplitudes) will be due solely to the difference in their *masses*. This can be understood in a qualitative manner as follows. A specific physical situation is always characterized by a typical spatial dimension (examples: Bohr radius $a_B = \hbar^2/e^2m$, Compton wavelength $\lambda\!\!\!^{-} = \hbar/mc$) and typical momenta (examples: momentum in a bound atomic state, momentum transfer in a scattering amplitude) which yield the bulk of the quantity that one wishes to calculate. However, the scale of these characteristic dimensions is set by the mass of the particle or, in some cases, by the ratio or difference of masses of different leptons (examples: vacuum polarization due to virtual electron-positron pairs in electronic and in muonic atoms, g-factor anomaly for electrons and for muons). We shall encounter many examples below, in this chapter and in Chap. 3.

[17] This is known to at least 2 ppm. Cf. the summary by H. Primakoff in "Muon physics" [MUP77].
[18] See e.g. Scheck (1978).

The *magnetic moment* of the muon relative to the magnetic moment of the proton is known very precisely from measurements in muonium:

$$|\mu_\mu|/\mu_\mathrm{p} = 3.18334547(47) \tag{2.139}$$

It is practically a normal Dirac moment,

$$\mu_\mu = \frac{1}{2} g_\mu \frac{Q}{2m_\mu} (Q = -|e|), \tag{2.140}$$

with $|g_\mu| \simeq 2$, the deviation of $|g_\mu|$ from 2, the so-called anomaly a_μ, being predictable on the basis of higher order radiative corrections. This anomaly is defined as $a_\mu = \frac{1}{2}\left(|g_\mu| - 2\right)$. The measured value of this anomaly is (Bailey et al. 1979).

$$a_\mu = 116592089(54) \times 10^{-11} \tag{2.141}$$

In the same experiment the equality of $g_{\mu-}$ and $-g_{\mu+}$ which is predicted by the invariance of the muon's interactions under the combined operation *CPT* (charge conjugation C, space reflection P, and time reversal T) has been tested with the result

$$\frac{g_+ - g_-}{g_\mathrm{average}} = -0.11 \pm 0.12 \tag{2.141'}$$

In contrast to the electron, the muon is unstable. Its primary decay mode is

$$\mu^- \to e^- \bar{\nu}_e \nu_\mu \quad (\mu^+ \to e^+ \nu_e \bar{\nu}_\mu);$$

its lifetime is

$$\tau_\mu = 2.197034(21) \times 10^{-6}\mathrm{s} \tag{2.142}$$

(see Chap. 3). This time is very long compared to typical time scales of electromagnetic processes of muons in a target.

2.6.2 Muonic Atoms, Qualitative Discussion

As the Pauli exclusion principle is not effective between muons and electrons, the trapped muon runs through its Bohr cascade towards the 1s-state, irrespective of the presence of the electronic shells of the host atom. Before we turn to the quantitative analysis of muonic atoms let us first discuss their characteristic spatial dimensions, energy scales and time scales.

Energy scales and spatial dimensions. Since the Bohr radius $a_\mathrm{B} = 1/Z\alpha m$ is inversely proportional to the mass of the charged lepton (more precisely: the *reduced* mass of the lepton-nucleus system) the orbits of a muonic atom are smaller by a

factor of about 207 [see(2.136)] than the orbits of the electrons of the host atom. If the principal quantum number is smaller than n_0, where

$$n_0^2 a_{\mathrm{B}}(m_\mu) \lesssim a_B(m_e),$$

the muonic orbits $(n, l = n-1)$ lie inside the electronic 1s-orbit. This happens for

$$n \lesssim n_0 \simeq \sqrt{m_\mu/m_e} \simeq 14.$$

Therefore, the states with $n \lesssim n_0$ of the muonic atom are essentially hydrogen-like up to screening effects by the electronic shells of the host atom. Screening will be the smaller, the lower the orbit. Thus, for a first qualitative orientation we may use the equations for the nonrelativistic hydrogen atom. The binding energy of a bound state with principal quantum number n is

$$E_n^{(\mathrm{n.r.})} = -m_\mu (Z\alpha)^2/2n^2. \tag{2.143}$$

The first relativistic correction to this is of order $(Z\alpha)^4$ but its magnitude relative to (2.143) is independent of the mass. Thus, the relative importance of relativistic effects in muonic atoms is approximately the same as in electronic atoms. The relevant parameter is $Z\alpha$. For light nuclei these effects will be small, for heavy nuclei such as lead $(Z = 82)$ where $Z\alpha \simeq 0.6$ they will be important. For most estimates and qualitative considerations the formulae of the hydrogen atom will be adequate. The wave functions are [see (6.52)]:

$$\psi_{nlm}(\boldsymbol{r}) = \frac{1}{r} y_{nl}(r) Y_{lm}(\theta, \varphi), \tag{2.144}$$

$$y_{nl}(\boldsymbol{r}) = \sqrt{\frac{(l+n)!}{a_B(n-l-1)!}} \frac{1}{n(2l+1)!} z^{l+1} e^{-z/2} \times {}_1F_1(-n+l-1; 2l+2; z), \tag{2.145}$$

where

$$a_B = 1/Z\alpha\mu, \tag{2.145a}$$

μ being the reduced mass, and z is the dimensionless variable

$$z = \frac{2}{n a_{\mathrm{B}}} r. \tag{2.145b}$$

The symbol ${}_1F_1$ denotes the confluent hypergeometric function [ABS65].

Let us calculate the Bohr radius for a light, two medium weight and a heavy nucleus, and let us compare it to the nuclear r.m.s. radius:

Nucleus	$\langle r^2\rangle^{1/2}$[fm]	$a_B(m)$[fm]
^{4}He($Z=2$)	3.1	128
^{16}O($Z=8$)	2.6	32
^{40}Ca($Z=20$)	3.5	12.8
^{208}Pb($Z=82$)	5.5	3.12

We see from this comparison that from about $Z = 20$ upwards the low muonic orbits start penetrating into the nucleus more and more. Accordingly, the low muonic states must become more and more sensitive, as Z increases, to the finite size of the nucleus and, in particular, to the deviation of the nuclear charge distribution from a point charge. Of course, for large Z the estimates for the binding energies and the radii of low-lying orbits given above become unrealistic. Let us illustrate this by comparing the 2p–1s transition energy in *lead*, for a point charge and for a realistic charge distribution[19]:

$$(E_{2p1/2} - E_{1s})_{\substack{\text{point charge}\\(Z=82)}} = (-5.38 + 20.99)\,\text{MeV} = 15.61\,\text{MeV},$$

$$(E_{2p1/2} - E_{1s})_{\text{finite size}} = (-4.78 + 10.52)\,\text{MeV} = 5.74\,\text{MeV}.$$

We note that the 1s state of this heavy atom shows a much weaker binding than in the pure $1/r$ potential. The 2p state is also shifted upwards, but by a much smaller proportion than the 1s state. At the same time the radial wave functions are also affected by the finite extension of the nuclear charge density. As the states are less bound than for a point-like charge, the radial functions are driven towards larger values of r. Nevertheless, it is still true that the muon in a 1s state of a heavy atom penetrates strongly into the nuclear interior.

Time scales in muonic atoms. The fate of the muon between the moment of its creation, say, from pion decay,

$$\pi^- \to \mu^- + \bar{\nu}_\mu \tag{2.146}$$

in a continuum state until it is trapped in some high-lying Bohr orbit of a target atom, i.e. the moderation of the muon from its initial positive energy down to zero kinetic energy through ionization and inelastic scattering processes in the target, is complicated and, in fact, not too well known. For our purposes it will be sufficient to know that these early stages take a relatively short time, of the order of 10^{-10}–10^{-12} s. The muon eventually lands in some bound state with quantum numbers (n, l). The question as to what the initial distribution in n and l is, can be (and has been) studied experimentally by looking at the intensities of γ-transitions

[19]The point charge values are calculated from (2.162) below. The finite size values are taken from Engfer et al. (1974).

between these highest states of the cascade. There is, as yet, no satisfactory theory of these initial distributions–a fact that may not seem so surprising if one realizes that the initial (n, l) distribution is a complicated function of the structure and chemical composition of the target material.

The cascade proceeds predominantly through

Auger transitions, i.e. through emission of electrons in the host atom, and *electric dipole* γ-radiation.

Auger transitions are important mainly in the upper part of the cascade. They are relatively more important for the lighter elements.[20]

In the lower part of the cascade the transition energies become large, and E1 γ-transitions quickly take over. The selection rules of Auger and of γ(E1)-transitions are

$$\text{Auger}: \quad l_\mathrm{f} = l_\mathrm{i} \pm 1, \quad \Delta n = \text{minimal}, \tag{2.147}$$

$$\text{E1}: \quad l_\mathrm{f} = l_i \pm 1, \quad \Delta n = \text{maximal}. \tag{2.148}$$

The selection rule for Δl is a strict one, the rules for Δn are somewhat empirical. They arise from the energy dependence of the rates and from the n-dependence of the transition matrix elements.

The selection rules have the effect of favouring *circular orbits* $(n, l = n-1)$; the lower n, the higher are the relative intensities for transitions between circular orbits. Transitions between inner, non-circular states have comparatively low intensities.

It is not difficult to estimate the time scale of these γ-transitions. The transition probability for an electric dipole transition is given by

$$T(\mathrm{E1}) = 8\pi c \frac{2\alpha}{9} \left(\frac{\Delta E}{\hbar c}\right)^3 \frac{1}{2l_\mathrm{i}+1} (l_\mathrm{f} \,\|Y_1\|\, l_\mathrm{i})^2 \,\langle n_\mathrm{f} l_\mathrm{f}|r|n_\mathrm{i} l_\mathrm{i}\rangle^2 . \tag{2.149}$$

Let us calculate T(E1) for a transition between circular orbits $(n_\mathrm{i} \equiv n, l_\mathrm{i} = n-1)$ $(n_\mathrm{f} = n-1,\ l_\mathrm{f} = n-2)$ with the wave functions (2.144). We have

$$\begin{aligned}
(l_\mathrm{f} \,\|Y_1\|\, l_\mathrm{i}) &= (-)^{l_\mathrm{i}+1} \sqrt{\frac{3}{4\pi}} \sqrt{(2l_\mathrm{i}+1)(2l_\mathrm{i}-1)} \begin{pmatrix} l_\mathrm{i} & 1 & l_\mathrm{i}-1 \\ 0 & 0 & 0 \end{pmatrix} \\
&= -\sqrt{\frac{3(n-1)}{4\pi}}, \\
\Delta E \equiv E_n - E_{n-1} &= \frac{2n-1}{2n^2(n-1)^2} (Z\alpha)^2 \mu c^2, \\
\langle n, n-1|r\,|n-1, n-2\rangle &= a_\mathrm{B} \frac{2^{2n+1} n^{n+1} (n-1)^{n+2}}{(2n-1)^{2n} \sqrt{2(2n-1)(n-1)}}.
\end{aligned}$$

[20] See Vol. I, Chap. III of [MUP77].

Putting these results together, we find

$$\overline{h}T(\mathrm{E1}; n \to n-1) = \frac{2^{4n} n^{2n-4} (n-1)^{2n-2}}{3(2n-1)^{4n-1}} \alpha^5 \mu c^2 Z^4,$$

or, expressing μ in terms of the electron mass,

$$T(\mathrm{E1}; n \to n-1) \simeq 5.355 \times 10^9 \frac{2^{4n} n^{2n-4} (n-1)^{2n-2}}{(2n-1)^{4n-1}} \times \frac{\mu}{m_\mathrm{e}} Z^4 [\mathrm{s}^{-1}]. \quad (2.150)$$

The transition probability is proportional to the reduced mass and to the fourth power of the nuclear charge. For the sake of illustration let us calculate the transition time

$$\tau(\mathrm{E1}; n \to n') = 1/T(\mathrm{E1}; n \to n')$$

for the transitions $\{(n = 14,\ l = 13) \to (n = 13,\ l = 12)\}$ and $\{2\mathrm{p} \to 1\mathrm{s}\}$:

$$\tau(\mathrm{E1}; 14 \to 13) \simeq 2.26(1 + 0.113/A)10^{-7}/Z^4 \mathrm{s}, \quad (2.150a)$$

$$\tau(\mathrm{E1}; 2 \to 1) \simeq 7.72(1 + 0.113/A)10^{-12}/Z^4 \mathrm{s}. \quad (2.150b)$$

[The correction factor stems from the reduced mass $1/\mu \simeq (1/m_\mu)(1 + m_\mu/Am_\mathrm{N})$]. These times must be compared with the lifetime (2.142) of the muon, $\tau \simeq 2.2 \times 10^{-6}$ S. In a very light system such as hydrogen ($Z = 1$) the upper part of the cascade is relatively slow, so that many muons will decay during the cascade before they reach the 1s state. In a heavy atom such as lead ($Z = 82$), however, the cascade times are scaled down by the factor Z^4. Rough interpolation between $n = 14$ and $n = 2$ shows that the whole cascade (assuming E1 transitions only) will take about 10^{-14} s. This time is extremely short as compared to τ_μ.

We conclude: For medium and heavy nuclei the trapping time and the cascade are very short as compared to the muon lifetime. In these atoms the muon behaves exactly like a stable heavy electron. In very light atoms such as muonic hydrogen, however, the upper part of the cascade is affected appreciably by muon decay, at the expense of the intensities of the cascade γ-transitions. These qualitative considerations are confirmed by detailed cascade calculations on computers. A detailed knowledge of the cascade is important in many experimental situations. For instance, if one sets out to study properties of inner states such as the metastable 2s state, these calculations are essential in predicting the relative populations of these states.

After having reached the 1s state the muon either decays, or is captured by the nucleus through the weak interaction process

$$\mu^- + (Z, A) \to (Z-1, A) + \nu_\mu.$$

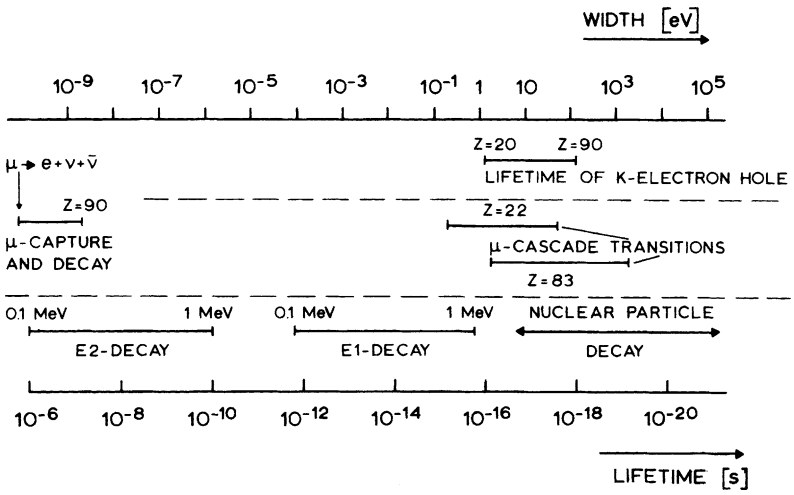

Fig. 2.9 Comparison of various lifetimes which are relevant for the dynamics in a muonic atom. The lower part of the figure shows typical times for nuclear γ-and particle decays. Taken from [MUP77] Vol. I, Chap. III

The capture rate Γ_{cap}, roughly, increases like Z^4. In light elements decay width and capture width are of similar magnitude. However, as Z increases, the capture reaction becomes predominant. In the heavy atoms, the lifetime of the muon is reduced, due to capture, to about 10^{-7} s.

These time scales of the muonic atom are illustrated in Fig. 2.9. They should be compared to typical time scales in the electronic shell as well as in the nuclear excitation spectrum. As to the former, we show, as an example, the lifetime of a hole state in the K-shell. As may be seen from the figure this atomic lifetime is comparable to cascade times of the muon. One consequence is this: If the muon, in the upper part of the cascade, has created a hole in e.g. the K-shell, it will make the rest of its cascade in presence of an incomplete electronic shell. This may be relevant in precision measurements of muonic transitions if the screening of the nuclear charge by the electrons has to be taken into account.

Regarding the nuclear excitation spectrum it can happen that due to accidental (near) degeneracy between muonic transition energies and the energies of certain nuclear excited states, the nucleus remains in an excited state when the muon has reached the 1s orbit. Comparison of typical lifetimes of such nuclear states with the lifetime $\tau(1s)$ of the muon in its 1s state (due to free decay and capture) shows a remarkable fact: The nuclear lifetimes are generally much shorter than $\tau(1s)$. Therefore, the nucleus can return to its ground state, through emission of a γ-ray, *while the muon remains in the 1s orbit*. This offers the unique possibility of observing a nuclear transition in the presence of the muon in the 1s orbit which,

as we know, penetrates strongly into the interior of the nucleus. The additional charge – e leads to *isomer shifts*, the interaction of the nuclear magnetic moment with the muon's magnetic moment to *magnetic hyperfine structure*.

On the basis of these qualitative considerations we may group the information obtainable from muonic atoms according to the spatial extension of the orbits in question.

(a) For *intermediate and heavy elements* we distinguish

(a.1) *High-lying orbits*: These are the ones which overlap strongly with the electronic cloud. These states are affected in an essential way by the state of the host atom and by the chemical composition and physical structure of the target.

(a.2) *Very low orbits*: As the muon moves well inside the lowest electronic shell, screening effects are very small and often negligible. These orbits penetrate into the nucleus and, therefore, are sensitive to the spatial structure of nuclear charge, magnetization and current densities. As the transition energies are comparable to nuclear excitation energies and as the overlap with nuclear states is large, dynamical mixing effects between muonic and nuclear states can occur. Also, instead of emitting γ-rays the muon can transfer its energy to the nucleus which then decays via fission or via emission of neutrons. These radiationless transitions are especially important in heavy elements. Muon induced fission is an important tool for the study of fission in transuranium elements (fission barriers, fission isomers).

(a.3) *Intermediate orbits* ($3 \lesssim n \lesssim 6$): These are the ones which are the most hydrogen-like. Indeed, effects due to the finite size of the nucleus are small and can be calculated to a high degree of accuracy. Likewise, the screening effects due to the electronic cloud are small and under good control. Energies and wave functions of these states can be calculated to very high precision. These orbits are ideally suited for model-independent measurements of *static nuclear moments* (especially electric quadrupole and hexadecapole moments), and of *radiative corrections*.

Figure 2.10 shows the densities $R_{nl}^2(r)\cdot r^2$ of selected muonic circular orbits in a heavy element (bismuth, $Z = 83$), in comparison to the nuclear charge density and to the density of K and L electrons. The figure illustrates quite clearly the three groups of orbits discussed above.

(b) In *very light elements* (such as hydrogen and helium) we have essentially only orbits of type (a.3). The electrons of the host atom are completely stripped off by the Auger effect so that the muon sees the bare charge of the nucleus. On the nuclear side, the muonic orbit radii are such that penetration effects are small. Thus, the study of energies of very light muonic atoms concerns primarily tests of radiative corrections as predicted by quantum electrodynamics.

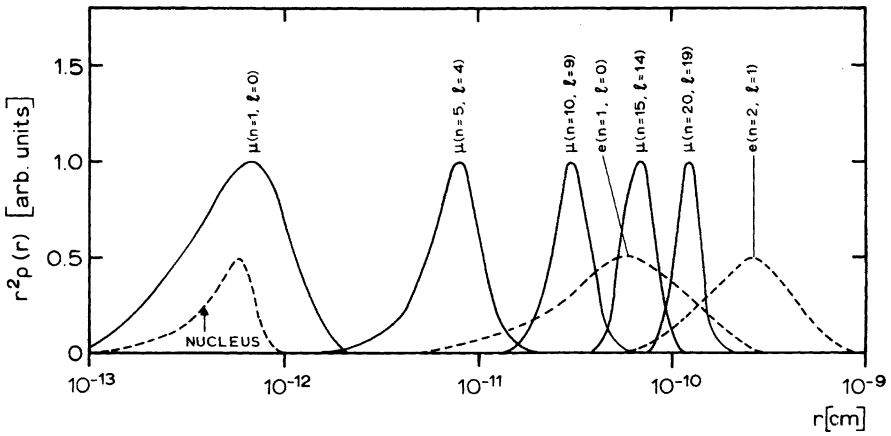

Fig. 2.10 Spatial structure of a heavy muonic atom. The scale in r (abscissa) is logarithmic; the densities are not normalized. Take from [MUP77] Vol. I, Chap. III

2.6.3 Dirac Bound States in a Central Field

In a quantitative analysis of data on muonic atoms (i.e. transition energies and X-ray intensities) we need the exact bound state solutions of the Dirac equation. In the case of a spherically symmetric potential (central field) the total angular momentum $\boldsymbol{j} = \boldsymbol{l} + \boldsymbol{s}$ commutes with the energy and can be chosen diagonal. The problem is then reduced to the calculation of the radial wave functions $f_\kappa(r)$ and $g_\kappa(r)$ of the central field solutions [QP07]

$$\phi_{km}(\boldsymbol{r}) = \begin{pmatrix} g_\kappa(r)\ \varphi_{km} \\ \mathrm{i} f_\kappa(r)\ \varphi_{-\kappa m} \end{pmatrix}. \tag{2.151}$$

We recall the meaning of the symbols in (2.151):

$$\kappa = \pm 1,\ \pm 2,\ \pm 3,\ \ldots \text{ (Dirac quantum number)},$$

$$j = |\kappa| - \tfrac{1}{2} \text{ and } \begin{cases} l = \kappa & \text{for } \kappa > 0, \\ l = -\kappa - 1 & \text{for } \kappa < 0, \end{cases}$$

$$\varphi_{\kappa m} \equiv \varphi_{jlm} = \sum_{m_l, m_s} \left(l m_l \frac{1}{2}\ m_s | j m \right) Y_{lm} \chi_{m_s}.$$

$f(r)$ and $g(r)$ satisfy a system of first-order differential equations, (2.105), which contains the spherically symmetric potential $V(r)$, viz.

$$\frac{\mathrm{d}f_\kappa}{\mathrm{d}r} = \frac{\kappa - 1}{r} f_\kappa - \{E - V(r) - m\} g_\kappa,$$
$$\frac{\mathrm{d}g_\kappa}{\mathrm{d}r} = -\frac{\kappa + 1}{r} g_\kappa + \{E - V(r) + m\} f_\kappa. \tag{2.152}$$

g_κ is called the "large" component, f_κ the "small" component: in the nonrelativistic limit $m - |E| \ll 1$, f_κ vanishes, whilst g_κ goes over into the corresponding Schrödinger wave function (see below).

Case (a): Potential of a point-like charge
As nuclei are well confined systems the electrostatic potential (2.117) around any nucleus approaches rapidly the potential of a point charge, $V_\mathrm{c} = -Z\alpha/r$, outside the nuclear radius. Therefore, this potential is the reference case to which the actual potential should be compared. The bound states of the true potential are shifted with respect to the case of the point charge. The corresponding wave functions are more or less distorted Coulombic wave functions. Information about the true potential is primarily contained in the shifts of the energy levels, to some extent also in the wave functions and in observables derived from them.

Technically, the bound state problem is different for the two cases and the potential of the point charge must be considered separately. The reason for this technical difference is easy to understand: The true potential of an extended charge distribution is regular at the region, $r = 0$. (Consider, for instance, the homogeneous density, for which $V(r) \sim C_0 + C_1 r^2$ is parabolic.) $V_\mathrm{c}(r)$, on the contrary, is singular at $r = 0$. In any relativistic wave equation, both V_c and its square enter. This is obvious in the Klein–Gordon equation (6.36) where the term $(E - V_\mathrm{c}(r))^2$ is added to the kinetic energy. In the case of Dirac spinors we know that each component also satisfies the Klein–Gordon equation. Alternately, this may be recovered directly from (2.152) by deriving from them uncoupled second-order equations for $f(r)$ and $g(r)$ separately (so-called "iterated form" of the Dirac equation).

In either case, the term ${V_\mathrm{c}}^2(r)$, being proportional to $1/r^2$, has the same type of singularity at the origin as the centrifugal potential $l(l+1)/r^2$. This singularity, as is well-known, determines the behaviour of the radial wave functions at $r = 0$. Thus, for a regular potential we expect the standard behaviour r^l or r^{-l-1}, while for the $1/r$ potential the characteristic exponent is modified by terms of order $Z\alpha$. At $r \to \infty$, on the other hand, the two cases are obviously the same. So only the solutions inside a suitably defined matching radius R, where the two potentials differ substantially, must be derived separately. After this long introduction we now turn to the derivation of the bound Coulomb states.

For very large r the differential equations (2.152) give the approximate equation

$$g''(r) - (m^2 - E^2)\, g(r) \simeq 0$$
$$f'(r) \simeq -(E - m) g(r)\,, \quad (\text{large}\, r)$$

For bound states $E < m$ and $\lambda := \sqrt{m^2 - E^2}$ is real positive. Thus $g(r)$ behaves like $\mathrm{e}^{-\lambda r}$, $f(r)$ like $\sqrt{(m-E)/(E+m)}g(r)$. For convenience we take out a factor $1/r$, in f and g, and we make the ansatz

$$g(r) = \frac{1}{r}\mathrm{e}^{-\lambda r} \sqrt{E+m}\,\{y_1(r) + y_2(r)\},$$
$$f(r) = \frac{1}{r}\mathrm{e}^{-\lambda r} \sqrt{m-E}\,\{y_1(r) - y_2(r)\}. \tag{2.153}$$

The asymptotic behaviour of $y_1(r)$ and $y_2(r)$ must be such that the exponential factor $\mathrm{e}^{-\lambda r}$ is not compensated. Let $x := 2\lambda r$, then y_1 and y_2 satisfy the system

$$\frac{\mathrm{d}y_1}{\mathrm{d}x} = \left(1 - \frac{Z\alpha E}{\lambda x}\right) y_1 - \left(\frac{\kappa}{x} + \frac{Z\alpha m}{\lambda x}\right) y_2,$$
$$\frac{\mathrm{d}y_2}{\mathrm{d}x} = \left(-\frac{\kappa}{x} + \frac{Z\alpha m}{\lambda x}\right) y_1 + \frac{Z\alpha E}{\lambda x} y_2. \tag{2.154}$$

The behaviour at $r = 0$ remains to be determined, keeping in mind the remarks made before. For that purpose, we write

$$y_{1,2}(x) = x^\gamma \phi_{1,2}(x), \tag{2.155}$$

with $\phi_{1,2}(0) \neq 0$ but finite and determine γ from (2.154): For $x = 0$ we obtain the linear system

$$\gamma\phi_1(0) = -\frac{Z\alpha E}{\lambda}\,\phi_1(0) - \left(\kappa + \frac{Z\alpha m}{\lambda}\right)\phi_2(0),$$
$$\gamma\phi_2(0) = \left(-\kappa + \frac{Z\alpha m}{\lambda}\right)\phi_1(0) + \frac{Z\alpha E}{\lambda}\,\phi_2(0)\,.$$

This homogeneous system has a nontrivial solution only if the determinant of the coefficient matrix

$$\begin{pmatrix} \gamma + Z\alpha E/\lambda & \kappa + Z\alpha m/\lambda \\ \kappa - Z\alpha m/\lambda & \gamma - Z\alpha E/\lambda \end{pmatrix}$$

vanishes. This gives $\gamma^2 = \kappa^2 - (Z\alpha)^2$. The solutions regular at the origin require the positive square root,

$$\gamma = \sqrt{\kappa^2 - (Z\alpha)^2}. \tag{2.156}$$

With the ansatz (2.155), where γ is given by (2.156), one derives easily the differential equations satisfied by $\phi_1(x)$ and $\phi_2(x)$

$$\frac{\mathrm{d}\phi_1}{\mathrm{d}x} = \left\{1 - \left(\gamma + \frac{Z\alpha E}{\lambda}\right)\frac{1}{x}\right\}\phi_1 - \left(\kappa + \frac{Z\alpha m}{\lambda}\right)\frac{1}{x}\phi_2,$$
$$\frac{\mathrm{d}\phi_2}{\mathrm{d}x} = -\left(\kappa - \frac{Z\alpha m}{\lambda}\right)\frac{1}{x}\phi_1 - \left(\gamma - \frac{Z\alpha E}{\lambda}\right)\frac{1}{x}\phi_2. \tag{2.157}$$

The functions $\phi_i(x)$ represent what remains of the radial functions f and g after we have taken out the characteristic exponent (x^γ) near the origin and the exponential factor ($\mathrm{e}^{-x/2}$) at infinity. Our experience with analogous problems in nonrelativistic quantum mechanics suggests that $\phi_i(x)$ are simple polynomials (they must be orthogonal for fixed κ). In fact, one can show that they can be written in terms of the well-known confluent hypergeometric function. One way of seeing this is the following: Starting from (2.157) derive a second-order differential equation for ϕ_2 (or ϕ_1) alone. One finds

$$x\frac{\mathrm{d}^2\phi_2}{\mathrm{d}x^2} + (2\gamma + 1 - x)\frac{\mathrm{d}\phi_2}{\mathrm{d}x} - \left(\gamma - \frac{Z\alpha E}{\lambda}\right)\phi_2 = 0. \tag{2.158}$$

This is, indeed, Kummer's equation with $a \equiv \gamma - Z\alpha E/\lambda$, $b \equiv 2\gamma + 1$. The solution with the required properties is [ABS65, ART31]

$$\phi_2(x) = {}_1F_1\left(\gamma - \frac{Z\alpha E}{\lambda};\ 2\gamma + 1;\ x\right). \tag{2.159a}$$

ϕ_1 is found from the second equation (2.157) and the recurrence relation

$$x\,{}_1F_1'(a;\ b;\ x) + a\,{}_1F_1\,(a;\ b;\ x) = a\,{}_1F_1\,(a + 1;\ b;\ x)$$

for the confluent hypergeometric function. Thus

$$\phi_1(x) = \frac{Z\alpha E/\lambda - \gamma}{\kappa - Z\alpha m/\lambda}\,{}_1F_1\,(1 + \gamma - Z\alpha E/\lambda;\ 2\gamma + 1;\ x). \tag{2.159b}$$

The asymptotic behaviour of ${}_1F_1$ is, to leading order in $1/x$,

$${}_1F_1\,(a;\ b;\ x) \sim \frac{\Gamma(b)}{\Gamma(b-a)}\,(-x)^{-a} + \frac{\Gamma(b)}{\Gamma(a)}\mathrm{e}^x x^{a-b}. \tag{2.160}$$

Obviously, the second term of this must vanish if we do not wish to destroy the exponential decrease of the bound state solutions, i.e. the factor $\mathrm{e}^{-x/2}$ in (2.153). This can only be achieved if the parameter a is zero or a negative integer because in that case $1/\Gamma(a)$ vanishes. When applied to ϕ_2, this gives the condition

$$Z\alpha E/\lambda - \gamma = n', \tag{2.161}$$

with

$$\lambda = \sqrt{m^2 - E^2},\ n' = 0,\ 1, 2, \ldots$$

Does the same condition also make $\phi_1(x)$ of (2.159b) remain regular at infinity? For $n' \geq 1$ this is obvious. For $n' = 0$, a little more care is necessary: The function ${}_1F_1\ (1;\ 2\gamma + 1; x)$ is not regular but the factor $Z\alpha E/\lambda - \gamma = 0$ in front of it makes ϕ_1 vanish, provided the denominator $(\kappa - Z\alpha m/\lambda)$ does not vanish. This is what has to be checked. With $\gamma = Z\alpha E/\lambda$ we have

$$\kappa^2 = \gamma^2 + (Z\alpha)^2 = (Z\alpha)^2\ \frac{\lambda^2 + E^2}{\lambda^2} = \left(Z\alpha \frac{m}{\lambda}\right)^2$$

and therefore $\kappa = \pm Z\alpha m/\lambda$. The solution $\kappa = +Z\alpha m/\lambda$ must indeed be excluded, whilst $\kappa = -Z\alpha m/\lambda$ is acceptable. Therefore, for $n' = 0$ only negative κ is allowed.

For convenience, we set $n' = n - |\kappa|$ with $n = 1, 2, \ldots$ Our results can then be summarized as follows. From (2.161) we find

$$E_{n|\kappa|} = m \left\{ 1 + \left(\frac{Z\alpha}{n - |\kappa| + \sqrt{\kappa^2 - (Z\alpha)^2}} \right)^2 \right\}^{-1/2}, \tag{2.162}$$

where the quantum numbers n, κ and $|\kappa| - 1/2$ assume the following values:

$$\begin{aligned} &n = 1, 2, \ldots, \\ &\kappa = \pm\ 1,\ \ \pm 2,\ \ \ldots,\ \ \pm(n-1), -n, \\ &j = |\kappa| - \frac{1}{2} = \frac{1}{2},\ \frac{3}{2},\ \ \ldots,\ n - \frac{1}{2}. \end{aligned} \tag{2.163}$$

$\kappa = +n$, as we said above, is excluded. The integer n is the familiar principal quantum number of the nonrelativistic hydrogen atom. This can be seen, for instance, by expanding the energy eigenvalues (2.162) in terms of $Z\alpha$,

$$E_{n|\kappa|} \simeq m \left\{ 1 - \frac{(Z\alpha)^2}{2n^2} - \frac{(Z\alpha)^4}{2n^4} \left(\frac{n}{|\kappa|} - \frac{3}{4} \right) \right\}, \tag{2.164}$$

the first term of which is the rest mass, whilst the second gives the binding energy (2.143) of the nonrelativistic hydrogen atom. The third term is the first relativistic correction. This term is independent of the mass (relative to the others) but depends on the angular momentum $j = |\kappa| - \frac{1}{2}$. For constant n it is relatively more important for small values of j than for large values.

As may be seen from the exact formula (2.162) the dynamical l-degeneracy of the nonrelativistic hydrogen atom is almost completely lifted. Only energy eigenvalues of equal n and $|\kappa|$ are degenerate. As κ can be positive and negative, except for the

largest value of κ where $\kappa = -n$, all j-values except for the highest $j = n - \frac{1}{2}$ have a *two*fold dynamical degeneracy in addition to the usual directional degeneracy in m_j, the magnetic quantum number. Thus, the $2s_{1/2}$ and $2p_{1/2}$ states are degenerate, the $3s_{1/2}$ and $3p_{1/2}$ states, the $3p_{3/2}$ and $3d_{3/2}$ states, and so on.

This remaining degeneracy of the relativistic atom is lifted eventually by radiative corrections (Lamb shift).

The eigenfunctions are given by our equations (2.153, 2.155, 2.159). The normalization to 1 is best performed by making use of well-known integrals involving confluent hypergeometric functions, exponentials and powers. The result is

$$\begin{aligned} g_{n\kappa}(r) &= 2\lambda N(n,\kappa)\sqrt{m+E}\, x^{\gamma-1}\mathrm{e}^{-x/2} \\ &\quad \times \Bigg\{ -(n-|\kappa|)_1F_1(-n+|\kappa|+1;2\gamma+1;x) \\ &\quad + \left(\frac{Z\alpha m}{\lambda} - \kappa\right)_1F_1(-n+|\kappa|;2\gamma+1;x)\Bigg\} \qquad (2.165a) \\ f_{n\kappa}(r) &= -2\lambda N(n,\kappa)\sqrt{m-E}\, x^{\gamma-1}\mathrm{e}^{-x/2} \\ &\quad \times \Bigg\{ (n-|\kappa|)_1F_1(-n+|\kappa|+1;2\gamma+1;x) \\ &\quad + \left(\frac{Z\alpha m}{\lambda} - \kappa\right)_1F_1(-n+|\kappa|;2\gamma+1;x)\Bigg\}. \qquad (2.165b) \end{aligned}$$

The normalization constant $N(n,\ \kappa)$ is given by

$$N(n,\kappa) = \frac{\lambda}{m}\frac{1}{\Gamma(2\gamma+1)}\left\{\frac{\Gamma(2\gamma+n-|\kappa|+1)}{2Z\alpha(Z\alpha m/\lambda-\kappa)\Gamma(n-|\kappa|+1)}\right\}^{1/2}. \qquad (2.166a)$$

As before,

$$x = 2\lambda r, \qquad (2.166b)$$

$$\lambda = \sqrt{m^2 - E_{n|\kappa|}^2} = \frac{Z\alpha m}{\sqrt{n^2 - 2(n-|\kappa|)(|\kappa|-\gamma)}}, \qquad (2.166c)$$

$$\gamma = \sqrt{\kappa^2 - (Z\alpha)^2}. \qquad (2.166d)$$

Strictly speaking, the orbital angular momentum l is not a good quantum number. However, in the limit of weakly relativistic motion, i.e. for $Z\alpha \ll 1$, $\sqrt{m-E} = \mathcal{O}(Z\alpha)$ is small compared to $\sqrt{m+E} \simeq \sqrt{2m}$. This shows that the wave function $g_{n\kappa}(r)$ is large compared to the wave function $f_{n\kappa}(r)$. Thus, the upper component in $\phi_{n\kappa m}$, (2.151), is large compared to the lower one, and its angular momentum l can be used to label the state, even though the lower component carries a different

angular momentum $\bar{l} = l \pm 1$. The nomenclature is approximate and refers to the corresponding nonrelativistic situation. As an example let us consider all states with $n = 2$. Here we have

$$n = 2, \kappa = -1, j = \frac{1}{2} : \begin{pmatrix} l = 0 \\ \bar{l} = 1 \end{pmatrix} \text{“}2s_{1/2}\text{-state”},$$
$$n = 2, \kappa = +1, j = \frac{1}{2} : \begin{pmatrix} l = 1 \\ \bar{l} = 0 \end{pmatrix} \text{“}2p_{1/2}\text{-state”},$$
$$n = 2, \kappa = -2, j = \frac{3}{2} : \begin{pmatrix} l = 1 \\ \bar{l} = 2 \end{pmatrix} \text{“}2p_{3/2}\text{-state”}.$$

The example shows that in the relativistic case (i.e. $Z\alpha$ not small compared to 1), the $2p_{1/2}$-state is a closer parent to the $2s_{1/2}$ than to the $2p_{3/2}$. We expect relativistic effects in the $2p_{1/2}$ to be more important than in the $2p_{3/2}$.

The limit of the purely nonrelativistic case can be verified on the expressions (2.165) for the wave functions. As

$$\lambda \simeq \frac{Z\alpha m}{n}\left(1 + \frac{(Z\alpha)^2}{2n^2}\frac{n - |\kappa|}{|\kappa|}\right),$$

this means calculating the wave functions to lowest nonvanishing order in $Z\alpha$. In this limit $m - E \simeq 0$ and $f_{n\kappa}(r) \simeq 0$. For $\kappa > 0$ we have $l = \kappa$,

$$x \simeq \frac{2Z\alpha m}{n} r = \frac{2r}{n a_B} =: z,$$

and

$$g_{n\kappa=l} \simeq 2\frac{Z\alpha m}{n}\frac{Z\alpha}{n}\frac{1}{\Gamma(2l+1)}\sqrt{\frac{\Gamma(n+l+1)}{2Z\alpha(n-l)\Gamma(n-l+1)}}\sqrt{2mz}^{l-1}\mathrm{e}^{-z/2}$$
$$\times(n-l)\left\{{}_1F_1(-n+l;2l+1;z) - {}_1F_1(-n+l+1;2l+1;z)\right\},$$

which equation, by means of the recurrence relation

$$b\left\{{}_1F_1(a;b;z) - {}_1F_1(a-1;b;z)\right\} = z\ {}_1F_1(a;b+1;z) \tag{2.167}$$

goes over into the nonrelativistic wave function $(1/r)y_{nl}(r)$ of (2.145). For negative k, $\bar{l} = -\kappa - 1 = |\kappa| - 1$, $g_{n\kappa}(r)$ must go over into $(1/r)y_{n,\bar{l}}(r)$, since in the nonrelativistic limit the states $\left(n, j = i + \frac{1}{2}\right)$ and $\left(n, j = i - \frac{1}{2}\right)$ have the same radial wave function. That this is indeed so may be verified from (2.165), and the recurrence relation

$$(1 + a - b)\ {}_1F_1(a;b;z) - a\ {}_1F_1(a+1;b;z) + (b-1)\ {}_1F_1(a;b-1;z) = 0 \tag{2.168}$$

(see exercise 2.8).

Case (b): Potential of a spherically symmetric charge distribution of finite size
For simplicity we consider a *spherically symmetric* charge distribution $\rho(r)$ of finite size. (The more general case of an arbitrary density $\rho(r)$ is dealt with in Sect. 2.8) Unlike the case of a point charge, $\rho(r)$ is assumed to be regular at the origin and to admit a Taylor expansion around $r = 0$,

$$\rho(r) = \rho_0 + \rho_1 r + \frac{1}{2!}\rho_2 r^2 + \mathcal{O}(r^3). \tag{2.169}$$

Inserting this series into the formula (2.117) for the potential this yields a similar expansion for $V(r)$:

$$V(r) = -4\pi Z\alpha^2 \left\{ \int_0^\infty \rho(r')r'\,\mathrm{d}r' - \frac{1}{6}\rho_0 r^2 - \frac{1}{12}\,\rho_1 r^3 - \frac{1}{40}\rho_2 r^4 + \mathcal{O}(r^5) \right\}. \tag{2.170}$$

This shows that $V(r)$ behaves like a parabola, $V_0 + V_1 r^2$, close to the origin. As a consequence, the behaviour of the radial solutions $f(r)$ and $g(r)$ near the origin is determined entirely by the centrifugal potential and not by the electrostatic potential. For $\kappa > 0$ the upper component of the spinor (2.151) carries the orbital angular momentum $l = \kappa$, whilst the lower component carries $\bar{l} = \kappa - 1$. We expect, therefore, the solutions regular at the origin to behave according to

$$\kappa > 0 \quad \begin{cases} g_\kappa(r) \sim r^\kappa \\ f_\kappa(r) \sim r^{\kappa-1} \end{cases} . \tag{2.171a}$$

Similarly, for $\kappa < 0$, the upper component has $l = -\kappa - 1$, the lower component has $\bar{l} = -\kappa$, so that we expect

$$\kappa < 0 \begin{cases} g_\kappa(r) \sim r^{-\kappa-1} \\ f_\kappa(r) \sim r^{-\kappa}. \end{cases} \tag{2.171b}$$

It is not difficult to prove these assertions. The second-order differential equations for $f(r)$ and $g(r)$ alone, which one derives from the system (2.152), contain the centrifugal terms $\kappa(\kappa-1)/r^2$ and $\kappa(\kappa+1)/r^2$, respectively. The characteristic exponents α and β in the ansatz $f(r) = r^\alpha \Sigma a_n r^n$ and $g(r) = r^\beta \Sigma b_n r^n$ are found to satisfy the equations

$$\alpha(\alpha+1) = \kappa(\kappa-1), \quad \beta(\beta+1) = \kappa(\kappa+1),$$

whose solutions are $\alpha_1 = \kappa - 1$, $\alpha_2 = -\kappa$ and $\beta_1 = \kappa$, $\beta_2 = -\kappa - 1$. In fact, the two cases of positive and negative κ, can be written in a particularly simple and compact form if we introduce the definitions:

$$\kappa > 0 \begin{cases} g_\kappa(r) = r^\kappa G_\kappa(r), \\ f_\kappa(r) = r^{\kappa-1} F_\kappa(r), \end{cases} \tag{2.171c}$$

$$\kappa < 0 \begin{cases} g_\kappa(r) = r^{-\kappa-1} F_\kappa(r), \\ f_\kappa(r) = -r^{-\kappa} G_\kappa(r). \end{cases} \tag{2.171d}$$

The function F_κ and G_κ obey the system of first-order differential equations

$$\begin{aligned} \frac{\mathrm{d}F_\kappa}{\mathrm{d}r} &= \{V(r) - E + m\ \mathrm{sign}\,\kappa\}\, r G_\kappa, \\ \frac{\mathrm{d}G_\kappa}{\mathrm{d}r} &= -\frac{1}{r}\{(2|\kappa|+1)G_\kappa + [V(r) - E - m\,\mathrm{sign}\,\kappa]F_\kappa\}. \end{aligned} \tag{2.172}$$

with initial conditions

$$\begin{aligned} F_\kappa(0) = a_0 \neq 0, \quad G_\kappa(0) &= -\frac{V(0) - E - m\,\mathrm{sign}\,\kappa}{2|\kappa|+1} a_0, \\ \frac{\mathrm{d}F_\kappa}{\mathrm{d}r}(0) = \frac{\mathrm{d}G_\kappa}{\mathrm{d}r}(0) &= 0. \end{aligned} \tag{2.173}$$

The system (2.172) with the initial conditions (2.173) is well adapted for numerical integration of the wave functions F and G, from which f and g are then obtained by means of (2.171c or d), respectively. These solutions, which by construction are regular at the origin, must also be regular at infinity. This condition fixes the eigenvalues $E_{n\kappa}$ for given κ. In order to achieve this, it is convenient to use the following trick.

The density $\rho(r)$ has a finite extension, i.e. beyond a certain radius R_M the density is zero or negligibly small. (In case of nuclei R_M is typically 2 to 3 times the nuclear radius.) Therefore, for $r \gtrsim R_\mathrm{M}$ the potential $V(r)$ is practically indistinguishable from $V_c = -Z\alpha/r$, the potential of a point-like charge, and the true wave functions (2.171c, d) must be linear combinations of two linearly independent solutions of the system of differential equations treated above, case (a). One such set of independent solutions for V_c could be the solution (2.165), regular at the origin, together with another solution which is singular at the origin.

The trick now consists in constructing that specific linear combination which, for *arbitrary* energy E, decreases exponentially at infinity (i.e. is regular at infinity), irrespective of its behaviour at $r = 0$. Call this solution $(f_\infty,\ g_\infty)$. It then suffices to vary E until the inner solutions $f_0,\ g_0$ which are regular at $r = 0$ and which are obtained by numerical integration, match the outer solution continuously at the point $r = R_\mathrm{M}$, i.e.

$$[f_\infty(r) g_0(r) - g_\infty(r) f_0(r)]_{r=R_\mathrm{M}} = 0. \tag{2.174}$$

For the construction of $(f_\infty,\ g_\infty)$ we return to (2.158). It is not difficult to verify that a solution independent of the regular one $\phi_2^{\mathrm{R}}(x) = {}_1F_1(a;b;x)$, where $a = \gamma - Z\alpha E/\lambda,\ b = 2\gamma + 1$, is this:

$$\begin{aligned}\phi_2^{\mathrm{I}}(x) &= x^{1-b}\,{}_1F_1(1+a-b;2-b;x)\\ &= x^{-2\gamma}\,{}_1F_1(-\gamma - Z\alpha E/\lambda;-2\gamma+1;x).\end{aligned}$$

According to the defining equations (2.153) and (2.155) ϕ^{R} and ϕ^{I} enter into f and g with the factor $x^\gamma \mathrm{e}^{-x/2}$. Thus, rf and rg are linear combinations of the functions

$$M(\varepsilon, s; x) = x^s \mathrm{e}^{-x/2}\,{}_1F_1(s-\varepsilon;2s+1;x), \tag{2.175}$$

where $\varepsilon := Z\alpha E/\lambda$ and $s = \pm\gamma$.

The asymptotic behaviour of $M(\varepsilon, s, x)$ is determined by the asymptotic form (2.160) of the confluent hypergeometric function. For real and positive x the second term in (2.160) dominates and we have

$$M(\varepsilon, \pm\gamma; x) \underset{x\to\infty}{\sim} \frac{\Gamma(\pm 2\gamma + 1)}{\Gamma(\pm\gamma - \varepsilon)} x^{-\varepsilon-1}\mathrm{e}^{x/2}. \tag{2.176}$$

We now combine the two solutions for positive and negative γ in such a way as to cancel out the exponentially increasing term (2.176). Noting that $\Gamma(\pm 2\gamma + 1) = \pm 2\gamma\Gamma(\pm 2\gamma)$, this is achieved by taking the combination

$$W(\varepsilon, s; x) := \frac{\Gamma(-2\gamma)}{\Gamma(-\gamma-\varepsilon)} M(\varepsilon, \gamma; x) + \frac{\Gamma(2\gamma)}{\Gamma(\gamma-\varepsilon)} M(\varepsilon, -\gamma; x). \tag{2.177}$$

This specific linear combination is regular at infinity for all values $\varepsilon = Z\alpha E/\lambda$.[21]

Repeating some of the steps of case (a) it is straightforward to construct the radial solution (f_∞, g_∞) from (2.177). One finds, barring arbitrary normalization,

$$rf_\infty(r) = \sqrt{m-E}\left\{\left(\kappa + \frac{Z\alpha m}{\lambda}\right)\right\} W(\varepsilon - 1, \gamma; x) - W(\varepsilon, \gamma; x)\Big\}, \tag{2.178a}$$

$$rg_\infty(r) = \sqrt{m+E}\left\{\left(\kappa + \frac{Z\alpha m}{\lambda}\right)\right\} W(\varepsilon - 1, \gamma; x) + W(\varepsilon, \gamma; x)\Big\}, \tag{2.178b}$$

Note that these solutions are indeed regular at infinity for any value of the energy E. (This still remains true when E becomes complex. This occurs if the Dirac equation contains a complex optical potential.)

Remarks. (i) The functions (2.178) are, in general, not regular at the origin because of the factor $x^{-\gamma}$ in the second term of (2.177). (ii) If one imposes regularity at the

[21] W is a Whittaker function, except for an extra factor $x^{1/2}$ on the right-hand side of (2.177).

origin, too, this term must vanish and one recovers the eigenvalue condition of the previous case (a), cf. (2.161).

2.7 Muonic Atoms and Quantum Electrodynamics

In a sense, vacuum polarization is the simplest and most fundamental radiative effect in the quantized theory of photons in interaction with matter. What is this effect and why is it fundamental? In the quantized Maxwell theory the electromagnetic forces which act between charged particles are described by the exchange of photons between these particles. The exchanged photon, through its quantum nature, can go over into all possible intermediate states which are allowed by the conservation laws of the theory. These intermediate states can annihilate and go over into the same photon state again, as sketched in Fig. 2.11. In this diagram the hatched loop stands for the sum of all many-particle and photon states which are allowed by the rules of the theory. The net effect of these insertions is a modification of the photon propagator or, in other words, of the classical forces between charged matter particles. The range of these modifications, in coordinate space, is a function of the masses of the particles in the intermediate states. The phenomenon occurs in any local gauge theory (the photon being replaced by the vector gauge bosons of the theory), and it reflects fundamental properties of the theory. This can be understood qualitatively by cutting the diagram in Fig. 2.11 as indicated by the broken line: If we change the external momenta such that the particle lines at the left and at the right of this figure represent incoming and outgoing particle-antiparticle pairs respectively, then the cut diagrams represent the total pair annihilation cross sections.

In quantum electrodynamics (QED), to lowest order in the fine structure constant α, vacuum polarization is represented by the virtual creation and re-annihilation of all possible pairs of one fermion and its antifermion, as shown in Fig. 2.12(a). This diagram (and likewise all diagrams of higher order in α), when added to the single photon exchange, leads to a modification of the photon propagator and has two basic effects: The first effect is an infinite, logarithmically divergent, contribution which, however, is the same in any diagram where the photon couples to a given particle of charge e_0. The presence of this divergent term indicates that the *bare* charge e_0 (i.e. the coupling constant appearing in the original Lagrangian), is renormalized, by an infinite amount, to the *physical* charge e. The infinity can be circumvented formally by a redefinition of the coupling constant which means replacing the bare

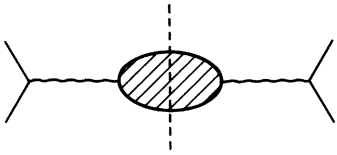

Fig. 2.11 Vacuum polarization in quantum electrodynamics leading to modification of the photon propagator

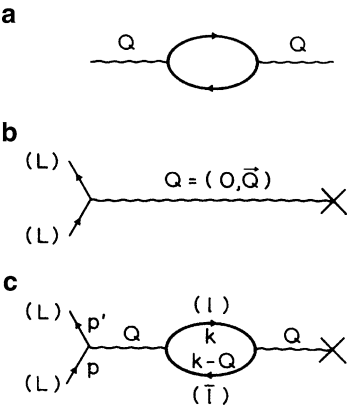

Fig. 2.12 (**a**) Modification of a photon propagator to order α, due to a loop of virtual charged particles (electron, muon, etc). (**b**) Interaction of a charged lepton (L) with an external potential (represented by the cross), (**c**) Modification of the interaction due to diagram (**b**) through lowest-order vacuum polarization

charge e_0 everywhere by the physical charge e. This prescription is formal because e_0 is necessarily infinite and yet the replacement is to be made, order by order, to the order α^n of perturbation theory to which we work, as if everything were finite. As the theory does not allow one to predict the magnitude of the charge e, this first and divergent effect of vacuum polarization is not observable.

In contrast to this, the remainder of vacuum polarization is finite and unique, and does have observable consequences. This second effect can be calculated uniquely, in successive orders of α, and can be confronted with precision measurements, as a test of QED. The physical effect of (finite) vacuum polarization is best understood in the case of an external, electrostatic potential. In this case vacuum polarization leads to a distortion of the given potential, over a distance which is characterized by the Compton wavelength $\lambda\!\!\!^{-}(i) = \hbar/m_i c$ of the particle that runs along the loop in the diagram of Fig. 2.12(a). Clearly, the longest range in this distortion effect is due to the lightest particle, the electron. Thus, vacuum polarization due to virtual *electron–positron pairs* is expected to distort the original potential over a distance of the order

$$\lambda\!\!\!^{-}(\mathrm{e}) \simeq 386\mathrm{fm}. \tag{2.179}$$

If we wish to see the quantitative importance of this effect in atoms we must check whether the orbit radii are large as compared to $\lambda\!\!\!^{-}(\mathrm{e})$ or whether they are comparable to or smaller than $\lambda\!\!\!^{-}(\mathrm{e})$. Hydrogen and muonium ($\mu^+$ e$^-$) have Bohr radii $\sim 1/\alpha m \simeq 5 \times 10^4$ fm and belong to the first class. In those "dilute" systems vacuum polarization is a small effect as compared to other radiative corrections due to vertex modification and to the anomalous magnetic moments. In contrast to these, muonic atoms have sizes which are indeed comparable to $\lambda\!\!\!^{-}(\mathrm{e})$, eq. (2.179). As a consequence, vacuum polarization is the predominant radiative correction in muonic atoms. As far as tests of QED are concerned, weakly bound systems, such as ordinary light atoms and muonium, and muonic atoms are complementary. They test different and complementary predictions of QED. We discuss first the finite and observable parts of vacuum polarization, in lowest order. We then say a little more about higher orders and give some characteristic examples. The discussion

of muonium (which is an example for the complementary situation, similar to hydrogen) can be found e.g. in Scheck (1978).

2.7.1 Observable Part of Vacuum Polarization to Order $O(\alpha)$

For the sake of simplicity let us consider the case where the photon line in Fig. 2.12(a) represents the interaction of a fermion (L) with an *external* electrostatic potential of a *point charge c*. This potential is represented by a cross in Fig. 2.12(b) and (c). According to standard Feynman rules the translation of this cross and the photon line into a formula is

$$\tilde{A}_\mu(\boldsymbol{Q}^2) = \frac{c}{(2\pi)^3}\delta_{\mu 0}\frac{1}{\boldsymbol{Q}^2}, \tag{2.180}$$

which is the Fourier transform of the usual $1/r$-potential[22]

$$\tilde{A}_\mu(\boldsymbol{Q}^2) = \frac{1}{(2\pi)^3}\int \mathrm{d}^3 Q\, \mathrm{e}^{-\mathrm{i}Qx}\frac{c}{4\pi|\mathbf{x}|}\delta_{\mu 0}. \tag{2.180'}$$

Consider now the vacuum loop of a charged lepton l illustrated by Fig. 2.12(c). According to the Feynman rules the sum of diagrams b and c is given by

$$M = 2\pi \mathrm{i} e_0 \overline{u_\mathrm{L}(p')}\gamma_\mu u_\mathrm{L}(p) \times\left[g^{\mu\nu} + \frac{1}{Q^2}\frac{ie_0^2}{(2\pi)^4}\int \mathrm{d}^4 k\ \mathrm{tr}\left\{\gamma^\mu \frac{1}{\not{k} - m_l + \mathrm{i}\varepsilon}\gamma^\nu \frac{1}{\not{k} - \not{Q} - m_l + \mathrm{i}\varepsilon}\right\}\tilde{A}_\nu\right], \tag{2.181}$$

where $Q = p - p'$. In the specific case of elastic scattering of the fermion L in an external potential we have $p^0 = p'^0$, so that $Q^2 = -\boldsymbol{Q}^2$. In a more general diagram Q is the momentum carried by the photon lines entering and leaving the closed fermion loop (see Fig. 2.12(a)). In any such case the vacuum polarization loop of order e^2 is represented by the tensor

$$\Pi^{\mu\nu}(Q) := \frac{\mathrm{i}e_0^2}{(2\pi)^4}\int \mathrm{d}^4 k\,\mathrm{tr}\left\{\gamma^\mu \frac{1}{\not{k} - m_\ell + \mathrm{i}\varepsilon}\gamma^\nu \frac{1}{\not{k} - \not{Q} - m_\ell + \mathrm{i}\varepsilon}\right\}. \tag{2.182}$$

As it stands this integral is divergent and we must be very careful in performing algebraic manipulations on it. It is well-defined and finite only in a regularized form of QED. Methods of regularization are described in textbooks on quantum field

[22] In the standard formulation of Feynman rules one chooses natural units so that $e^2/4\pi = \alpha$.

theory. They are essential in identifying the precise nature of the singularities of divergent quantities and in isolating these from the finite parts. If the regularization respects Lorentz invariance and gauge invariance of the theory, these latter, finite parts are unique.

In what follows we assume that the tensor $\prod^{\mu\nu}(Q)$ is already regularized. For instance, using the method of Pauli and Villars, one finds

$$\Pi^{\mu\nu}_{\text{reg}}(Q) = (Q^\mu Q^\nu - Q^2 g^{\mu\nu})\ [C + \Pi(Q^2)], \tag{2.183}$$

where the first term depends on a fictitious regulator mass M,

$$C = \frac{\alpha_0}{3\pi}\ \ln\left(\frac{M}{m_\ell}\right)^2 \tag{2.184}$$

(and hence is logarithmically divergent), whilst the second term

$$\Pi(Q^2) = -\frac{2\alpha}{\pi}\int_0^1 \mathrm{d}z\ z\,(1-z)\ln\left(\frac{m_\ell^2 - Q^2 z\,(1-z)}{m_\ell^2 - \mathrm{i}\varepsilon}\right) \tag{2.185}$$

is finite and independent of the method of regularization used. It can be shown that the logarithmic divergence (2.184) represents a formal renormalization of the charge and that it can be absorbed if the bare charge is replaced by the physical charge,[23]

$$e = e_0\ \sqrt{1 - \frac{\alpha}{3\pi}\ \ln\left(\frac{M}{m_l}\right)^2}\,. \tag{2.186}$$

Finally, we note that the specific convariant form of $\Pi^{\mu\nu}$, (2.183), is a consequence of gauge invariance which requires

$$Q_\mu\ \Pi^{\mu\nu}_{\text{reg}}(Q) = 0 = \Pi^{\mu\nu}_{\text{reg}}(Q)\,Q_\nu.$$

In order to understand the physical content of the finite part $\Pi(Q^2)$ let us transform the integral (2.185) somewhat so that it may easily be transformed to coordinate space, by means of Fourier transformation. Let $z = (1-y)/2$ and, therefore, $1-z = (1+y)/2$. Then

$$\Pi(Q^2) = -\frac{\alpha}{2\pi}\int_0^1 \mathrm{d}y(1-y^2)\ \ln\left\{1 - \frac{Q^2}{m^2 - \mathrm{i}\varepsilon}\ \frac{1-y^2}{4}\right\}\ (m \equiv m_\ell).$$

[23] As we work in second order here, it is consistent to insert $\alpha = e^2/4\pi$, not $\alpha_0 = e_0^2/4\pi$ into (2.185) and the square root in (2.186).

By partial integration we can get rid of the logarithm and obtain

$$\Pi(Q^2) = \frac{\alpha}{\pi}\, Q^2 \int_0^1 \mathrm{d}y\, \frac{y^2(1-y^2/3)}{4m^2 - Q^2(1-y)^2 - \mathrm{i}\varepsilon}. \tag{2.187}$$

An equivalent representation is obtained by means of the substitution

$$\kappa^2 := \frac{4m^2}{1-y^2},$$

i.e.

$$y^2 = 1 - \frac{4m^2}{\kappa^2}, \quad \mathrm{d}\kappa^2 = \frac{\kappa^4}{2m^2}\, y\mathrm{d}y,$$

which gives

$$\Pi(Q^2) = \frac{\alpha Q^2}{3\pi} \int_{4m^2}^{\infty} \mathrm{d}\kappa^2\, \frac{(1+2m^2/\kappa^2)\ \sqrt{1-4m^2/\kappa^2}}{\kappa^2(\kappa^2 - Q^2 - \mathrm{i}\varepsilon)}. \tag{2.188}$$

Let us now return to the example of scattering in an external electrostatic potential. Inserting the result (2.188) into the amplitude (2.181), after having renormalized the charge (to the order at which we work), we obtain

$$\begin{aligned} M &= 2\pi \mathrm{i} e\, \overline{u_{\mathrm{L}}(p')}\, \gamma_\mu\, u_{\mathrm{L}}(p) \left[g^{\mu\nu} + \frac{1}{Q^2}(Q^\mu\, Q^\nu - Q^2 g^{\mu\nu})\ \Pi(Q^2) \right] \tilde{A}_\nu \\ &= 2\pi \mathrm{i} e\, \overline{u_{\mathrm{L}}(p')}\, \gamma^\nu\, u_{\mathrm{L}}\,(p)\ [1 - \Pi(Q^2)]\ \tilde{A}_\nu. \end{aligned}$$

In this example $Q^2 = -\boldsymbol{Q}^2, \tilde{A}_\nu$ is given by (2.180), $\Pi(Q^2 = -\boldsymbol{Q}^2)$ by (2.188). The factor $[1 - \Pi]\tilde{A}$ can be read as a modified external potential and may easily be transformed to coordinate space. Let

$$\tilde{V}(\boldsymbol{Q}^2) := -e[1 - \Pi\,(-\boldsymbol{Q}^2)]\tilde{A}_0(\boldsymbol{Q}^2). \tag{2.189}$$

The potential in coordinate space is the Fourier transform of $\tilde{V}$,

$$V(x) = \frac{C}{(2\pi)^3} \int \mathrm{d}^3\boldsymbol{Q} \mathrm{e}^{\mathrm{i}Qx} \left\{ \frac{1}{\boldsymbol{Q}^2} + \frac{\alpha}{3\pi} \int_{4m^2}^{\infty} \mathrm{d}\kappa^2 \frac{(1+2m^2/\kappa^2)\ \sqrt{1-4m^2/\kappa^2}}{\kappa^2(\kappa^2 + \boldsymbol{Q}^2 - \mathrm{i}\varepsilon)} \right\} \tag{2.189$'$}$$

where we set $-ce = C$.

The integrals over $\boldsymbol{Q}$ can be performed by means of the formula

$$\frac{1}{(2\pi)^3} \int \mathrm{d}^3\ Q\ \frac{\mathrm{e}^{\mathrm{i}Qx}}{\boldsymbol{Q}^2 + a^2} = \mathrm{e}^{-ar}/4\pi r \quad (r = |\boldsymbol{x}|),$$

taking $a = 0$ in the first term, $a = \kappa$ in the second term of (2.189′). This gives

$$V(r) = \frac{C}{4\pi}\left\{\frac{1}{r} + \frac{\alpha}{3\pi}\int_{4m^2}^{\alpha} \mathrm{d}\kappa^2 \frac{(1+2m^2/\kappa^2)\sqrt{1-4m^2/\kappa^2}}{\kappa^2}\frac{\mathrm{e}^{-\kappa r}}{r}\right\}. \quad (2.190)$$

Thus, the original $1/r$ potential is modified by a superposition of Yukawa terms with ranges greater or equal $1/2m = \frac{1}{2}\lambda\!\!\!^{-}(\mathrm{e})$.

For practical use one may replace the variable κ^2 by a dimensionless integration variable $\kappa^2 = 4m^2x^2$, so that (Uehling 1935)

$$V(r) = \frac{C}{4\pi r}\left\{1 + \frac{2\alpha}{3\pi}\int_1^{\infty} \mathrm{d}x \mathrm{e}^{-2mxr}\left(1+\frac{1}{2x^2}\right)\frac{\sqrt{x^2-1}}{x^2}\right\}. \quad (2.190')$$

Remember that C is the external charge. For instance, if this is a proton then $C = |e|$; if it is a point-like nucleus then $C = +Z|e|$. (The case of an extended charge distribution is treated below).

There are two limiting situations where it is easy to estimate the integral in (2.190′). If $rm \gg 1$, i.e. if r is very large compared to $\lambda\!\!\!^{-}(\mathrm{e})$, the integrand is large only close to the lower limit of the integral. We approximate

$$\left(1+\frac{1}{2x^2}\right)\frac{\sqrt{x^2-1}}{x^2} \simeq \frac{3}{2}\sqrt{2(x-1)}$$

near $x = 1$ and substitute $x - 1 = u$, so that

$$\int_1^{\infty} \mathrm{e}^{-2mxr}\left(1+\frac{1}{2x^2}\right)\frac{\sqrt{x^2-1}}{x} \simeq \mathrm{e}^{-2mr}\int_0^{\infty}\mathrm{d}u\,\mathrm{e}^{-2mru}\frac{3}{2}\sqrt{2u}$$
$$= \frac{3\sqrt{\pi}}{8}\frac{\mathrm{e}^{-2mr}}{(mr)^{3/2}},$$

and therefore

$$V(r) = \frac{C}{4\pi r}\left\{1 + \frac{\alpha}{4\sqrt{\pi}}\frac{\mathrm{e}^{-2mr}}{(mr)^{3/2}}\right\}. \quad r \gg \lambda\!\!\!^{-}(\mathrm{e}). \quad (2.191a)$$

This limit is relevant in normal atoms whose orbital radii are indeed large compared to $\lambda\!\!\!^{-}(\mathrm{e})$. Because of the exponential the correction term is very small. This is in contrast to muonic atoms whose orbital radii are comparable with or smaller than $\lambda\!\!\!^{-}(\mathrm{e})$. Here vacuum polarization is a large effect.

Similarly, if $rm \ll 1$ i.e. if $r \ll \lambda\!\!\!^{-}(\mathrm{e})$ the integral (2.190′) can be solved approximately, too, and is found to be (Blomqvist 1972)

$$V(r) \simeq \frac{C}{4\pi r}\left\{1 - \frac{2\alpha}{3\pi}[\ln(mr) + C_{\mathrm{E}} + 5/6]\right\}, \tag{2.191b}$$

where $C_{\mathrm{E}} = 0.577216$ (Euler's constant).

2.7.2 *Illustration and Interpretation of Vacuum Polarization of Order $\alpha Z\alpha$*

Figure 2.13 illustrates the $1/r$ potential and the vacuum polarization potential of (2.190′): In order to get rid of dimensional quantities and of the numerical factors in front of the integral, we have multiplied $V(r)$, (2.190′), by $(-6\pi^2/\alpha Cm)$. Thus the upper curve represents the reduced vacuum polarization potential

$$\upsilon_{\mathrm{vacpol}}(u) = -\frac{1}{u}\int_1^\infty \mathrm{d}x \mathrm{e}^{-2ux}\left(1 + \frac{1}{2x^2}\right)\frac{\sqrt{x^2-1}}{x^2} \tag{2.192}$$

as a function of $u = rm \mathrel{\hat{=}} r/\lambda\!\!\!^{-}(\mathrm{e})$. The figure shows that $\upsilon_{\mathrm{vacpol}}$ is small compared to the uncorrected $1/r$ potential for distances $r \gtrsim \lambda\!\!\!^{-}(\mathrm{e})$, but becomes strong at small distances $r \ll \lambda\!\!\!^{-}(\mathrm{e})$. Furthermore, the potential due to vacuum polarization has the same sign as the $1/r$ potential everywhere. Thus, in an attractive $1/r$ potential, vacuum polarization leads to even more attraction. This result contradicts naive expectations if we think of vacuum polarization in analogy to electric polarizability of ordinary matter. Indeed, for a positive point charge, we would expect the virtual positrons to be pushed away from the origin and the virtual electrons to be pulled towards the origin. As the total induced charge is zero, this would mean that the original positive point charge effectively is smeared out over a certain region of space. However, this would lead to an effective screening of the charge and hence to a *reduction* of its field, not to the increase seen in the figure.

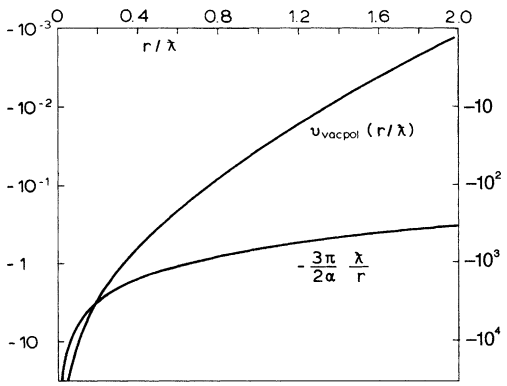

Fig. 2.13 Potential due to vacuum polarization, in dimensionless form, as a function of $r/\lambda\!\!\!^{-}$ where λ is the Compton wavelength of the virtual particle in the loop of Fig. 2.12(a). Also shown is the $1/r$ potential, scaled by the same factor as the former. The right-hand scale holds for the latter

This result becomes even more puzzling if we consider the induced charge density $\rho_{\mathrm{Pol}}(r)$ pertaining to the vacuum polarization potential: $\rho_{\mathrm{Pol}}(r) = -\Delta V_{\mathrm{Pol}}(r)$ (for technical reasons we introduce a convergence factor into the integral),

$$V_{\mathrm{Pol}}(r) = \frac{C}{4\pi r}\frac{2\alpha}{3\pi}\lim_{M\to\infty}\int_1^\infty \mathrm{d}x \mathrm{e}^{-(m/M)x}\mathrm{e}^{-2mrx}\left(1+\frac{1}{2x^2}\right)\frac{\sqrt{x^2-1}}{x^2}.$$

Using the well-known formula

$$(\Delta-\kappa^2)\frac{\mathrm{e}^{-\kappa r}}{r} = -4\pi\delta(\boldsymbol{r})$$

and taking $\kappa = 2mx$, one finds

$$\rho_{\mathrm{Pol}}(r) = \frac{C}{4\pi}\frac{2\alpha}{3\pi}\lim_{M\to\infty}\left\{4\pi\delta(\boldsymbol{r})\int_1^\infty \mathrm{d}x\mathrm{e}^{-(m/M)x}\left(1+\frac{1}{2x^2}\right)\frac{\sqrt{x^2-1}}{x^2}\right.$$
$$\left.-\frac{4m^2}{r}\int_1^\infty \mathrm{d}x\mathrm{e}^{-(m/M)x}\mathrm{e}^{-2mrx}\left(1+\frac{1}{2x^2}\right)\sqrt{x^2-1}\right\}. \qquad (2.193)$$

(The convergence factor is needed in the first term of this expression because the integral diverges logarithmically; it is irrelevant in the second term.) This polarization charge density has rather curious properties: For finite argument $r \neq 0$ it has the same sign everywhere. At $r = 0$ it has two singularities, a δ-distribution with a linearly divergent coefficient

$$4\pi\delta(r)\ln(M/m) \qquad (2.194)$$

and a $1/r^3$ pole which comes from the second term [see (2.197a) below] Yet, the integral of ρ_{Pol} over all space vanishes, as it should. This is seen by making use of the formula

$$\int_0^\infty \frac{\mathrm{e}^{-\kappa r}}{r}r^2\mathrm{d}r = 1/\kappa^2$$

with $\kappa = 2mx$:

$$\int \rho_{\mathrm{Pol}}(r)\mathrm{d}^3r = 4\pi\frac{C}{4\pi}\frac{2\alpha}{3\pi}\lim_{M\to\infty}\left\{\int_1^\infty \mathrm{d}x\mathrm{e}^{-(m/M)x}\left(1+\frac{1}{2x^2}\right)\frac{\sqrt{x^2-1}}{x^2}\right.$$
$$\left.-\int_1^\infty \mathrm{d}x\mathrm{e}^{-(m/M)x}\left(1+\frac{1}{2x^2}\right)\frac{\sqrt{x^2-1}}{x^2}\right\} = 0. \qquad (2.195)$$

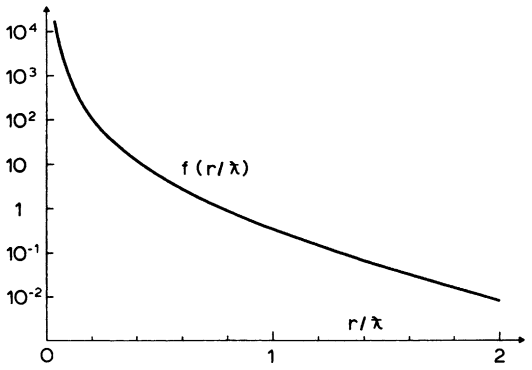

Fig. 2.14 Induced polarization charge density (2.196) in dimensionless form and as a function of $r/\lambda\!\!\!^{-}$. Note that this density is positive (attractive) for all finite r, but is singular at $r = 0$ so that its integral over all space vanishes

Figure 2.14 shows the polarization charge density for $r \neq 0$. Again, in order to get rid of dimensional quantities we have plotted the function

$$f(u) = \left(-\frac{6\pi^2}{\alpha C m^3}\right)\rho_{\mathrm{Pol}}(r)$$
$$= \frac{4}{u}\int_0^\infty \mathrm{d}x \mathrm{e}^{-2ux}\left(1+\frac{1}{2x^2}\right)\sqrt{x^2-1} \qquad (r \neq 0), \qquad (2.196)$$

where $u = mr \mathrel{\hat{=}} r/\lambda\!\!\!^{-}(\mathrm{e})$, as a function of this variable. The connection to the function (2.192) is

$$\frac{1}{u^2}\frac{\mathrm{d}}{\mathrm{d}u}\left(u^2\frac{\mathrm{d}\upsilon(u)}{\mathrm{d}u}\right) = -f(u), \quad u \neq 0.$$

From the approximate expressions (2.191a, b) for the potential at large and small r, respectively, we derive the corresponding limiting behaviour of the polarization density (2.196), viz. ($u = mr \mathrel{\hat{=}} r/\lambda\!\!\!^{-}(\mathrm{e})$),

$$r \ll \lambda\!\!\!^{-} \quad f(u) \simeq 1/u^3, \qquad (2.197a)$$

$$r \gg \lambda\!\!\!^{-} \quad f(u) \simeq \frac{3\sqrt{\pi}}{8}u^{-5/2}\mathrm{e}^{-2u}. \qquad (2.197b)$$

Clearly, the polarization charge density is not very intuitive. It has the expected property (2.195) but it is qualitatively different from a polarization density in ordinary matter. The singular term (2.194) at $r = 0$ is reminiscent of the charge renormalization (2.184). The only semi-physical statement one may make is this: When a test charge or a photon probes the field of our point charge at large distances, i.e. at low momentum transfers, then it sees what is called the *physical* charge. The closer it approaches the point charge (i.e. the larger the momentum transfers), the more the test particle sees of the *bare* charge. As the bare charge is larger than the physical charge (see (2.186)) the test particle sees an enhanced field at short

distances. The closer it comes the more enhanced the field. Unfortunately, the bare charge is infinite. The phenomenon of vacuum polarization evades simple analogies to classical polarization phenomena because infinite charge renormalization is not intuitive.

2.7.3 Radiative Corrections in Muonic Atoms

The polarization potential of order $O(\alpha C)$, (2.190′), which we have discussed so extensively, yields the dominant contribution to radiative corrections to the energies of muonic atoms. In this section we give some illustrative examples. We then discuss other radiative corrections such as the Lamb shift and vacuum polarization of higher order.

It is not difficult to generalize the result (2.190′) for a point-like charge to the case of the extended charge density of a nucleus. Here $C = -Ze^2 = -4\pi Z\alpha$ and

$$V(\boldsymbol{r}) = -Z\alpha \int \mathrm{d}^3 r' \frac{\rho(\boldsymbol{r}')}{|\boldsymbol{r}-\boldsymbol{r}'|} \times \left\{ 1 + \frac{2\alpha}{3\pi} \int_1^\infty \mathrm{e}^{-2m|\boldsymbol{r}-\boldsymbol{r}'|x} \left(1 + \frac{1}{2x^2}\right) \frac{\sqrt{x^2-1}}{x^2} \mathrm{d}x \right\}, \tag{2.198}$$

where $\rho(\boldsymbol{r})$ is the charge density normalized to one.

Clearly, the singular properties of the polarization potential and charge density remain unchanged by the integration over the finite charge density.

If the charge density is spherically symmetric the expression (2.198) simplifies somewhat. The first term on the r.h.s. transforms into the uncorrected spherical potential (2.117). The integral over angular variables in the polarization potential can be done by elementary means (exercise!) giving

$$V_{\mathrm{vacpol}}(r) = -Z\alpha \frac{2\alpha}{3m} \int_0^\infty \mathrm{d}r' \frac{r'}{r} \rho(r') \{ I(|r-r'|) - I(r+r') \} \tag{2.199}$$

with

$$I(z) = \int_1^\infty \mathrm{e}^{-2mzx} \left(1 + \frac{1}{2x^2}\right) \frac{\sqrt{x^2-1}}{x^3} \mathrm{d}x.$$

In a deformed nucleus, the multipole expansion (2.133) of the charge density should be inserted into (2.198). (We see from this, in particular, that vacuum polarization will also contribute to electric quadrupole hyperfine structure.)

Let us now illustrate the importance of vacuum polarization of order ($O(\alpha Z\alpha)$ by a few practical examples and let us compare this correction to the remaining radiative corrections.

In the second column of Table 2.4 we give the transition energy $2\mathrm{p}_{1/2} - 1\mathrm{s}_{1/2}$ in four typical atoms. The third column shows the order $\alpha Z\alpha$ vacuum polarization whilst the fourth and fifth columns show vacuum polarization corrections of higher

Table 2.4 Realistic $2p_{1/2} - 1s_{1/2}$ transition energies and radiative corrections in muonic atoms. (The transition energies contain all corrections.) Numbers taken from Engfer et al. (1974)

Nucleus	Trans. energy [keV]	Vac. pol. $\alpha Z\alpha$ [keV]	Vac. pol., higher orders [keV]	Lamb shift [keV]
$^{12}_{6}$C	75.25	0.372	0.002	−0.006
$^{\text{nat}}_{20}$Ca	783.79	6.049	0.044	−0.208
$^{116}_{50}$Sn	3418.99	25.455	0.109	−1.548
$^{208}_{82}$Pb	5778.01	34.804	−0.106	−2.683

Table 2.5 Lamb shifts in muonic hydrogen and helium. All energies in meV (= 10^{-3} eV). Calculated values from Borie and Rinker (1982). Experimental values from Carboni et al. Nucl. Phys. A278(1977)381, Pohl et al. Nature 466 (2010) 213

	$^{1}_{1}$H	$^{4}_{2}$He		
Lamb shift	$2p_{3/2} - 2s_{1/2}$	$2p_{1/2} - 2s_{1/2}$	$2p_{3/2} - 2s_{1/2}$	$3d_{3/2} - 3p_{3/2}$
fine structure	8.4	0	145.7	0
vac. pol. $\alpha Z\alpha$	204.9	1665.8	1666.1	110.560
vac. pol., higher	1.5	12.0	12.0	0.925
vertex correction	−0.6	−11.1	−10.8	−0.069
recoil	~ 0	−0.2	−0.2	0.005
finite size of nucleus	-3.4 ± 0.1	$-103\langle r^2\rangle$[a)]	$-103\langle r^2\rangle$[a)]	~ 0
polarizability	$\sim 2 \times 10^{-2}$	3.1 ± 0.6	3.1 ± 0.6	~ 0
total theoretical	210.8 ± 0.1	1380.9(4.2)	1527.2(4.2)	111.42
experiment	206.295 ± 0.003	1381.3(0.5)	1527.5(0.3)	

[a)] $\langle r^2\rangle^{1/2} = 1.674 \pm 0.012$ fm.

order and the remainder of the Lamb shift, respectively. Clearly, the $O(\alpha Z\alpha)$ term is the dominant correction in all cases.

Table 2.5 shows the radiative corrections for muonic hydrogen and helium 4. The second column contains the radiative and other contributions to the energy splitting of the $2p_{3/2}$ and $2s_{1/2}$ states in hydrogen. The origin of individual contributions is indicated in the first column. The correction labeled "polarizability" is explained in the next section. The third and fourth column give the details of the Lamb shift in the $n = 2$ states of muonic ^{4}He. The last column, finally, shows an example for the Lamb shift in the $n = 3$ levels of helium.

The bottom line shows the experimental results obtained for the $n = 2$ system in helium. The agreement with the theoretical predictions is excellent. However, the uncertainty on the theoretical numbers is about a factor of ten larger than the experimental error bar. As may be seen from the table, this uncertainty stems almost entirely from the finite-size correction, i.e. from the experimental error bar of the r.m.s. radius of ^{4}He. The polarizability shift is also sizeable but is believed to be calculable to at least the accuracy indicated in the table. In this respect, the $n = 3$ states in helium and the Lamb shift in hydrogen are somewhat clearer tests of

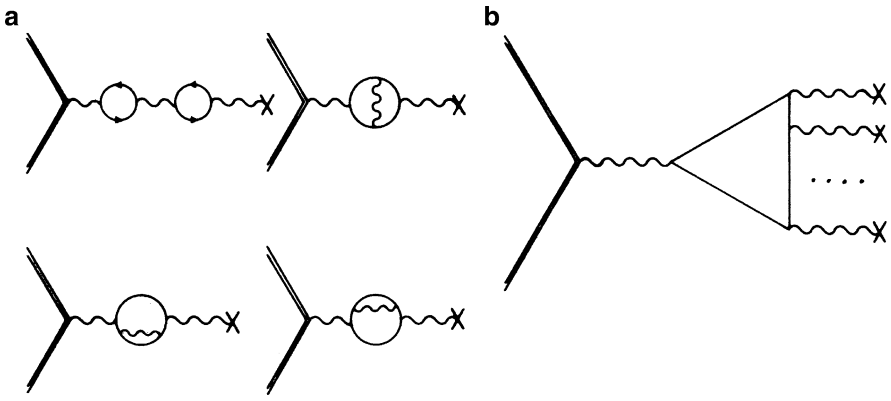

Fig. 2.15 (**a**) Vacuum polarization to order $\alpha^2(Z\alpha)$, Z being the charge of the external potential. The double line represents the external, bound muon. (**b**) Vacuum polarization of order $\alpha(Z\alpha)^{2n+1}$ for $n = 1$ and higher

radiative corrections as both the finite size and polarizability corrections are small. So far, these shifts have not been measured.

In the examples shown in Tables 2.4, 2.5 the corrections due to vacuum polarization of order higher than $\alpha Z\alpha$ are due primarily to

(i) the terms of order $\alpha^2 Z\alpha$ which are depicted in Fig. 2.15(a),
(ii) terms of order $\alpha(Z\alpha)^3$ (more generally $\alpha(Z\alpha)^{2n+1}$) which are illustrated by Fig. 2.15(b). These latter terms, even though they are proportional to α^4, appear enhanced in heavy nuclei because $(Z\alpha)$ is no longer small compared to one. For example, in lead we have $Z\alpha \simeq 0.6$. Here the correction to the $2p - 1s$ transition energy due to diagram (b) is as large as 40 eV. Other corrections such as vacuum polarization due to a virtual *muon* loop are found to be very small.

Finally, the remaining radiative corrections, i.e. the Lamb shift and the anomalous magnetic moment interaction, can be represented by additional potentials in the muon's wave equation. The details and references to the literature are found in Vol. I, Chapter III of [MUP77].

We may summarize this section by saying that vacuum polarization of order $\alpha Z\alpha$ is tested at a level of a few parts per million. The higher order terms of vacuum polarization are tested to about 20%. This provides another piece of evidence for the success of quantum electrodynamics, which is complementary to the very impressive classical tests of QED in electronic atoms and in the g-factor anomaly of electron and muon.

2.8 Deep Inelastic Scattering

2.8.1 Inclusive Electron Scattering

Scattering experiments of electrons on hadronic targets may be designed in yet another, qualitatively different, manner. Suppose the experimental arrangement is such that, while the energy of the incident electron $E \gg m_e$ is held fixed, the energy E' and the angular distribution of the outgoing electron are measured, irrespective of the final state into which the hadron has turned. This means, in other words, that the experiment determines the doubly differential cross section for *inclusive scattering*

$$\frac{d^2\sigma(E - E', \theta)}{dE' d\Omega'}(e + h \to e' + X), \tag{2.200}$$

where h is a nucleon (proton or neutron), or a nucleus, X stands for the sum and integral over all final hadronic states that can be reached by electro-excitation at the energy transfer $E - E'$ and momentum transfer $q^2 = -(k - k')^2$ (corresponding to the scattering angle θ). Both elastic scattering and inelastic scattering to specific final states probe coherent properties such as (ground state or transition) charge and current densities. If both the energy transfer and the momentum transfer are chosen large enough, inclusive scattering becomes insensitive to coherent properties such as wave functions describing the target h but, in turn, probes the "granularity" of the target. As both nuclei and nucleons are made up of constituents whose spatial size is smaller than the target's size, this means that inclusive, deep inelastic scattering probes the constituents rather than the hadron h which they form. This is particularly interesting in the case of nucleonic targets because this is one of the ways to study the nature of quarks, or, more generally, partons in hadrons. Neither quarks nor gluons can exist as free particles. Only composite states with certain well-defined quantum numbers describe physical hadrons. Indeed, historically, deep inelastic scattering was essential in unravelling the constituent structure of proton and neutron.

In the approximation which assumes that electro-excitation is due to the exchange of *one* virtual photon, the cross section (2.200) can be expressed in terms of a few Lorentz scalar, hadronic *structure functions* and some known functions of energy and scattering angle. The structure functions which are extracted from experiment, can then be analyzed in terms of the internal structure of the target h.

For the sake of definiteness take h to be a proton of four-momentum p, and let k and k' denote the four-momenta of the electron before and after the scattering process. In a first step we write down the cross section for the process $e + p \to e + m$ where m is a final state, containing m particles, which carries the right quantum numbers and is in accord with conservation of energy and momentum. A process of this type is sketched in Fig. 2.16. According to the Feynman rules for quantum

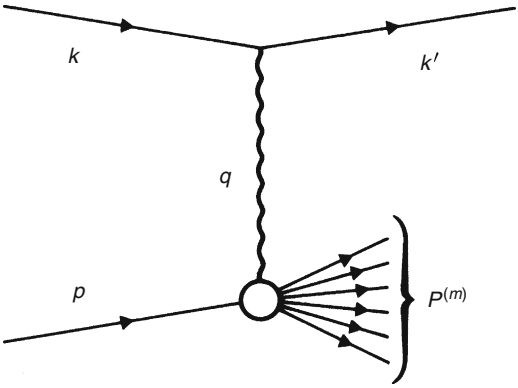

Fig. 2.16 An electron of momentum k converts a proton (momentum p) to an m-particle state, via exchange of a virtual photon

electrodynamics, App. C, the transition amplitude corresponding to the diagram of Fig. 2.16 reads

$$R^{(m)} = -\mathrm{i}\frac{2\pi e^2}{q^2}\overline{u(k')}\gamma_\mu u(k)\langle m|j^\mu(0)|p\rangle\delta(p+k-k'-P^{(m)}).$$

Here, $P^{(m)}$ is the sum of four-momenta in the final state m, i.e. $P^{(m)} = p_1 + p_2 + \ldots + p_m$, $k - k'$ is the momentum transfer delivered by the electron, $j^\mu(x)$ denotes the electromagnetic current operator. Thus, in the approximation of one-photon exchange $q := k - k'$ is the four-momentum of the virtual photon. The T-matrix element needed in the expression (B.3) for the cross section is obtained from $R^{(m)}$ by the defining relation (B.2). In the laboratory system, the struck proton is at rest, $p = (M, \mathbf{0})$, while $k = (E, \boldsymbol{k})$, and $k' = (E', \boldsymbol{k}')$. As the energy of the incident electron is large compared to the rest mass, $E \gg m_\mathrm{e}$, the electron mass can be neglected in the kinematics so that

$$|\boldsymbol{k}| \approx E, \quad |\boldsymbol{k}'| \approx E', \quad \text{and} \quad q^2 = (k-k')^2 \approx -2EE'(1-\cos\theta),$$

where q^2 is the same as t, (2.51b). In the same approximation the flux factor (B.4) is approximately ME. Thus, integrating over the momenta of the hadronic final state and summing over all spin orientations,

$$\begin{aligned}\mathrm{d}^2\sigma^{(m)} = {} & \frac{(2\pi e)^4}{2MEq^4}\left(\frac{1}{2}\sum_{\text{spins}}\ell^*_\mu\ell_\nu\right) \\ & \frac{1}{2}\sum_{\text{spins}}\int\frac{\mathrm{d}^3p_1}{2E_1}\cdots\int\frac{\mathrm{d}^2p_m}{2E_m}\langle p|j^{\mu\dagger}(0)|m\rangle\langle m|j^\nu(0)|p\rangle\delta(p+k-P^{(m)}) \\ & \times\frac{\boldsymbol{k}'^2 d\,|\boldsymbol{k}'|\mathrm{d}\Omega'}{2E'}.\end{aligned}$$

Here ℓ_μ stands for the matrix element of the electromagnetic current taken between electron spinors in momentum space, $\ell_\mu = \overline{u(k')}\gamma_\mu u(k)$, $\boldsymbol{k}'^2 \approx E'^2$, and $\mathrm{d}|\boldsymbol{k}'| \approx \mathrm{d}E'$. Summing over all final states which are allowed by the selection rules and by energy-momentum conservation, one obtains the inclusive cross section (with $e^2/4\pi = \alpha$, in natural units)

$$\frac{\mathrm{d}^2\sigma}{\mathrm{d}E'\mathrm{d}\Omega'} = \alpha^2 \frac{E'}{ME}\frac{1}{q^4} w_{\mu\nu} W^{\mu\nu}. \tag{2.201}$$

In this expression the Lorentz tensors $w_{\mu\nu}$, $W^{\mu\nu}$ are defined as follows. The *leptonic* contribution is contained in the tensor $w_{\mu\nu} := \left(\Sigma_{\text{spins}} \ell^*_\mu \ell_\nu\right)/2$, where the sum over all spin orientations is taken. It is easily evaluated by means of the trace formulae (C.2) and (C.4) of App. C2, viz.

$$w_{\mu\nu} = \frac{1}{2}\mathrm{tr}\{(\not{k} + m_\mathrm{e})\gamma_\mu(\not{k}' + m_\mathrm{e})\gamma_\nu\} \approx 2(k_\mu k'_\nu + k'_\mu k_\nu - (kk')g_{\mu\nu}), \tag{2.202}$$

the second, approximate, equality holding if m_e is neglected. The *hadronic* tensor is defined by

$$\begin{aligned} W^{\mu\nu} := 2\pi^2 \left(\frac{1}{2}\sum_{\text{spins}}\right) {\sum_m}' \langle p|j^\mu(0)|m\rangle\langle m|j^\nu(0)p\rangle (2\pi)^4 \\ \times \delta(P^{(m)} + k' - p - k), \end{aligned} \tag{2.203}$$

where $P^{(m)} = p_1 + \cdots + p_m$, the ${\sum_m}'$ being shorthand for

$${\sum_m}' = \sum_m \int \frac{\mathrm{d}^3 p_1}{2E_1} \cdots \int \frac{\mathrm{d}^3 p_m}{2E_m}, \quad \text{with} \quad E_i = p^{(i)0}.$$

In (2.203) we have made use of the fact that the electromagnetic current operator is hermitean. Note that $W^{\mu\nu}$ depends only on matrix elements of j^μ between on-shell states. Owing to the delta distribution in the four-momenta, the sum Σ'_m can be understood to stand for the completeness relation for states with total energy–momentum equal to $P^{(m)} = (p + k - k') = p + q$. As a consequence $\Sigma'_m|m\rangle\langle m|$, taken between $\langle p|j^\mu$ and $j^\nu|p\rangle$, can be replaced by unity. Furthermore, writing the delta distribution as an integral and making use of a translation formula of the type (2.42′), we have

$$\begin{aligned} (2\pi)^4\delta(p + q - P^{(m)})\langle p|j^\mu(0)|m\rangle &= \int \mathrm{d}^4 x \mathrm{e}^{\mathrm{i}(p+q-P^{(m)})}\langle p|j^\mu(0)|m\rangle \\ &= \int \mathrm{d}^4 x \mathrm{e}^{\mathrm{i}qx}\langle p|j^\mu(x)|m\rangle. \end{aligned}$$

Hence, an alternative way of writing (2.203) is the following

$$W^{\mu\nu} = 2\pi^2 \left(\frac{1}{2}\sum_{\text{spins}}\right) \int \mathrm{d}^4x \mathrm{e}^{\mathrm{i}q\cdot x} \langle p|j^\mu(x) j^\nu(0)|p\rangle, \quad (q = k - k'). \tag{2.204}$$

In this expression one can replace the product $j^\mu(x)j^\nu(0)$ by the commutator of these operators because the extra term that is added vanishes due to energy–momentum conservation. This is seen as follows: Making use again of a translation formula,

$$\begin{aligned}\int \mathrm{d}^4x \mathrm{e}^{\mathrm{i}q\cdot x} \langle p|j^\nu(x) j^\mu(x)|p\rangle &= \sum_m{}' \int \mathrm{d}^4x \mathrm{e}^{\mathrm{i}q\cdot x} \mathrm{e}^{-\mathrm{i}(p-P^{(m)})\cdot x} \langle p|j^\nu(0)|m\rangle\langle m|j^\mu(0)|p\rangle \\ &= \sum_m{}' (2\pi)^4 \delta^{(4)}(q + P^{(m)} - p) \langle p|j^\nu(0)|m\rangle\langle m|j^\mu(0)|p\rangle.\end{aligned}$$

The 0-component of the delta distribution takes care of energy conservation and reads $\delta^{(1)}(E - E' + P^{(m)0} - M)$, in the laboratory system. As $E - E' \geq 0$ and $P^{(m)0} > M$, the argument of this delta distribution can never be zero, hence the whole expression vanishes. Thus, we find the following, general expression for $W^{\mu\nu}$

$$W^{\mu\nu} = 2\pi^2 \left(\frac{1}{2}\sum_{\text{spins}}\right) \int \mathrm{d}^4x \mathrm{e}^{\mathrm{i}q\cdot x} \langle p|[j^\mu(x), j^\nu(0)]|p\rangle. \tag{2.204'}$$

This form of the hadronic tensor is often useful in deriving, for instance, general properties of the hadronic contribution (such as crossing symmetry or Ward identities).

The following result, although not needed in the definition of structure functions and the derivation of cross sections which follows, is nonetheless of intuitive interest.

Remark: One shows that the amplitude (2.204) is intimately related to the Compton amplitude for the scattering of a photon with mass $q^2 \neq 0$, hence a virtual photon, from a proton. The exact relation is

$$\text{Im } T(\gamma(q) + p \to \gamma(q) + p, \theta = 0) = \frac{e^2}{(2\pi)^5} \varepsilon_\mu \varepsilon_\nu W^{\mu\nu},$$

where ε_μ denotes the polarization of the photon. Thus $W^{\mu\nu}$ is proportional to the imaginary part of the Compton amplitude in the forward direction, for a photon that is not on its mass shell. By the optical theorem (Sect. 6.1.3) this means that it is proportional to the total cross section for scattering of virtual photons of mass q^2 on protons.

2.8.2 Covariant Decomposition of $W^{\mu\nu}$ and Cross Section

Clearly, $W^{\mu\nu}$ is a Lorentz tensor in momentum space and, as such, must be decomposable into covariants multiplied by Lorentz scalar functions, in close analogy to the decomposition (2.46) of a current matrix element. Conservation of the electromagnetic current, $\partial_\mu j^\mu(x) = 0$, implies the relations

$$q_\mu W^{\mu\nu} = 0, \qquad W^{\mu\nu} q_\nu = 0. \tag{2.205}$$

The first of these follows if we make the replacement $q_\mu e^{iq\cdot x} = (\partial_\mu e^{iq\cdot x})/i$ and shift the partial derivative to $j^\mu(x)$ by partial integration. The second follows by observing that the argument x in (2.204) can be shifted to the second operator by means of the translation $\langle p|j^\mu(x)j^\nu(0)|p\rangle = \langle p|j^\mu(0)j^\nu(-x)|p\rangle$, and by substituting $x \to -x$. An analysis of physical dimensions in (2.201) shows that $W^{\mu\nu}$ is dimensionless. Indeed, the left-hand side of (2.201) has dimension E^{-3}. The kinematic factor on its right-hand side has dimension E^{-5}, while the electron tensor $w_{\mu\nu}$ has dimension E^2.

The only Lorentz tensors constructed from the available momenta and the invariant tensors $g_{\mu\nu}$ and $\varepsilon_{\mu\nu\sigma\tau}$ which obey the conservation conditions above are

$$\left(g^{\mu\nu} - \frac{q^\mu q^\nu}{q^2}\right), \left(p^\mu - q^\mu \frac{(pq)}{q^2}\right)\left(p^\nu - q^\nu \frac{(pq)}{q^2}\right), \qquad \varepsilon_{\mu\nu\sigma\tau} q^\sigma p^\tau.$$

While the first two of these are genuine Lorentz tensors (i.e. transform with $\Lambda \otimes \Lambda$, where Λ is a Lorentz transformation), the third is a pseudotensor (i.e. transforms with $(\det\ \Lambda)\ (\Lambda \otimes \Lambda)$. As the two current operators in (2.204) both have the same, definite parity, their product is even and $W^{\mu\nu}$ can depend only on the first two tensors, not on the third. Therefore, the most general decomposition of the hadronic tensor must have the form

$$W^{\mu\nu} = -\left(g^{\mu\nu} - \frac{q^\mu q^\nu}{q^2}\right) W_1 + \frac{1}{M^2}\left(p^\mu - q^\mu \frac{(pq)}{q^2}\right)\left(p^\nu - q^\nu \frac{(pq)}{q^2}\right) W_2. \tag{2.206}$$

The functions W_1 and W_2 which are called *structure functions* are Lorentz *scalars* and, as such, can depend only on scalar variables. In inclusive scattering the only Lorentz scalar variables are

$$\begin{aligned} q^2 &= (k - k')^2 \overset{\text{lab}}{=} 2(m_e^2 - EE' + \boldsymbol{k}\cdot\boldsymbol{k}') \approx -4EE'\sin^2(\theta/2), \\ \nu &:= \frac{(pq)}{M} \overset{\text{lab}}{=} E - E'. \end{aligned} \tag{2.207}$$

(The third kinematic invariant p^2 is constant and equals M^2.) The variable ν is defined such as to be equal to the energy loss of the electron in the laboratory

system. The factor M^2 in the denominator of the second term in the defining equation (2.206) is introduced in order to make both structure functions dimensionless. In summary, the Lorentz scalar functions

$$W_1(\nu, q^2),\ W_2(\nu, q^2) \tag{2.208}$$

contain all the information on the structure of the target that can be extracted by means of electron scattering at any transfer of energy and momentum.

The cross section for inclusive scattering is computed as follows. Since q^2 and ν, as defined in (2.207), are the relevant variables, it is convenient to derive the doubly differential cross section with respect to these variables instead of E' and θ. From $E' = E - \nu,\ \cos\theta = 1 + q^2/(2E(E-\nu))$ the Jacobian $\partial(E',\ \cos\theta)/\partial(\nu,\ q^2)$ is found to be $(2EE')^{-1}$. Thus

$$\frac{\mathrm{d}^2\sigma}{\mathrm{d}\nu \mathrm{d}q^2} = \frac{\pi}{EE'}\frac{\mathrm{d}^2\sigma}{\mathrm{d}E'\mathrm{d}\Omega}.$$

Inserting the result (2.202) and the decomposition (2.206) into the expression (2.201) one finds

$$\frac{\mathrm{d}^2\sigma}{\mathrm{d}\nu \mathrm{d}q^2} = \frac{\pi}{EE'}\frac{2\alpha^2 E'}{q^4 EM}\left\{W_1\left[(kk') + \frac{2}{q^2}(kq)(k'q)\right] - \frac{W_2}{M^2}\left[(kk')\left(M^2 - \frac{(pq)^2}{q^2}\right)\right.\right.$$
$$\left.\left. -2\left((kp) - \frac{1}{q^2}(qp)(qk)\right)\left((k'p) - \frac{1}{q^2}(qp)(qk')\right)\right]\right\}.$$

Indeed, to take an example, the term that multiplies W_1 is

$$(k_\mu k'_\nu + k'_\mu k_\nu - (kk')g_{\mu\nu})\left(\frac{q^\mu q^\nu}{q^2} - g^{\mu\nu}\right) = 2\frac{(qk)(qk')}{q^2} - 3(kk') + 4(kk'),$$

the last term following because $g_{\mu\nu}g^{\mu\nu} = 4$.

Remembering that the electron mass is neglected we have

$$(kq) \approx -(kk') \approx -(k'q), q^2 \approx -2(kk'), (kk') \approx EE'(1-\cos\theta),$$

so that W_1 obtains a factor $2EE'(1-\cos\theta)$ while W_2 appears multiplied with

$$-EE'(1-\cos\theta) - \frac{1}{2}(E-E')^2 + \frac{1}{2}(E+E')^2 = EE'(1+\cos\theta).$$

This gives the final result

$$\frac{\mathrm{d}^2\sigma}{\mathrm{d}\nu \mathrm{d}q^2} = \frac{4\pi\alpha^2 E'}{q^4 EM}\left(2W_1(\nu, q^2)\sin^2\frac{\theta}{2} + W_2(\nu, q^2)\cos^2\frac{\theta}{2}\right) \tag{2.209}$$

It should be clear from the discussion above that this general formula contains all scattering processes that occur if an electron with fixed energy E hits a proton. For instance, in elastic scattering the kinematic variables (2.207) are related by $q^2 + 2Mv = 0$. This is easily verified: Energy–momentum conservation requires $p + k = p' + k'$. The process is elastic if $p'^2 = M^2 = p^2$. Thus, with $q = k - k'$ we have $p'^2 = (q + p)^2$ and, hence, $q^2 + 2(qp) = q^2 + 2Mv = 0$. As a consequence we expect the structure functions W_1 and W_2 to contain additive contributions proportional to $\delta(v + q^2/2M)$ which reproduce the expression (2.57′) for elastic scattering that we calculated in Sect. 2.4.2,3. Similarly, if the scattering process leads to an isolated resonance, viz. $e + p \to e + \Delta$, $p'^2 = M_\Delta^2$ where M_Δ is the mass of that resonance. The structure functions should then contain terms proportional to $\delta\left(v + q^2/2M - \left(M_\Delta^2 - M^2\right)/2M\right)$.

The general kinematic situation will be as sketched in Fig. 2.17: In the plane spanned by the variables v and $(-q^2)$ the kinematics of the elastic process is the straight line $q^2 + 2Mv = 0$ and the kinematics of production of a single resonance is the straight line $q^2 + 2Mv - \left(M_\Delta^2 - M^2\right) = 0$. The threshold for the continuum where more than one particle is produced at the hadronic vertex lies somewhere in between. Figure 2.17 also shows typical kinematic lines which are obtained if the energy loss is varied, while the scattering angle is held fixed, $\theta = \text{const}$.

The kinematic domain where both $(-q^2)$ and v are large i.e. the domain far to the right in Fig. 2.17, is called the deep inelastic region. It is this domain which is the most revealing with regard to the constituent structure of the proton.

2.8.3 An Example: Elastic Scattering from the Proton

In the case of elastic scattering the final state is again the proton, the momentum transfer is $q = k - k' = p' - p$. The sum over intermediate states Σ'_m reduces to $m = 1$ and to an integral over the momentum p' of the proton in the final state. The hadronic matrix element has the familiar decomposition (2.46) with $F_3(Q^2) \equiv 0$, or, when transformed by means of the Gordon identity, the covariant form (2.46′). We consider first the integration over the delta distribution in (2.203). With $\{\ldots\}$ denoting the remainder of the integrand, we have

$$\int \frac{\mathrm{d}^3 p'}{2E'_p} \delta^{(4)}(k + p - k' - p')\{\cdots\} = \delta^{(1)}(E + E_p - E' - \omega') \frac{1}{2\omega'} \{\cdots\}_{p'=p+q}$$

$$\overset{\text{lab}}{=} \frac{1}{2\omega'} \delta^{(1)}(v + M - \omega')\{\cdots\},$$

where we have set $\omega' = \sqrt{M^2 + (\boldsymbol{k} - \boldsymbol{k}')^2} = \sqrt{M^2 + v^2 - q^2}$. Since (2.209) depends on v, not on ω', we must rewrite the argument of the delta distribution in terms of the variable v. This is done by means of the formula

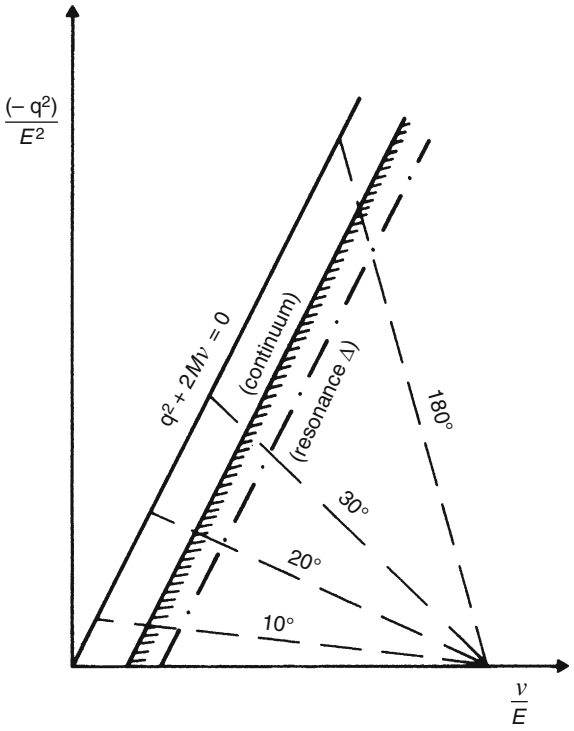

Fig. 2.17 Kinematics of electron–proton scattering to any final state. For a given final hadronic state the variables ν and q^2 are linearly dependent, as shown. Also, lines of constant scattering angle are drawn

$$\delta(f(x)) = \frac{\delta(x_0)}{|f'(x_0)|}, \text{ with } x_0 \text{ a single zero of } f(x).$$

Thus, with $\mathrm{d}(\nu + M - \omega'(\nu))/\mathrm{d}\nu = 1 - \nu/\omega'$,

$$\frac{1}{2\omega'}\delta(\nu + M - \omega') \to \frac{1}{2\omega'}\frac{\omega'}{\omega' - \nu}\delta\left(\nu + \frac{q^2}{2M}\right) \to \frac{1}{2M}\delta\left(\nu + \frac{q^2}{2M}\right).$$

The hadronic tensor for elastic scattering becomes

$$W^{\mu\nu}_{\text{elastic}} = \frac{1}{4}\sum_{r,s=1}^{2}\delta\left(\nu+\frac{q^2}{2M}\right)\frac{1}{2M}\overline{u^{(r)}(p)}\left\{(F_1+F_2)\gamma^\mu - (p+p')^\mu\frac{F_2}{2M}\right\}u^{(s)}(p').$$

$$\overline{u^{(s)}(p')}\left\{(F_1+F_2)\gamma^\nu - (p+p')\nu\frac{F_2}{2M}\right\}u^{(r)}(p).$$

The traces are the same as in Sect. 2.4.2. and we do not repeat their calculation here. However, instead of expressing the kinematic invariants in terms of s and t (as we did in Sect. 2.4.2.) we write the result such as to conform to the general form (2.206). Using $(pq) = -q^2/2$, and $(pp') = M^2 - q^2/2$ one finds

$$W^{\mu\nu}_{\text{elastic}} = \delta\left(\nu + \frac{q^2}{2M}\right)\frac{1}{2M}\left\{-\left(g^{\mu\nu} - \frac{q^\mu q^\nu}{q^2}\right)\left(-\frac{q^2}{2}(F_1 + F_2)^2\right)\right.$$
$$+\frac{1}{M^2}\left(p^\mu - q^\mu\frac{(pq)}{q^2}\right)\left(p^\nu - q^\nu\frac{(pq)}{q^2}\right)2M^2$$
$$\left.\times\left(F_1^2 - \frac{q^2}{4M^2}F_2^2\right)\right\}.$$

It is convenient to replace F_1 and F_2 by the electric and magnetic (Sachs) form factors (2.58) and (2.61), with $t = q^2$ as defined in (2.51b). Then

$$F_1^2 - \frac{q^2}{4M^2}F_2^2 = \frac{1}{1 - q^2/(4M)}\left(G_{\text{E}}^2 - \frac{q^2}{4M^2}G_{\text{M}}^2\right),$$

so that the structure functions describing elastic scattering are found to be

$$W_1^{\text{elastic}} = -\delta\left(\nu + \frac{q^2}{2M}\right)\frac{q^2}{4M}G_{\text{M}}^2 \tag{2.210}$$

$$W_2^{\text{elastic}} = \delta\left(\nu + \frac{q^2}{2M}\right)\frac{M}{1 - q^2/(4M^2)}\left[G_{\text{E}}^2 - \frac{q^2}{4M^2}G_{\text{M}}^2\right]. \tag{2.211}$$

It remains to insert this result into (2.209) and to integrate over the variable ν. Finally, the resulting cross section $\mathrm{d}\sigma/\mathrm{d}q^2$ is easily converted to the form $\mathrm{d}\sigma/\mathrm{d}\Omega'$ through

$$\frac{\mathrm{d}\sigma}{\mathrm{d}q^2} = \frac{\mathrm{d}\sigma}{\mathrm{d}\Omega'}2\pi\frac{\mathrm{d}(\cos\theta)}{\mathrm{d}q^2}.$$

q^2 is the same as the variable t for which we derived the expression (2.36) in the laboratory system (neglecting m_{e}). There we also calculated the derivative

$$\frac{\mathrm{d}t}{\mathrm{d}(\cos\theta)} \equiv \frac{\mathrm{d}q^2}{\mathrm{d}(\cos\theta)} = \frac{2E^2}{[1 + (E/M)(1 - \cos\theta)]^2}.$$

Using the relation (in the laboratory system) $E' = E/[1 + E/M(1 - \cos\theta)]$ and collecting results, one indeed rediscovers the formula (2.57′) for the elastic differential cross section due to Rosenbluth (1950).

2.8.4 Counting Quark Generations

The annihilation of positrons on electrons in a *colliding beam* experiment, in principle, is a simple and direct way of discovering new quark generations. Indeed, at the level of the hadronic constituents, e^+e^--annihilation into quark-antiquark pairs may be compared to the well-known QED process $e^+e^- \to \mu^+\mu^-$. For s large as compared to m_μ^2 the production cross section for the latter is calculated to be

$$\sigma^{\text{tot}}(e^+e^- \to \mu^+\mu^-) \simeq \frac{4\pi\sigma^2}{3s}.$$

(For a derivation of this formula see e.g. [QP07], Chap. 10.) All quarks carry nonvanishing electric charge. Therefore, a pair of a quark f of mass M_i and charge e_i, and its antiquark $\bar{f}$ is created in e^+e^--annihilation as soon as the squared center-of-mass energy is larger than the corresponding threshold $s_i = (2M_i)^2$, $s \geq s_i$. The ratio of the cross section for creation of all such pairs up to this threshold to the cross section for creation of a $\mu^+\mu^-$-pair is found to be (see, e.g., [QP07])

$$\frac{\sigma_{\text{tot}}(e^+e^- \to \sum (f_i^+ f_i^-))}{\sigma_{\text{tot}}(e^+e^- \to \mu^+\mu^-)} \simeq 1 + \sum e_i^2 \sqrt{1 - 12M_i^2/s^2 - 16M_i^4/s^3}, \quad (2.212)$$

e_i being the electric charge of the quark f_i. Thus, at every threshold for the production of a new pair $\left(f_i^+ f_i^-\right)$ the ratio (2.212) is expected to increase by an amount roughly proportional to the square e_i^2 of the charge. As an example, it may be instructive for the reader to draw this ratio for the known quark generations, in the order of increasing masses,

$(\bar{s}s)$ (mass 95 MeV, charge $-1/3$),
$(\bar{c}c)$ (mass 1.27 GeV, charge $+2/3$),
$(\bar{b}b)$ (mass 4.68 GeV, charge $-1/3$), and
$(\bar{t}t)$ (mass 171.2 GeV, charge $+2/3$).

Indeed, this stepwise increase of the ratio (2.212) as a function of the variable s is born out by experiment. Up to the inclusion of colour (see Sect. 3.5.1 below) and of corrections that are calculable from Quantum ChromoDynamics (QCD), there is good agreement between data and predictions.

2.8.5 Deep Inelastic Scattering and Parton Structure of Nucleons

The technique of deep inelastic scattering on protons and neutrons is very powerful in unravelling the internal structure of these particles in terms of their constituents. Historically the first empirical evidence for the fact that quarks were indeed genuine constituents of nucleons, and not merely mathematical tools for classifying hadrons in SU(3) multiplets, came from hadronic total cross sections such as $\sigma(pp)$ and

$\sigma(\pi p)$ whose ratio seemed to be determined by the number of quarks or antiquarks contained in protons and pions, respectively[24]. The amazing observation was that, e.g., $\sigma(pp)/\sigma(\pi p)$ at sufficiently high energy was equal to 3/2, reflecting the fact that a proton is made predominantly out of three quarks while a pion is predominantly a quark-antiquark state. In analogy to atomic physics the three quarks *uud* in the proton, and *udd* in the neutron are called *valence quarks*. This picture of nucleons in an *additive quark model*, does not exclude the presence of other stuff in a proton, depending on the momentum scale at which it is being probed. Once the quark structure of nucleons was established, some obvious questions that came up were: How to confirm the third-integral electric charges of quarks? How does the spin of the nucleon arise, from the spins of the constituent quarks, from relative angular momenta, or from other components of its ground state?

Remarkably, deep inelastic scattering of electrons, and also of neutrinos, after the necessary generalization to the charged and neutral weak interactions (see below), allows to probe the nucleon's structure in much more detail. The information that can be obtained by deep inelastic scattering of electrons is contained in the structure functions W_1, W_2, cf. the definition (2.206), and a third such function if spin-sensitive measurements are made. In (2.207) the invariants $q^2 = (k - k')^2$ and $\nu = (pq)/M$ were defined. It is customary to use instead of these the variables

$$Q^2 := -q^2, \tag{2.213a}$$

defined such as to be positive everywhere in the physical region, and

$$x := \frac{Q^2}{2M\nu}, \tag{2.213b}$$

$$y := \frac{(qp)}{(kp)}, \tag{2.213c}$$

both of which have simple physical interpretations. For example, with respect to the nucleon's rest frame,

$$y := \frac{(qp)}{(kp)} = \frac{\nu}{E} = \frac{E - E'}{E}$$

is the fraction of the energy of the electron lost in the collision. The variable x, in turn, is the fraction of the nucleon's momentum carried by the quark which is struck in the process. This can be seen as follows.

The proton or neutron is assumed to be an ensemble of a small number of loosely bound constituents. These constituents which are called *partons*, in the simplest case, are just the quarks of the additive quark model. In this picture the quarks move almost freely along the momentum of the proton so that quark number i carries a

[24]H.J. Lipkin, F. Scheck; Phys. Rev. Lett **16** (1965) 71; E.M. Levin, L.L. Frankfurt; JETP Letters **2** (1965) 65.

fraction $p_i = \xi p$ of the proton's momentum with $0 < \xi < 1$. Neglecting all masses the Mandelstam squared energy variable of the electron-quark system is

$$s^{(i)} = (p_i + k)^2 \simeq 2(p_i k) = 2\xi(pk).$$

If s denotes the corresponding invariant for the electron-*proton* system, $s = (p + k)^2 \simeq 2(pk)$, then $s^{(i)} = \xi s$. It seems natural to assume that the scattering of the electron on quark i is elastic, so that $p_i' = p_i + q$. The mass of the quark in the final state being negligible, too, one has

$$0 \simeq (p_i + q)^2 = 2(p_i q) + q^2 = 2\xi(pq) - Q^2 = 2\xi M\nu - Q^2 = 2M\nu(\xi - x).$$

Therefore, in the limit of vanishing masses $x = \xi$, as was to be shown.

The invariant cross section is obtained from (2.56) above with $F_1 \equiv 1$ and $F_2 \equiv 0$, and by neglecting the masses M and m,

$$\begin{aligned}\frac{\mathrm{d}\sigma}{\mathrm{d}t^{(i)}} &\simeq \frac{4\pi\alpha^2 e_i^2}{t^{(i)2}} \frac{s^{(i)2} + t^{(i)} s^{(i)}}{s^{(i)2}} \left\{1 + \frac{t^{(i)2}}{2(s^{(i)2} + t^{(i)} s^{(i)})}\right\} \\ &= \frac{2\pi\alpha^2 e_i^2}{t^{(i)2}} \frac{s^{(i)2} + (s^{(i)} + t^{(i)})^2}{s^{(i)2}}. \end{aligned} \tag{2.214}$$

The distribution of the proton's momentum p among the partons/quarks is measured by a *parton distribution function* $f_i(\xi)$ for each species i. These functions describe the internal structure of the proton. Since there is no known method for calculating them, they are usually taken from empirical fits to a set of scattering data.

With $t^{(i)} = q^2 = -Q^2$, $s^{(i)} = \xi s$, and $\xi = x$ the cross section for the proton is obtained from (2.214) by integration over the distribution function and reads

$$\frac{\mathrm{d}\sigma}{dQ^2} = \frac{2\pi\alpha^2 e_i^2}{Q^4} \int_0^1 \mathrm{d}x \; f_i(x) \left\{1 + \left(1 - \frac{Q^2}{xs}\right)^2\right\},$$

from which one obtains the double-differential cross section

$$\frac{\mathrm{d}\sigma}{dQ^2 \mathrm{d}x} = \frac{2\pi\alpha^2 e_i^2}{Q^4} \; f_i(x) \left\{1 + \left(1 - \frac{Q^2}{xs}\right)^2\right\}, \tag{2.215a}$$

This formula exhibits a remarkable feature: If one divides the cross section by the factor

$$\left\{1 + \left(1 - \frac{Q^2}{xs}\right)^2\right\},$$

which, obviously is of a purely kinematic origin, then there remains an expression which depends on the variable x only,

$$\left\{1+\left(1-\frac{Q^2}{xs}\right)^2\right\}^{-1}\frac{\mathrm{d}\sigma}{dQ^2\mathrm{d}x}=\frac{2\pi\alpha^2e_i^2}{Q^4}\ f_i(x). \tag{2.215b}$$

This result from a simple constituent model for the proton, is called *Bjorken scaling*[25]. It rests on the assumption that during the time scale which is typical for the scattering process the quarks in the proton behave as if they were free particles. Interactions between them are neglected at this level.

The analysis of deep inelastic scattering on nucleons with electrons and neutrinos as projectiles, is an important branch of modern elementary particle physics, both in experimental high energy physics and in theory[26]. Here we restrict our summary to electrons only, without terms depending on polarization.

There are many ways of defining the structure functions. A conventional choice adopted in the Review of Particle Physics quoted above is the following. Instead of the structure functions W_i, cf. (2.206), and without polarization dependence, one uses

$$F_1(x,Q^2):=W_1(\nu,Q^2),\qquad F_2(x,Q^2):=\frac{(pq)}{M^2}W_2(\nu,Q^2), \tag{2.216}$$

in terms of which the cross section becomes

$$\frac{\mathrm{d}^2\sigma}{\mathrm{d}x\mathrm{d}y}=\frac{4\pi\alpha^2}{xyQ^2}\left\{xy^2F_1(x,Q^2)+\left(1-y-\frac{x^2y^2M^2}{Q^2}\right)F_2(x,Q^2)\right\}. \tag{2.217}$$

It is instructive to verify that this formula is the same as (2.209). The Jacobian of the transformation from the variables $(x,\ y)$ to the variables $(\nu,\ Q^2)$ is

$$\frac{\partial(x,y)}{\partial(\nu,Q^2)}=\left|\det\begin{pmatrix}-Q^2/(2M\nu^2) & 1/(2M\nu)\\ y/\nu & 0\end{pmatrix}\right|=\frac{y}{2M\nu^2},$$

so that

$$\frac{\mathrm{d}^2\sigma}{\mathrm{d}x\mathrm{d}y}=\frac{2M\nu^2}{y}\frac{\mathrm{d}^2\sigma}{\mathrm{d}\nu\mathrm{d}Q^2}.$$

For example, in the limit of large energy, neglecting the masses of the electron and the quarks, one has in the laboratory system

$$\nu\simeq E-E',\quad x\simeq\frac{EE'}{M(E-E')}(1-\cos\theta),\quad y\simeq\frac{E-E'}{E}.$$

[25] J.D. Bjorken, E.A. Paschos; Phys. Rev. **185**, 1975 (1969).

[26] A good summary is the review on structure functions by B. Foster, A.D. Martin, M.G. Vincter, in K. Nakamura et al. (Particle Data Group), J. Phys. G 37, 075021 (2010), *Reviews, Tables, and Plots*, p.188 where many recent references are given. The Review of Particle Physics can also be found at http://pdg.lbl.gov/

The cross section (2.217) is then given by

$$\frac{\mathrm{d}^2\sigma}{\mathrm{d}x\mathrm{d}y} \simeq \frac{4\pi\alpha^2 E'}{Q^4}\{(E-E')2(1-\cos\theta)F_1(x,Q^2) + M(1+\cos\theta)F^2(x,Q^2)\},$$

so that, upon insertion of the definitions (2.216) with $(pq)/M^2 = (E-E')/M$

$$\begin{aligned}\frac{\mathrm{d}^2\sigma}{\mathrm{d}\nu\mathrm{d}Q^2} &= \frac{y}{2Mv^2}\frac{\mathrm{d}^2\sigma}{\mathrm{d}x\mathrm{d}y} \simeq \frac{4\pi\alpha^2 E'}{Q^4}\frac{1}{2ME} \\ &\times\left\{2(1-\cos\theta)F_1(x,Q^2) + \frac{M}{E-E'}(1+\cos\theta)F_2(x,Q^2)\right\} \\ &= \frac{4\pi\alpha^2 E'}{Q^4 EM}\{2\sin^2(\theta/2)W_1(\nu,Q^2) + \cos^2(\theta/2)W_2(\nu,Q^2)\}.\end{aligned}$$

This is what we obtained in (2.209).

In the case of longitudinally polarized electrons there is a third structure function $F_3(x,\ Q^2)$ whose contribution depends on the helicity $\lambda = \pm 1$ of the electron. If weak interactions are taken into account, i.e. instead of photon exchange there is Z^0- and/or $W^{\pm}$–exchange, and if, alternatively, neutrino scattering is measured, there are additional coupling terms and more structure functions (see reference quoted above).

References

Alder, K., A. Bohr, T. Huus, B. Mottelson and A. Winther, 1956, *Rev. Mod. Phys*. 28, 432.

Alder, K. and T.H. Schucan, 1963, *Nucl. Phys*. 42, 498.

Bailey, J., K. Borer, F. Combley, H. Drumm, C. Eck, F.J.M. Farley, J.H. Field, W. Flegel, P.M. Hattersley, F. Krienen, F. Lange, G. Lebée, E. McMillan, G. Petrucci, E. Picasso, O. Runolfsson, W. von Rüden, R.W. Williams and S. Wojcicki, 1979, *Nucl. Phys*. B150, 1.

Blomqvist, J., 1972, *Nucl. Phys*. B48, 95.

Borie, E.F. and G.A. Rinker, 1982, *Rev. Mod. Phys*. 54, 67.

Borkowski, F., G.G. Simon, V.H. Walther and R.D. Wendling, 1975, *Nucl. Phys*. B93, 461.

Borkowski, F., G. Höhler, E. Pietarinen, I. Sabba-Stefanescu, G.G. Simon, V.H. Walther and R.D. Wendling, 1976, *Nucl. Phys*. B114, 505.

De Forest, T. and J.D. Walecka, 1975, *Adv. in Phys*. 15, 1.

Donnelly, T.W. and J.D. Walecka, 1975, *Ann. Rev. Nucl. Sci*. 25, 329.

Elton, L.R.B., 1953, *Proc. Roy. Soc*. (London) A66, 806.

Engfer, R., H. Schneuwly, J.L. Vuilleumier, H.K. Walter and A. Zehnder, 1974, *Atomic and Nuclear Data Tables* 14, 509.

Friedrich, J. and F. Lenz, 1972, *Nucl. Phys*. A183, 523.

Friar, J.L. and J.W. Negele, 1973, *Nucl. Phys*. A212, 93.

Frois, B. and C.N. Papanicolas, 1987, *Ann. Rev. Nucl. Part. Sci*. 37, 133.

Griffy, T.A., D.S. Onley, J.T. Reynolds and L.C. Biedenharn, 1963, *Phys. Rev*. 128, 833 and 129, 1698.

Lenz, F., 1969, *Zeit. Physik* 222, 491.

Mott, N.F., 1929, *Proc. Roy. Soc.* (London) A124, 429.
Ravenhall, D.G., D.R. Yennie and R.N. Wilson, 1954, *Phys. Rev.* 95, 500.
Reynolds, J.T., D.S. Onley and L.C. Biedenharn, 1964, *J. Math. Phys.* 5, 411.
Rosenbluth, M.N., 1950, *Phys. Rev.* 79, 615.
Scheck, F., 1978, *Phys. Reports* 44, 187.
Scheck, F., 1966, *Nucl. Phys.* 77, 577.
Sick, I., 1974, *Nucl. Phys.* A218, 509 and *Phys. Lett.* 53B, 15.
Simon, G.G., Ch. Schmitt, F. Borkowski and V.H. Walther, 1980, *Nucl. Phys.* A333, 381.
Uehling, E.A., 1935, *Phys. Rev.* 48, 55.

Exercises

2.1. Show that (2.17b) can be transformed into (2.17a) by means of a rotation and a reflection. If the interaction is invariant with respect to these operations, the scattering amplitudes must be the same.

2.2. Derive the cross section (2.26,2.35) for electron scattering off a spin-zero target, on the basis of Feynman rules.

2.3. Prove (2.41) starting from (2.39). *Hint*: Consider first the case of an infinitesimal translation. Then make use of

$$\mathrm{e}^x = \lim_{n\to\infty} (1 + x/n)^n.$$

2.4. Prove relation (2.93) and use this relation to calculate the interaction term (2.92).

2.5. Derive the elastic form factor for a homogenous charge density (2.102). Calculate the cross section and discuss the result.

2.6. Prove the representation (2.129). *Hints*: First derive an equation for $(\mathrm{d}/\mathrm{d}r)W(r)$, with $W(r)$ as defined in (2.128), by combining the differential equations (2.105′) for the two potentials. Calculate $W(r = R_\infty)$ at some large radius, making use of the asymptotic forms of the radial functions, and let R_∞ go to infinity.

2.7. An unstable particle of lifetime τ is produced with a given energy E on a fixed target in the laboratory. Over which length can one reasonably hope to transport a beam of such particles? Consider the example of muons and pions at kinetic energies between 10 MeV and 200 MeV.

2.8. For $\kappa < 0$, $l = -\kappa - 1$, show that $rg_{n\kappa}(r) \simeq y_{nl}(r)$. This means that the states $\left(n,\ \kappa,\ j = -\kappa - \frac{1}{2} = l + \frac{1}{2}\right)$ and $\left(n, \kappa' = -\kappa - 1, j = -\kappa - \frac{3}{2} = l - \frac{1}{2}\right)$ have the same radial wave function in the nonrelativistic limit.

2.9. For circular orbits compare the fine structure splitting as predicted by (2.162) with the one obtained in first-order perturbation theory from

$$V_{ls} = \frac{1}{2m^2}\frac{1}{r}\frac{\mathrm{d}V}{\mathrm{d}r}\boldsymbol{l}\cdot\boldsymbol{s}.$$

and nonrelativistic wave functions.

2.10. In a muonic atom consider two potentials V_1 and V_2 which differ only over the nuclear domain. Expand the muonic density according to $|\Psi|^2 \simeq a + br + cr^2$ and show that the eigenvalues of the energy for V_1 and V_2 differ approximately by

$$\Delta E = Ze^2 \frac{2\pi}{3} a \left\{ \Delta \langle r^2 \rangle + \frac{b}{2a} \Delta \langle r^3 \rangle + \frac{3c}{10a} \Delta \langle r^4 \rangle \right\},$$

where $\Delta \langle r^n \rangle$ is the difference in the corresponding nuclear charge moments. Derive an approximate formula for $E_{2p1/2} - E_{2s1/2}$ as compared to the value of this difference in the case of the point charge.

2.11. Prove the following identity, starting from (1.84–1.84'):

$$(p + p')_\alpha \overline{u(\boldsymbol{p}')}\, u(\boldsymbol{p}) = \overline{u(\boldsymbol{p}')} \{ 2M\gamma_\alpha + \mathrm{i}\sigma_{\alpha\beta}(p - p')^\beta \} u(\boldsymbol{p}).$$

Springer

http://www.springer.com/978-3-642-20240-7

Electroweak and Strong Interactions
Phenomenology, Concepts, Models
Scheck, F.
2012, XX, 424 p., Hardcover
ISBN: 978-3-642-20240-7